Dissertations and Theses (Open Access)          MD Anderson UTHealth Houston Graduate School

5-2016

# The Notch Target Hes4 Promotes Osteosarcoma Tumor Growth And Metastasis By Inhibiting Osteogenic Differentiation, And Has Potential As A Prognostic Biomarker For Newly Diagnosed Patients With High Grade Osteosarcoma.

Madonna McManus

The TMC LIBRARY
Health Sciences Resource Center

THE NOTCH TARGET HES4 PROMOTES OSTEOSARCOMA TUMOR GROWTH AND

METASTASIS BY INHIBITING OSTEOGENIC DIFFERENTIATION, AND HAS

POTENTIAL AS A PROGNOSTIC BIOMARKER FOR NEWLY DIAGNOSED

PATIENTS WITH HIGH GRADE OSTEOSARCOMA.

by

Madonna M. McManus, B. S.

APPROVED:

_____
Eugenie S. Kleinerman, M.D.
Advisory Professor

_____
Keri L. Schadler, Ph.D.

_____
Candelaria Gomez-Manzano, M.D.

_____
Joya Chandra, Ph.D.

_____
Raymond J. Grill, Ph.D.

_____
Patrick A. Zweidler-McKay, M.D., Ph.D.

APPROVED:

_____
Dean, The University of Texas
Graduate School of Biomedical Sciences at Houston

THE NOTCH TARGET HES4 PROMOTES OSTEOSARCOMA TUMOR GROWTH AND

METASTASIS BY INHIBITING OSTEOGENIC DIFFERENTIATION, AND HAS

POTENTIAL AS A PROGNOSTIC BIOMARKER FOR NEWLY DIAGNOSED

PATIENTS WITH HIGH GRADE OSTEOSARCOMA.

A

DISSERTATION

Presented to the faculty of
The University of Texas
Health Science Center at Houston
and
The University of Texas
MD Anderson Cancer Center
Graduate School of Biomedical Sciences
in Partial Fulfillment

of the Requirements

for the Degree of

DOCTOR OF PHILOSOPHY

by

Madonna M. McManus, B.S.
Houston, Texas

May, 2016

**Dedication**

For my dad.

Thank you for the constellation maps, rock tumblers, garage sale microscopes

and subscriptions to National Geographic and Scientific American.

Your gifts taught me to be fascinated by the inner workings of our universe.

Above all, thank you for seeing potential in me that no one else really saw.

I couldn't have achieved this without a lifetime of your love and support,

and I miss you every day.

## Acknowledgements

Mom, thank you. You inspire within me a passion and fire that I'll never lose. You are the epitome of strength and generosity, and I feel so blessed to be your daughter.

Michael, my husband: thank you for encouraging and inspiring within me perseverance and kindness. Being your partner makes everything better.

Keri, my mentor and friend: without your brilliant guidance and ideas, and daily encouragement, I would not have made it through to the end. I wanted to quit at least three hundred times, and you never let me. You have impacted me in ways that you may never understand, and I couldn't be more grateful for all that you are. You are the embodiment of all that is good in science; your kindness, intelligence, thoughtfulness and generosity set you apart, and I couldn't possibly be more grateful that I got to be THE Keri Schadler's first student. I can't wait to see the positive impact your works makes on the world.

Dr. Kleinerman: there is a running joke in the department that all orphaned students come to you. This fact is a testament to how kindhearted and supportive you are to those around you. Your desire to support and guide students towards developing impactful work is inspiring, and I could not have succeeded without you. You have greatly impacted my education, and I admire you dearly. Your students love you, and it's very clear why.

I would also like to thank my committee members, Dr. Raymond Grill, Dr. Patrick Zweidler-McKay and Dr. Joya Chandra, for your years of support, advice and encouragement. I could not have been successful without your collective expertise. Thank you also Dr. Gomez-Manzano for your willingness to join my committee.

I am grateful for the Pediatric department, in particular Mandy Hall, Yanwen Yang, and Nancy Gordon. Thank you for your expertise, friendship, and willingness to help me with whatever I needed.

Thank you ETAP, specifically Dr. Varsha Gandhi and Lidia Vogelsang, for becoming a second family.

I would also like to express gratitude for the Deans of GSBS: Dr. Shelley Barton and Dr. Michael Blackburn. You made me feel supported and valued, and I am so grateful for your contributions to my education.

THE NOTCH TARGET HES4 PROMOTES OSTEOSARCOMA TUMOR GROWTH AND

METASTASIS BY INHIBITING OSTEOGENIC DIFFERENTIATION, AND HAS

POTENTIAL AS A PROGNOSTIC BIOMARKER FOR NEWLY DIAGNOSED

PATIENTS WITH HIGH GRADE OSTEOSARCOMA.

Madonna M. McManus, B. S.

Advisory Professor: Eugenie Kleinerman, M.D.

Mentor: Keri Schadler, Ph.D.

**Abstract**

Currently, there are no well-established prognostic biomarkers for osteosarcoma (OS) at the time of diagnosis. Although response to preoperative chemotherapy correlates with metastasis risk and overall survival, this information is obtained 3-4 months after the initial diagnosis. The major purpose of this study is to identify clinically relevant biomarkers that will allow for the stratification of patients into good or poor responders to chemotherapy at diagnosis. We also aim to understand the biology of these markers in OS pathogenesis. Because the development of OS is caused by genetic disruptions of osteogenic differentiation, we sought to identify pathways that are involved in normal bone development and homeostasis. One such pathway is the Notch signaling pathway. We hypothesized that the Notch downstream target Hairy/Enhancer of Split 4 (Hes4) is important in the pathogenesis of OS, and thus can be used as a biomarker for OS at the time of diagnosis.

The differentiation status of some cancers is linked with their metastatic behavior: the more immature the cell population, the more aggressive the disease. The Notch signaling pathway is a mediator of differentiation and a crucial component in normal bone

development. In normal bone marrow stromal cells, Hes4 was shown to regulate commitment to the osteogenic pathway. By contrast, we demonstrated that in a tumorigenic context, human OS cells that overexpress Hes4 inhibited the progression of preosteoblasts to early and mature osteoblasts and increased the invasive capacity *in vitro*. This was not universal to all Notch effectors, as Hes1 overexpression induced opposing effects. When injected into NSG mice, Hes4 overexpressing OS cells produced significantly larger, more lytic tumors and significantly more metastases than did GFP expressing cells. In patients with high grade OS, high Hes4 mRNA expression in diagnostic primary tumor biopsies correlated with an increased incidence of metastasis and decreased overall survival. Therefore, Hes4 may allow for the stratification of patients into good or poor responders to chemotherapy at diagnosis. Early stratification and prognosis of OS would allow for modification of therapy and may serve as the basis for future clinical trials of OS treatment.

Table of Contents

**List of Illustrations**

**List of Tables**

**CHAPTER 1. Introduction**

## Osteosarcoma

Osteosarcoma (OS) is the most common primary bone cancer in adolescents and young adults, occurring in 4 per million in the United States (1). The peak incidence of OS is between the ages of 11-20, and OS affects slightly more males than females (Campanacci instituto Rizzoli 2000). In most patients, OS occurs in areas of rapid bone growth, specifically, the metaphyseal periosteum of the distal femur, proximal tibia, and proximal humerus (2). OS is thought to arise from the transformation of mesenchymal stem cells and results in the disruption of osteogenic differentiation, resulting in the uncontrolled deposition of malignant osteoid (3). Histologically, OS can be characterized by the uncontrolled formation of both osteoblastic and osteolytic lesions.

The current standard of care in treating pediatric OS is 10-12 weeks of preoperative chemotherapy (high-dose methotrexate, doxorubicin, and cisplatin; MAP), followed by surgery and several more months of postoperative chemotherapy (4). The single most important prognostic factor in determining OS patient outcome is the histological response to preoperative chemotherapy within the surgically resected tumor (5-7). A good histological response is defined as >90% necrosis in a resected tumor specimen and results in a 5-year survival of 70-80%; the 5-year survival for poor responders (those with <90% tumor necrosis) is 30-60% (5-7). When OS metastasizes, most lesions occur in the lung, with more rare incidences of OS metastases in other bones, the heart, the liver, or the brain. Although 20% of OS patients present with detectable metastatic disease, up to 80% of patients have metastatic disease within 5 years of diagnosis (2).

Unfortunately, despite ongoing advances in the treatment of OS, there has not been a significant change in survivorship in the last 20 years. Survival rates remain at 15-30% for

patients who present with metastatic disease. New treatment strategies are needed, and a greater understanding of the biology that drives both the pathogenesis of OS and the metastatic spread of disease will allow for the development of new, more effective treatments.

## Normal Bone Development and Homeostasis

Because OS affects growing bones in growing adolescents, and because OS is thought to arise from mesenchymal stem cells (3), we hypothesized that OS develops and progresses as a result of a deregulation in bone development and homeostasis. Normal bone development can therefore lend insight to OS disease etiology. Normal bone development and homeostasis is a tightly regulated balance of bone formation (mediated by osteoblasts) and bone absorption (mediated by osteoclasts)(Figure 1). During development and growth, such as during adolescence, there is a shift in the balance in favor of new bone formation. This is due to the activation of the osteoblastic pathway.

Bone marrow stromal cells can differentiate into either mesenchymal stem cells (MSCs) or hematopoietic stem cells (HSCs). Further differentiation of MSCs results in bone formation. More specifically, bone formation relies on a multistep differentiation pathway in which various transcription factors control the progression from an immature stem-like state (MSC) through osteogenic lineage commitment to terminal differentiation into osteoblasts/osteocytes (8-17). This process is defined and regulated by the presence or absence of a number of transcription factors and can be divided into 4 main stages (Figure 2). Expression of each factor is transient and must peak then decline to allow progression to the next stage. The first stage, "pluripotency," is comprised of pluripotent MSCs which have the potential to differentiate into multiple downstream mesodermic pathways including

osteogenic differentiation (bone), chondrocytic differentiation (cartilage), and adipocyte generation (fat).  MSCs are characterized by the expression of Nanog, Sox2 and Oct4. The second stage is comprised of committed osteoprogenitors and is induced by the expression of RunX2 and osterix. These transcription factors promote the commitment of pluripotent mesenchymal stem cells into the osteogenic pathway, and are key transcriptional switches that allow for proper osteogenic differentiation. These osteoprogenitors have lost the ability to differentiate down a non-osteogenic lineage. Committed osteoprogenitors differentiate into early and mature osteoblasts, which give rise to bone forming osteocytes during the third and final stage. This final stage of differentiation results in the deposition of osteoid, a matrix that allows for bone formation. Early and mature osteoblasts are characterized by the presence of alkaline phosphatase, osteopontin, and osteocalcin.

Unlike osteoblasts, which are derived from MSCs, osteoclasts are derived from hematopoietic stem cells (HSCs). Interestingly, the regulation of osteoclast function is highly dependent on osteoblasts. Osteoblasts control the maturation of osteoclasts via their expression of the receptor activator of nuclear factor-kB ligand (RANKL). RANKL, expressed by osteoblasts, interacts with RANK receptors on the surface of osteoclast precursors, promoting the maturation of osteoclasts (18-20).

**Understanding the molecular mechanisms that regulate OS cell differentiation and that drive the cross-talk between blastic and lytic phenotypes in OS may lead to the identification of novel treatment strategies that target both.**
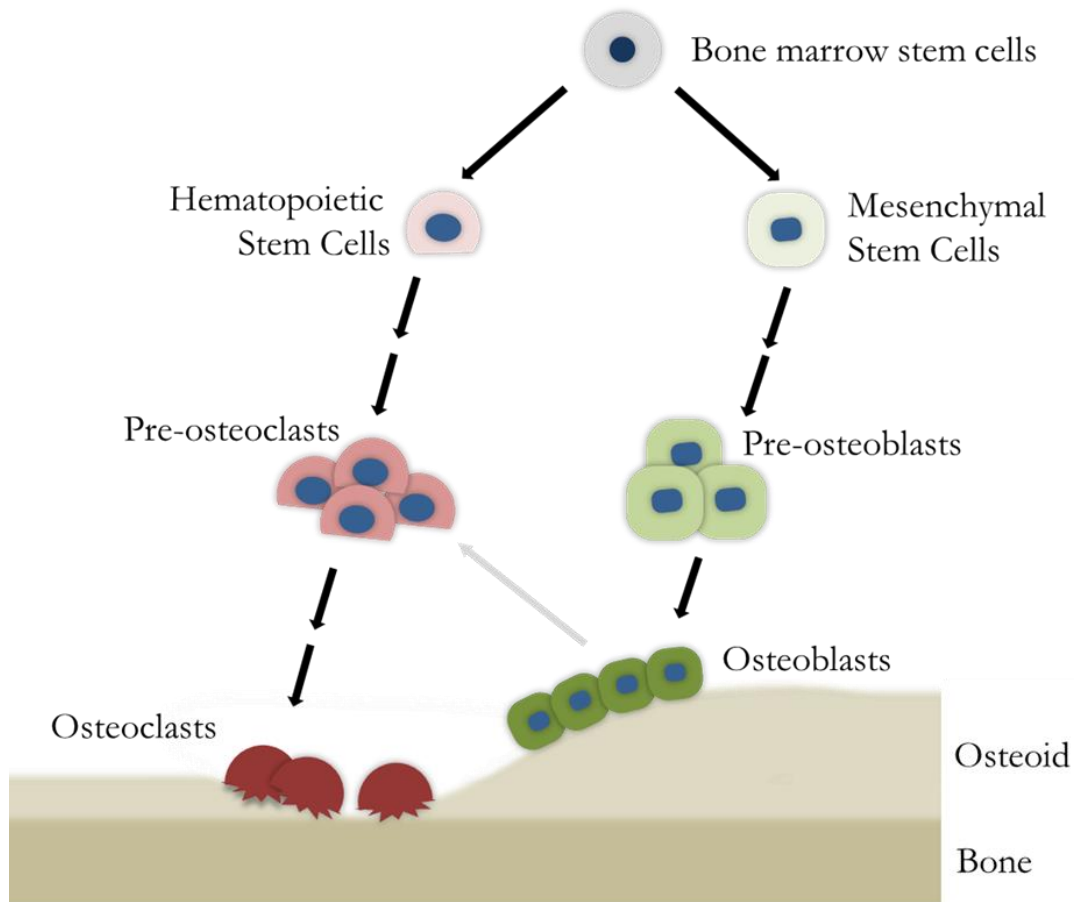
**Figure 1. Schematic depicting the highly regulated balance of osteoblasts and osteoclasts.**
Bone remodeling relies on both osteoclastic and osteoblastic activity. The formation of osteoclasts and osteoblasts is highly regulated by a multistep differentiation process. Osteoclasts originate from hematopoietic stem cells. Osteoblasts originate from mesenchymal stem cells. There is cross talk between osteoblasts and pre-osteoclasts that will be discussed again in Chapter 5.
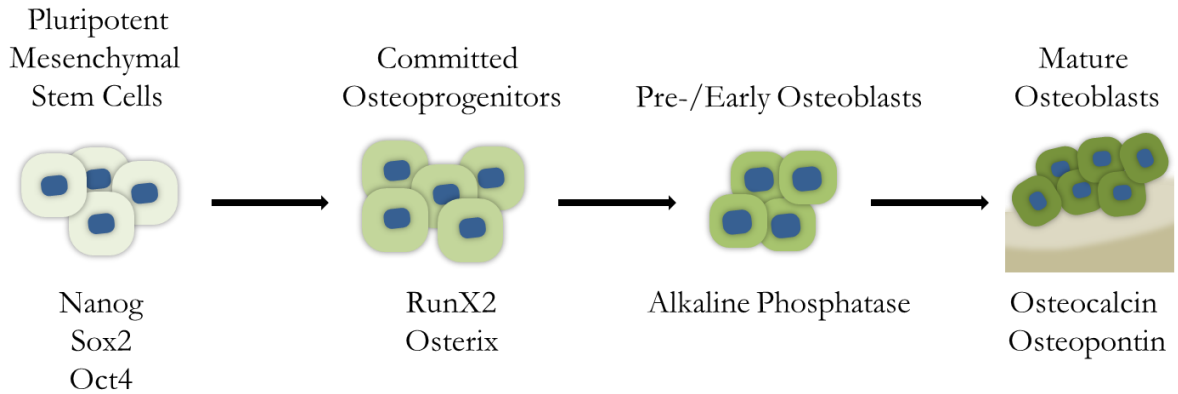
**Figure 2. A schematic of normal osteogenic bone differentiation and associated transcription factors.**
This process is defined and regulated by the presence or absence of a number of transcriptions factors and can be divided into 4 main stages: pluripotency, osteogenic commitment, pre/early osteoblast, and maturation.

## Deregulated and Tumorigenic Bone Homeostasis

Histologically, OS is a highly heterogeneous mixture of cells representing the full spectrum of osteoblastic and osteolytic differentiation, ranging from highly proliferative MSCs and HSCs, to terminally differentiated osteoblasts and osteoclasts, thus resulting in both osteoblastic and osteolytic characteristics (2, 3, 21). Osteoblastic tumors result in the formation of calcium rich, bone-like tumors, while osteolytic tumors result in the destruction of bone. Importantly, both OS types can be present within one tumor.

Interestingly, the differentiation status of OS is believed to be linked to metastatic behavior: the more immature the cell population, the more aggressive the disease (3). An immature tumor would be high in MSCs or HSCs and would have a reduced number of fully differentiated osteoblasts and osteoclasts. Indeed, in both human and murine OS, expression of osterix, the transcription factor responsible for osteogenic lineage commitment, is decreased in more aggressive, immature and tumorigenic phenotype (19, 22).

## Notch Signaling

OS may result from aberrations in the mechanisms that regulate bone development, remodeling and homeostasis. Because of this, we sought to identify signaling pathways that are involved in bone regulation. One such pathway is the Notch signaling pathway (Figure 3). The Notch signaling pathway is a well-known mediator of differentiation in many tissue types and a crucial component in normal bone development (23-27). Briefly, the Notch signaling pathway is activated when a membrane-bound ligand (Jag1, Jag2, Dll1, Dll3, or Dll4) on a signal-sending cell physically interacts with the extracellular domain of a membrane-bound Notch receptor (Notch1-4) on a signal-receiving cell. This interaction results in the two-step proteolytic cleavage of the intracellular domain of Notch by metalloprotease and then gamma secretase. Once cleaved, the intracellular domain of Notch translocates to the nucleus where it interacts with co-activator mastermind-like 1-3 (MAML) within CSL (C promoter binding factor-1 [CBF-1], suppressor of hairless, Lag-1) to form a transcriptional complex which promotes the expression of a number of target genes downstream from Notch (28-32). These genes include: c-Myc, p21, and cyclin D1 (cell cycle progression), Bcl-2 (inhibition of apoptosis), Hairy/Enhancer of Split (Hes1-7), Hey1-2, Hey-L family of proteins, and deltex (transcriptional repressors) (33). These Notch effectors are transcription factors that regulate expression of diverse targets, allowing Notch receptors to act as master regulators of gene cohorts to control cellular outcome (27, 34-36). Hes and Hey genes are transcriptional regulators of the basic helix-loop-helix (bHLH) class (37). Hes and Hey family members are known to form direct transcriptional repressors by binding to N- or E- box DNA sequences of target promoters as hetero- or homodimers. Hes and Hey

transcription factors can also indirectly regulate transcription by binding to other

transcriptional complexes or by sequestering transcriptional activators (37, 38).
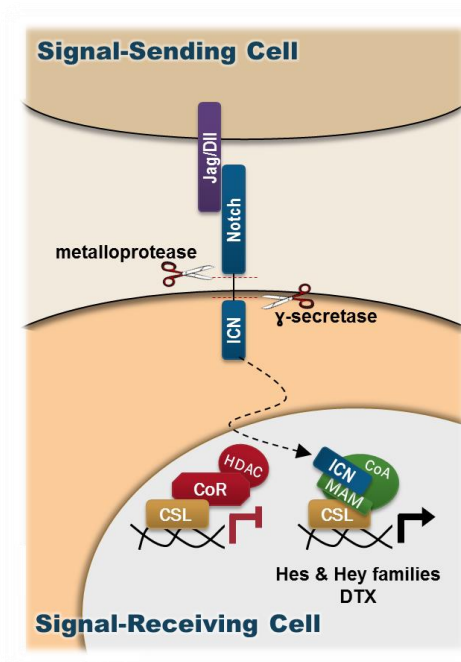


**Figure 3. Schematic of the Notch Signaling Pathway.**
The Notch signaling pathway is activated when a membrane-bound ligand (Jag1, Jag2, Dll1, Dll3, or Dll4) on a signal-sending cell physically interacts with the extracellular domain of a membrane-bound Notch receptor (Notch1-4) on a signal-receiving cell. This interaction results in the two-step proteolytic cleavage of the intracellular domain of Notch by metalloprotease and then gamma secretase. Once cleaved, the intracellular domain of Notch translocates to the nucleus to promote the expression of a number of target genes downstream from Notch. These genes include Hairy/Enhancer of Split (Hes1-7), Hey1-2, and deltex.

## Notch Signaling in Bone

Notch signaling plays a complicated role in bone formation and homeostasis (39). Notch Signaling promotes the development of osteoblasts from MSCs (40), while the expression of the Notch delta ligand inhibits the development of osteoclasts (41). Notch cleaving metallo-proteases are localized to sites of active bone formation (42). In mice and humans, Notch-deficiency results in severe skeletal abnormalities (43-45). In a mouse knockout of Notch1 and gamma secretase, there was an accumulation of bone in the marrow cavity which resulted in shorter long bones, along with an observed increase in sialoprotein, alkaline phosphatase, and collagen I (25). This resulted in an overall increase in osteoblastic differentiation.

## Notch Signaling in Osteosarcoma

Notch signaling is implicated in the development of numerous cancers, including OS. Inhibiting Notch receptor activity using genetic or pharmacologic inhibition resulted in decreased tumor growth in nude mice, indicating that Notch plays an important role in OS pathogenesis (46). Hes4, a Notch effector that is not yet well characterized, was first identified as a potential protein of interest in cancer when it was shown to be an important biomarker used to identify solid tumors likely to respond to GS inhibitor (GSI)-based therapies in breast cancer (47-49). Interestingly, Hes4 also plays an important role in differentiation; specifically, Hes4 regulates the lineage commitment of normal bone marrow stromal cells (BMSCs) into the osteogenic pathway (Figure 4) (27). When Hes4 is present, it interacts with Twist-1 to allow for RunX2 mediated expression of osterix followed by increases in osteopontin and osteocalcin. These together allowed for the terminal differentiation of BMSCs.
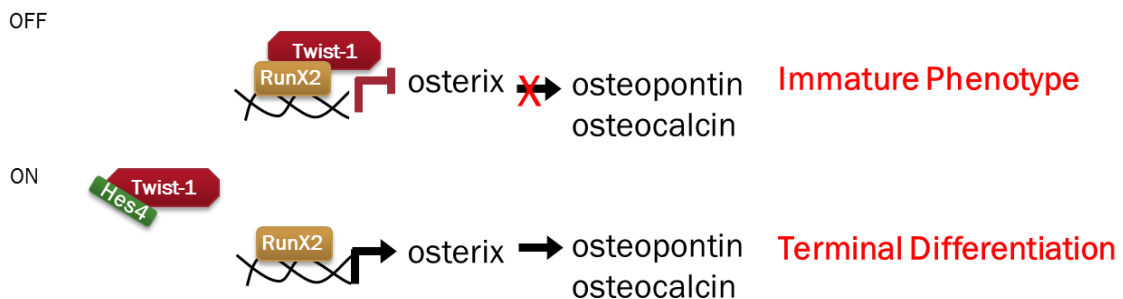


**Figure 4. Depiction of Hes4 signaling in Normal Bone Marrow Stromal Cells.**
Hes4 regulates the lineage commitment of normal bone marrow stromal cells into the osteogenic pathway.

## Hypothesis

Because disruption of osteogenic differentiation is thought to lead to the initiation and progression of OS (11, 50), we sought to expand our understanding of the underlying molecular mechanisms that drive bone remodeling to identify therapeutic targets for OS that have potential in treating both primary and metastatic tumors. Little is known about the roles of individual Notch effectors such as Hes1 and Hes4 in the development and progression of OS. Based on a lack of published data regarding the roles of Notch, we aimed to characterize the individual roles of Notch effectors.

**We hypothesized that Hes4 promotes the development and progression of primary and metastatic OS by inhibiting the differentiation of OS cells.** To test this hypothesis, we performed both *in vitro* and *in vivo* studies manipulating the expression of Hes4 and Hes1, and determined whether this promoted differentiation of OS and progression of primary and metastatic OS.

**CHAPTER 2. Blocking Notch Receptor signaling does not inhibit OS cell or tumor growth.**

**Rationale**

Because it can induce a wide range of outcomes, Notch signaling can contribute to both oncogenic or tumor suppressive phenotypes depending on the cancer type (51-53), and in some cases, can play both roles within the same tumor type (54-59). In Osteosarcoma, there have been several reports that suggest that Notch plays an oncogenic role (46, 60-62). For example, in 2013 Mu *et al.* demonstrated a correlation between the metastatic potential of murine cells and increased expression of Notch1, Notch2, Notch4, and Hes1 (61). Because of the potential oncogenic role Notch has played in osteosarcoma (46, 60-62), we first inhibited Notch signaling and examined the effect on OS tumor progression. There are numerous genetic and pharmacologic approaches to blocking Notch pathway activity (63-65). In this chapter, we will focus on the inhibition of MAM-mediated co-activation of the CSL transcriptional complex using dominant-negative MAM (dnMAM; a truncated version of MAM that can bind to ICN but not DNA). Though inhibition of Notch using GSIs are tested clinically due to the ease of delivery as a pharmacologic agent, more specific targeting of Notch pathway activity is achieved with dnMAM, which can be introduced by retroviral transduction into various experimental systems (46, 60, 66). [For results regarding GSI mediated inhibition of Notch signaling, see Appendix]

In 2008 it was shown in a subcutaneous OS model using nude mice that dnMAM expressing SJSA OS cells resulted in reduced OS tumor burden when compared to control SJSA cells (46). This suggests that inhibiting Notch may be a therapeutic target in preventing OS tumor progression. In this chapter, we explore the potential anti-tumorigenic role of blocking Notch signaling using dnMAM in an orthotopic OS tumor model using CCHD intratibially-injected NSG mice.

## Results

### Inhibiting Notch using dnMAM does not alter proliferation

We used dnMAM to look at how specifically preventing Notch's ability to regulate transcription would affect proliferation. In order to express dnMAM in OS cells, we transduced CCHD, HOS and CCHO human OS cells with GFP containing retroviral MigR1 constructs with and without dnMAM (control: "CCHD/HOS/CCHO-GFP"; dnMAM expressing: "CCHD/HOS/CCHO-dnMAM" (Figure 5). Because this construct expresses dnMAM and GFP as a fusion protein, each GFP protein equates to one dnMAM protein. In HOS cells transduced with GFP or GFP-dnMAM, there was no change in cell count over an 8 day period (Figure 6A). Similarly, in these same cells, there was not a change in the number of colonies formed in HOS cells transduced with GFP-dnMAM versus GFP control (Figure 6B). Using the dnMAM expression construct, we measured the effect of inhibiting CSL-dependent signaling on proliferation when compared to control CCHD/HOS/CCHO-GFP cells in a competitive proliferation assay. Expression of dnMAM does not affect the rate of proliferation of HOS, CCHD or CCHO cells relative to control cells in a competitive proliferation assay (Figure 6C).
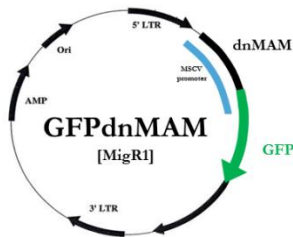


**Figure 5. dnMAM expression construct.**
Schematic representation of the dnMAM vector map depicting the orientation of GFP and dnMAM within the retroviral MigR1 backbone. Expression is controlled by constitutively active 5' LTR promoter. dnMAM and GFP are expressed as a fusion protein.
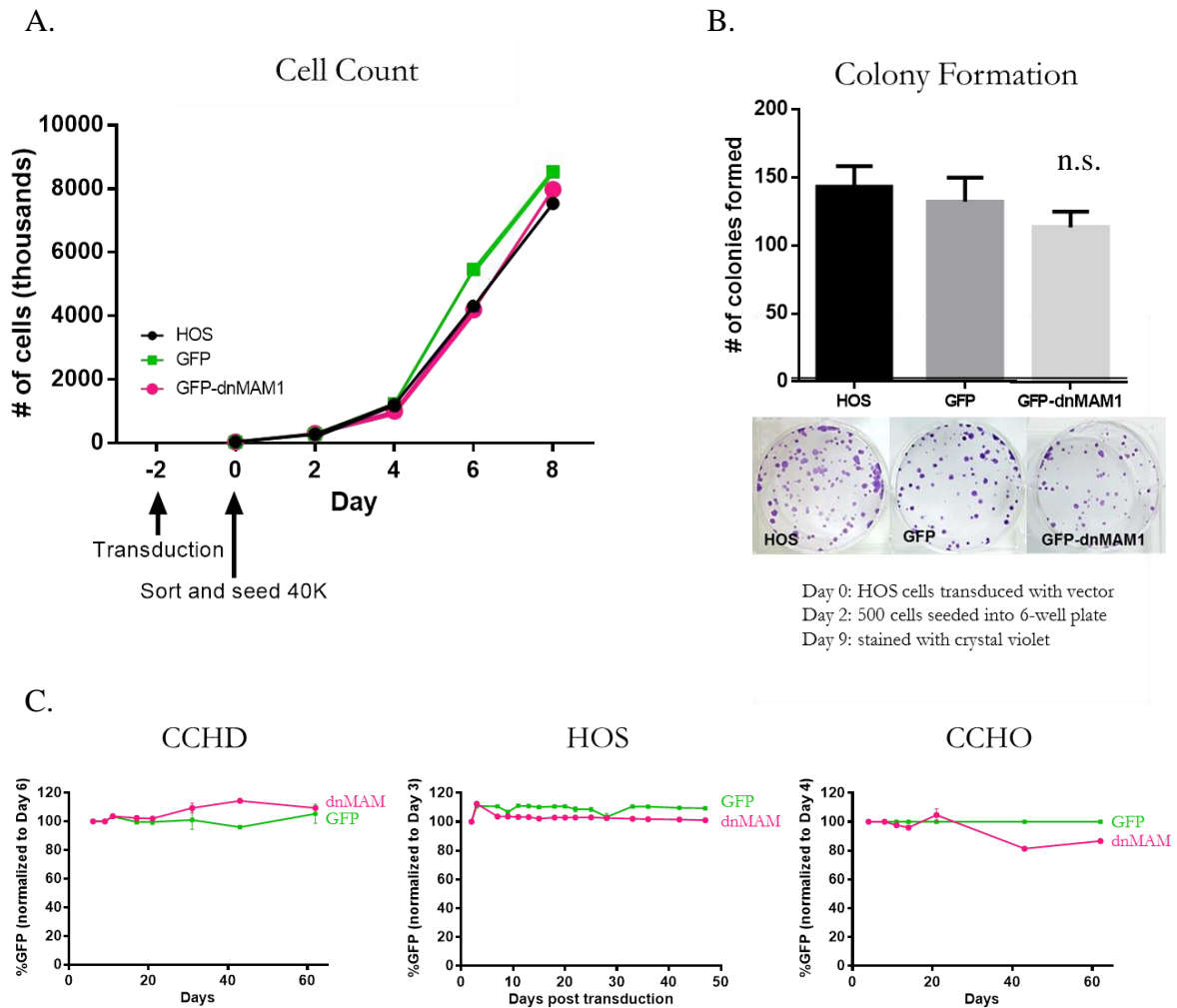
**Figure 6. Inhibiting CSL-dependent Notch signaling using dnMAM does not affect proliferation.**
(A) Cell counts of HOS cells transduced with GFP or GFP-dnMAM; counts made every two days over an 8 day period. (B) HOS cells were transduced with either GFP or GFP-dnMAM1, were sorted for GFP+. 500 cells were seeded on day 2 and stained for crystal violet on day 9. There was not a change in the number of colonies formed in HOS cells transduced with GF-dnMAM versus GFP control. (C) Graph of the percentage of GFP$^+$ OS cells (CCHD, HOS and CCHO) over time after stable retroviral transduction of vector alone (GFP) or containing dnMAM (normalized to day 6, 3, and 4, respectively, after transduction). n.s. is "not significant.

**Inhibiting Notch using dnMAM does not affect OS cell invasiveness.**

In order to determine any changes in migration or invasion in OS cells in response to dnMAM, we quantified the number of cells that were able to migrate through Matrigel and traverse an 8-μm pore membrane in HOS and CCHD cells transduced with dnMAM relative to cells transduced with GFP control cells. The presence of dnMAM did not alter the ability of HOS and CCHD cells to invade. (Figure 7).
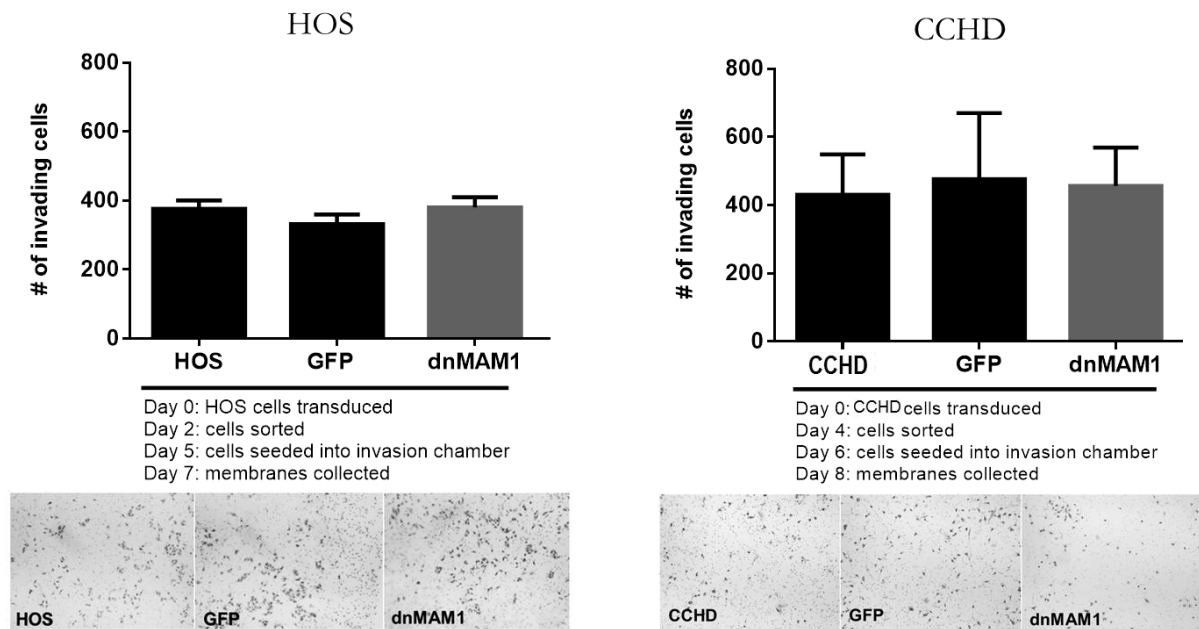


**Figure 7. Inhibiting CSL-dependent Notch signaling using dnMAM does not affect the ability for OS cells to invade.**
HOS and CCHD cells were transduced with GFP or GFP-dnMAM and were sorted for GFP. Invasiveness was measured using a 24-well BD BioCoat Matrigel invasion chamber with an 8-μm pore size. Graphs show average of 3 experiments +/- S.E.M.

**Inhibiting Notch using dnMAM does not alter *in vivo* tumor growth or number of metastases in an orthotopic OS model.**

To determine the role of blocking Notch using dnMAM in the progression of primary and metastatic OS, we used an *in vivo* CCHD xenograft mouse model (Figure 8). We used luciferase imaging to longitudinally monitor tumor growth and determined that there was no change in tumor growth in mice injected with CCHD-luc-GFP cells versus CCHD-luc-GFP-dnMAM cells (Figure 9A). Six weeks after inoculation, the experiment was terminated due to large tumor burden. The metastatic lesions within the lungs of all experimental mice were quantified, and no difference was detected (Figure 9B).
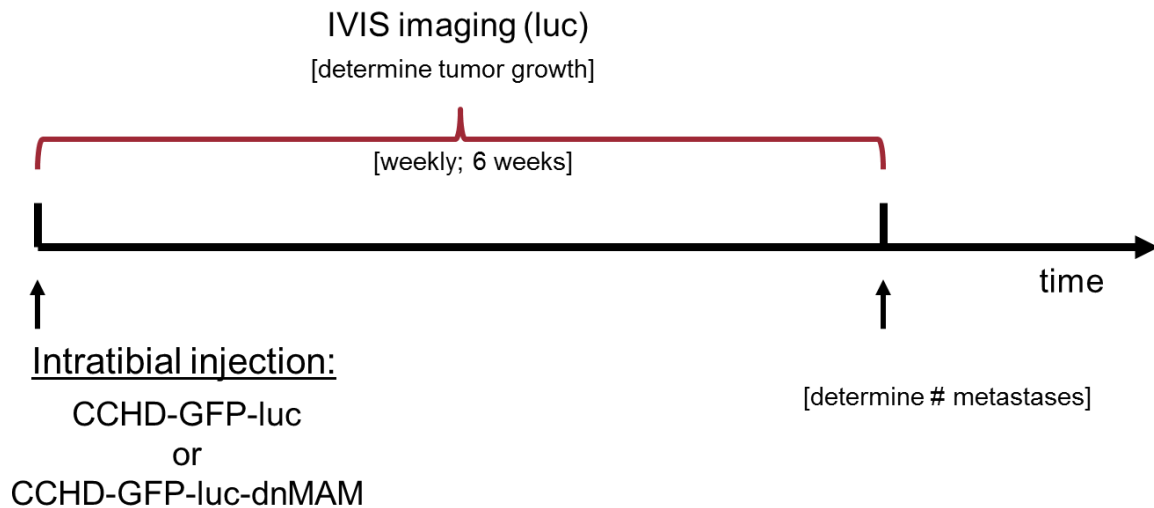


**Figure 8. Schematic diagram of *in vivo* GFP versus dnMAM experimental design.** Either CCHD-GFP-luc or CCHD-GFP-luc-dnMAM expressing cells (1 × 106 suspended in 15 μl of sterile PBS) were injected into the right tibias of 6-week-old NOD/SCID/IL2Rγ-deficient mice (The Jackson Laboratory, Bar Harbor, ME).

A.



B.
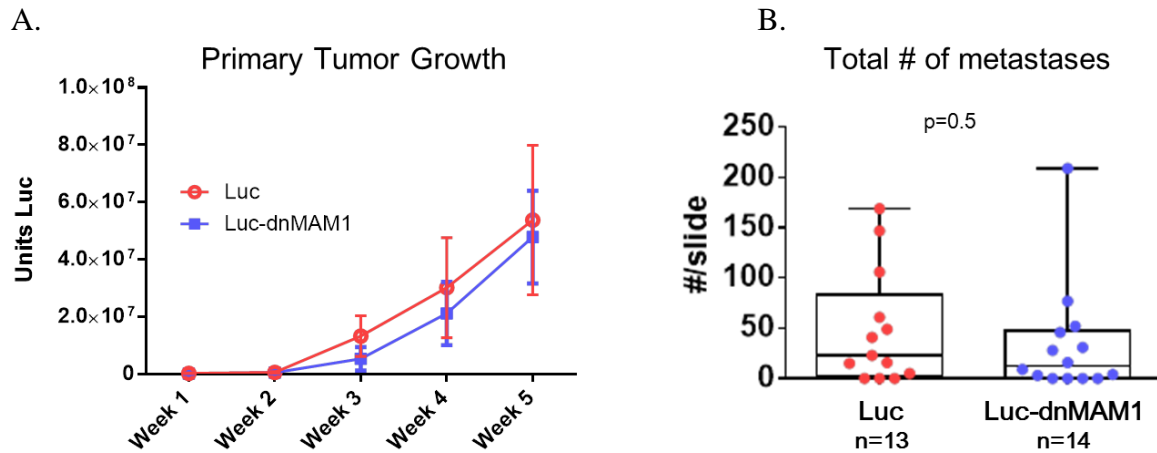


**Figure 9. Inhibiting CSL-dependent Notch signaling using dnMAM does not affect OS primary tumor growth or the number of metastases in an orthotopic OS tumor model.** Either CCHD-GFP-luc or CCHD-GFP-luc-dnMAM expressing cells were injected orthotopically in NOD/SCID/IL2Rγ-deficient mice. (A) Luciferase activity was quantified weekly for 5 weeks to monitor primary tumor growth. N=13 luc, N=14 luc-dnMAM. (B) Six weeks after the initial injection, mice were sacrificed, and lung metastases were quantified.

**Inhibiting Notch using dnMAM differentially affects Notch downstream target expression**

Although dnMAM is expressed as a fusion protein which allows us to confirm the presence of dnMAM expression by GFP fluorescence, we wanted to confirm that dnMAM is indeed inhibiting CSL-mediated expression of Notch downstream targets. We used RTq-PCR to monitor the expression of the Notch downstream target Hes1, the standard surrogate marker for Notch activation, in response to the presence of dnMAM in OS cells relative to GFP containing control cells. In HOS and CCHD cells, dnMAM induces a decrease in the expression of the Notch downstream target, Hes1, by over 40% (Figure 10). In order to understand how other Notch downstream targets are affected by dnMAM, we expanded our analysis to quantify the expression of Hes1-5, Hey1-2 and Deltex. Interestingly, the

17

transduction of dnMAM induces a variety of results on Notch downstream target expression in CCHD cells: Hes1 and Hey1 decrease, while Hes2, Hes4 and Hey2 slightly increase (though this increase is not significant). This suggests that there may be other factors regulating the expression of these targets.
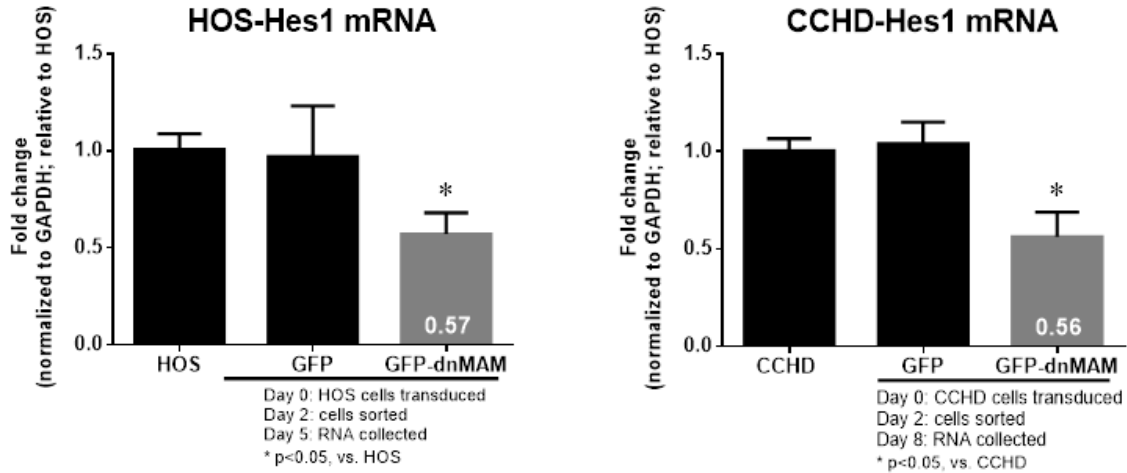


**Figure 10. Inhibiting CSL-dependent Notch signaling using dnMAM decreases the expression of the Notch downstream target, Hes1.**
RTq-PCR was used to quantify the expression of Hes1 in HOS and CCHD OS cells. Results are expressed as fold change relative to GFP control, and are normalized to GAPDH as an internal control. *p≤0.05, bars show mean +/- S.E.M, n=3.

## CCHD- changes in mRNA
## GFP vs. dnMAM1

* p<0.05, vs. GFP
ND- no RNA detected

Y-axis: Fold change (normalized to GAPDH; normalized to GFP)

X-axis: Hes1, Hes2, Hes4, Hes5, Hey1, Hey2, Deltex

Bar values: Hes1: 0.6, Hes2: 1.4, Hes4: 1.6, Hes5: ND, Hey1: 0.7*, Hey2: 1.1, Deltex: ND
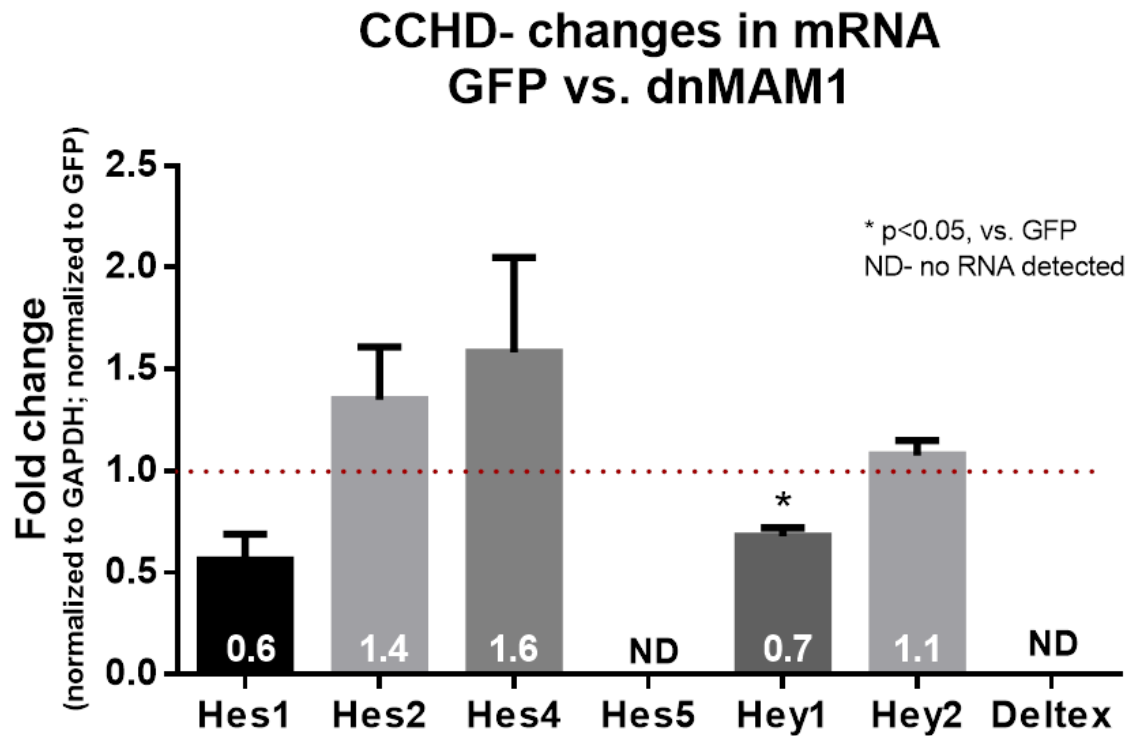
**Figure 11. Inhibiting CSL-dependent Notch signaling using dnMAM differentially affects the expression of Notch downstream target expression.**
RTq-PCR was used to quantify the expression of NDTs Hes1, Hes2, Hes4, Hes5, Hey1, Hey2 and Deltex in CCHD OS cells. Results are expressed as fold change relative to GFP, and are normalized to GAPDH as an internal control. *p≤0.05, bars show mean +/- S.E.M, n=3.

## Summary and Discussion

In this chapter, we showed that dnMAM does not affect OS cell proliferation, cell viability, the formation of colonies, or the invasiveness of OS cells (Figures 6&7). Although dnMAM expression was reported to induce a decrease in tumor burden in an OS subcutaneous model in nude mice (46), we did not observe a decrease in tumor burden using an orthotopic OS model in NSG mice (Figure 9). Orthotopic tumor models are considered more clinically relevant and better predictive models of tumor growth and metastasis than standard subcutaneous models due to the fact that tumor cells are implanted directly into the organ of origin. This allows injected tumor cells to interact with the microenvironment, and better mimics clinical OS. Together, this data suggests that blocking Notch receptor signaling dnMAM may not be a therapeutically beneficial objective in treating Pediatric OS tumors, and perhaps Notch signaling is not as simple as initially predicted.

In this chapter, we also showed that inhibiting Notch receptor signaling using dnMAM can have varying effects on Notch downstream targets (Figure 11). Although Hes and Hey family members are considered Notch downstream targets, they may also be transcriptionally activated by other signaling pathways. For example, there have been several reports that describe Notch-independent transcription of Hes1 by: sonic hedgehog (Shh) (67), activating transcription factor 2 (ATF2) (68), Nanog (69), c-Jun N-terminal kinase (JNK) (70, 71). This suggests that other pathways may play an important role in regulating the expression of Notch downstream targets, and further studies are needed to understand the mechanisms that drive these targets individually. Perhaps targeting a Notch downstream target instead of receptor signaling will be more effective in treating OS.

**CHAPTER 3. Ligand stimulation differentially promotes the activation of Notch downstream targets.**

## Rationale

Because blocking Notch receptor signaling may not be an effective approach in treating Pediatric OS, we sought to better understand Notch signaling both up- and downstream of the Notch receptor.

Notch signaling relies on the intercommunication of two nearby cells. A membrane bound ligand of a signal sending cell interacts with the extracellular domain of a membrane bound Notch receptor on a signal receiving cell to promote a two-step proteolytic cleavage of the receptor. This in turn results in the release and translocation of the intracellular portion of the signal receiving receptor into the nucleus where it promotes the transcription of any number of downstream targets. In the tumor microenvironment, Notch on tumor cells can be self-stimulated (cis activation), stimulated by Notch ligands on other tumor cells (trans-tumor activation), or stimulated by Notch ligands in the microenvironment surrounding tumor cells (trans-microenvironment activation).

To date, most researchers have focused their studies at the receptor level by monitoring the presence or absence of Notch receptors and/or ligands, and by developing genetic and pharmacologic inhibitors that block Notch receptor cleavage or Notch receptor mediated transcription. As seen in Chapter 2, blocking Notch using dnMAM had no effect on tumor growth *in vitro* and *in vivo* and had varying effects on Notch target expression (Figures 6-11).

In this chapter, we investigate how Notch can be activated physiologically using ligand based activation, and we explore how Notch downstream targets (NDTs) can be differentially expressed. Little is known about how the same Notch ligand and the same Notch receptor can induce differential expression of downstream targets. Because of our

observance of variant responses to dnMAM in Chapter 2, we sought to understand how

Notch ligands can produce differing results within the same population of tumor cells.

## Results

**Baseline expression of Notch downstream targets is variable in a panel of OS cell lines.**

        We first examined baseline expression of the NDTs Hes1, Hes2, Hes3, Hes4, Hes5, and Hey1 in a panel of unstimulated human OS cells, and found that unstimulated OS cells express varying levels of all targets investigated (Figure 12). This suggests that NDTs, in the absence of external stimulatory factors as well as in the presence of inhibitory factors like dnMAM (Chapter 2, Figure 11), are variably expressed.
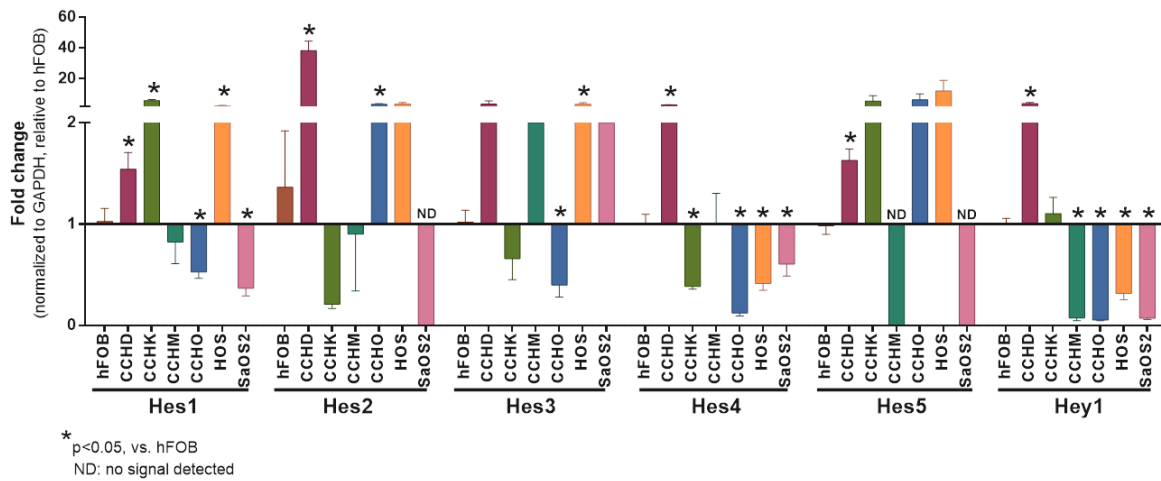


**Figure 12. The expression of Notch downstream targets is variable in a panel of OS cell lines.**
Baseline expression of Hes1, Hes2, Hes3, Hes4, Hes5, and Hey1 in a panel of unstimulated OS cell lines was measured using RTq-PCR, normalized to GAPDH as an internal control, and are expressed as fold change relative to hFOB control. *p≤0.05, bars show mean +/- S.E.M, n=3.

**Notch ligands Jag1 and DLL4 are expressed in low amounts in OS cells.**

We used RTq-PCR to quantify the Notch ligands present in a panel of human OS cell lines. In these OS lines, all 5 canonical Notch ligands were shown to be expressed in low quantities relative to human fetal osteoblasts, with the exception of higher Jag2 in CCHD and higher DLL3 in HOS cells (Figure 13). If OS cells were receiving cis- activation or trans-tumor activation by Jag2 or DLL3, NDTs would be present in unstimulated OS cells. However, because NDTs are low *in vitro*, but present *in vivo,* we focused on ligand stimulation from the tumor microenvironment. We hypothesized that ligands in the vasculature feeding and surrounding the tumor are providing for trans-microenvironmental activation. Vasculature is known to be rich in DLL4 and Jag1 ligands (72). We therefore examined the effect of DLL4 and Jag1 stimulation on NDT expression.
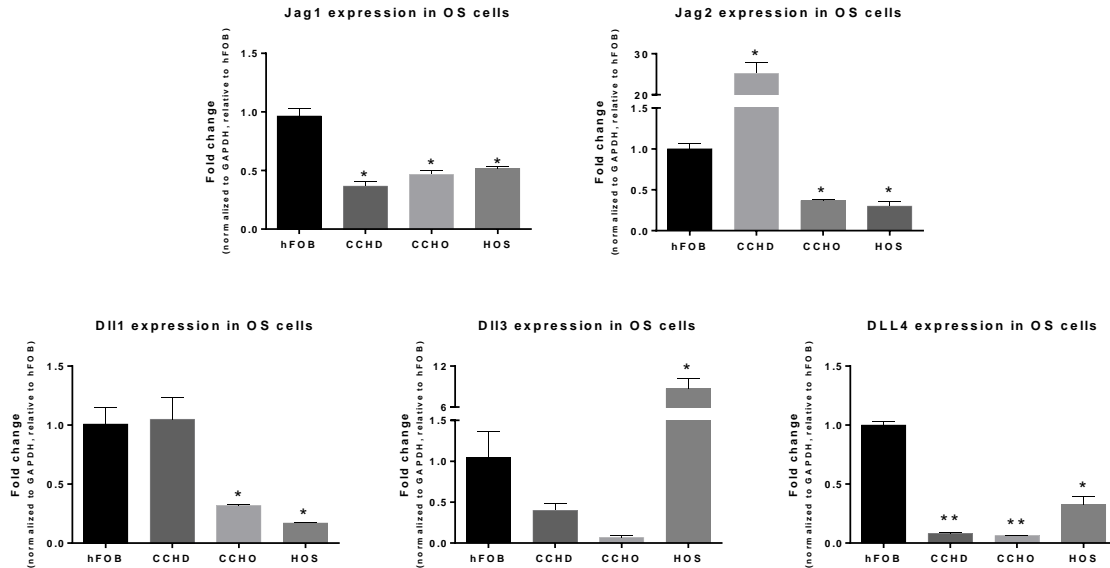


**Figure 13. Expression of Notch ligands in human OS cells lines.**
cDNA was prepared from RNA harvested from unaltered hFOB, CCHD, HOS and CCHO cells. Real-time quantitative polymerase chain reaction (RTqPCR) was done to measure levels of Jag1, Jag2, Dll1, Dll3, and Dll4, normalized to GAPDH, relative to hFOB cells. N=3, error bars= S.E.M., *$p<0.05$, **$p<0.01$.

**Jag1 and DLL4 increase the expression of Hes1, Hes4 and Hey1**

Because Notch is likely activated via trans-microenvironment activation, we decided to focus on Jag1 and Dll4, two ligands that are known to be expressed in tumor vasculature. In order to determine the effect of Jag1 and DLL4 stimulation on OS cells, we used plate bound ligand (2ug/ml) and PCR to quantify the expression of a panel of NDTs after 24hours of stimulation (Figure 14). In HOS and CCHD cells, the transcription of Hes1, Hes4 and Hey1 was increased in response to both Jag1 and Dll4. We focused on Hes1, the standard surrogate marker for Notch activation, and Hes4, which has been shown to be a prognostic factor for response to GSI and therefore may be indicative of OS cell response to Notch pathway modulation, for the following experiments. We next investigated the time and dose response of Hes1 and Hes4 expression to Jag1 or Dll4.
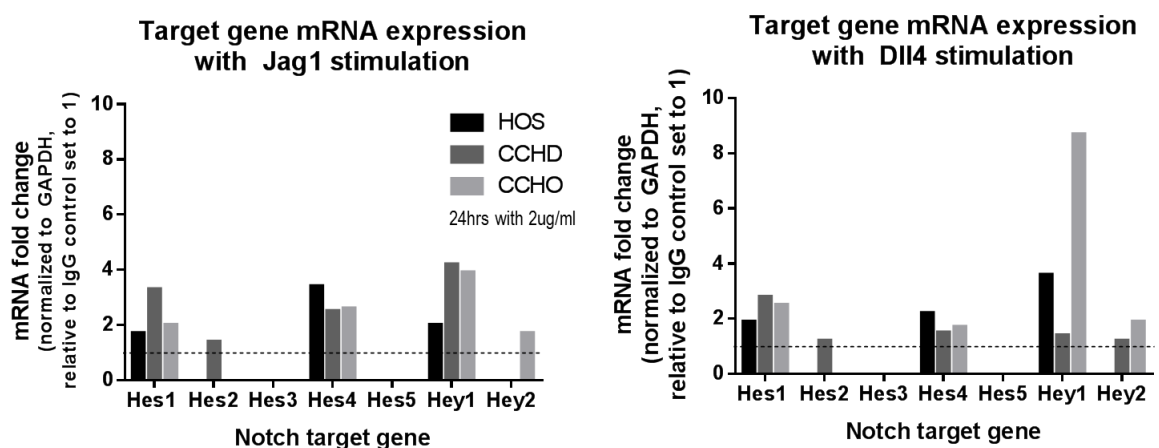


**Figure 14. Plate bound ligand stimulation of human OS cell lines using Jag1 and DLL4.** cDNA was prepared from RNA harvested from HOS cells exposed to either Dll4 or Jag1 (2μg/ml) plate bound ligand for 24 hours. Real-time quantitative polymerase chain reaction (RTqPCR) was done to measure levels of Hes1, Hes2, Hes3, Hes4, Hes5, Hey1 and Hey2, normalized to GAPDH, relative to IgG treated HOS cells. N=3, error bars= S.E.M.

**Hes1 and Hes4 are expressed at different time points after exposure to Dll4.**

In order to determine the kinetics of Jag1 and Dll4 stimulation on the expression of Hes1 and Hes4, we performed RTqPCR on HOS cells that were treated with increasing amounts of plate bound ligand (0.1, 0.5, 1 and 2 ug/ml) over multiple time-points (3, 6, 12, 24 and 48hours). Jag1 elicits a minimal response in the transcriptional expression of both Hes1 and Hes4, while DLL4 promotes significant time and dose dependent increases (only one dose shown; 1μg/ml) (Figures 15).

Interestingly, Hes1 and Hes4 are transcriptionally expressed at different time points in response to DLL4 stimulation (Figure 15). Hes4 peaks early (40-fold increase, 6 hours) in response to DLL4 stimulation, while the peak expression of Hes1 (26-fold increase) is observed at 12hours. This data demonstrates that it is possible to promote differential expression of NDTs despite similar contexts. This data is important because it further demonstrates the complexities within Notch signaling; NDTs are not simply turned on or off in response to ligand. This data suggests that further investigation is needed to more thoroughly understand how the downstream targets of Notch interact with one another and contribute to downstream signaling.
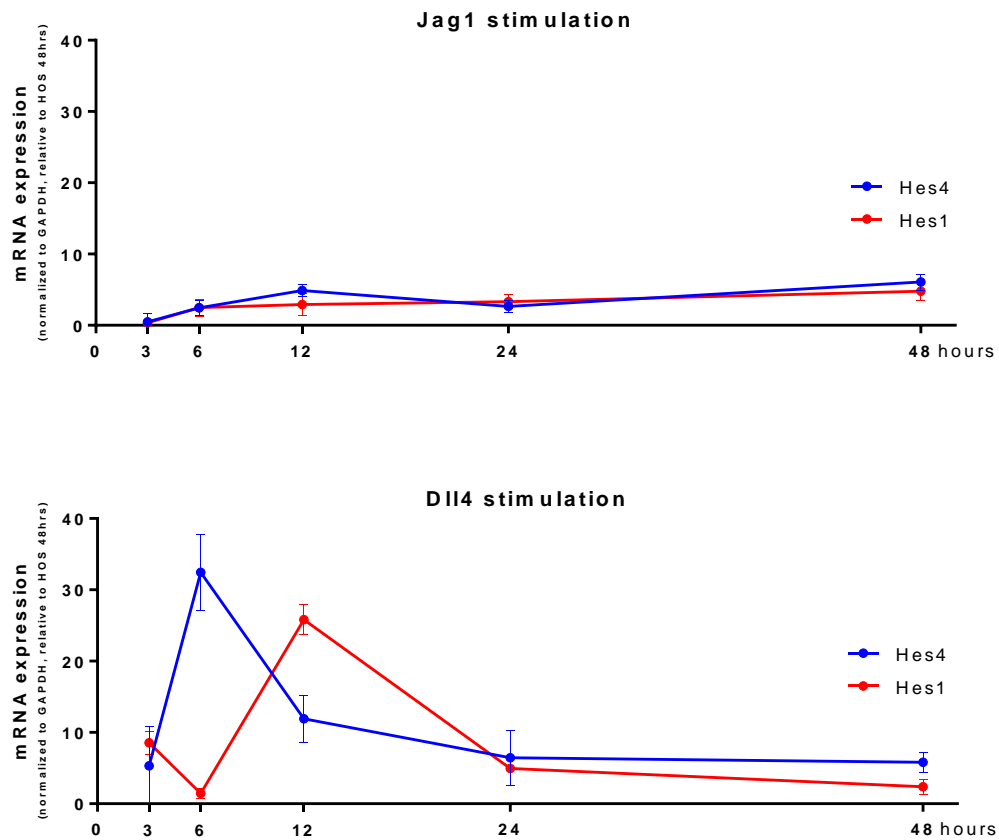
**Figure 15. Expression of Hes4 and Hes1 in HOS cells are more sensitive to DLL4 than Jag1 in response to plate bound ligand stimulation; Hes1 and Hes4 are expressed at different time points after exposure to Dll4.**
cDNA was prepared from RNA harvested from HOS cells exposed to either Dll4 or Jag1 (2μg/ml) plate bound ligand for 3, 6, 12, 24 and 48 hours. Real-time quantitative polymerase chain reaction (RTqPCR) was done to measure levels of Hes1 and Hes4 normalized to GAPDH, relative to IgG treated HOS cells. N=3, error bars= S.E.M.

## Summary and Discussion

In Chapter 2, we demonstrated that dnMAM promotes varying effects on OS NDT expression, with no effect on cell proliferation, invasion, primary tumor growth or the development of metastases *in vivo* (Figures 6-11). In this chapter, we show that Notch ligands are low in OS cells, suggesting trans- microenvironment activation (Figure 13). The microenvironment is made up of tumor vasculature (endothelial cells and pericytes) which is rich in the Notch ligands Dll4 and Jag1 (72-75). Plate bound Jag1 or Dll4 stimulation of human OS cell lines results in a dose and time dependent transcriptional increase of Hes1 and Hes4 (Figure 15). Interestingly, Hes1 and Hes4 expression are more sensitive to Dll4 than Jag1 stimulation (Figure 15). In vasculogenesis, Dll4 and Jag1 undergo complex signaling to promote lateral inhibition in the cells in which they are expressed; Dll4 promotes sprouting on one cell, and acts on Jag1 on nearby cells to inhibit sprouting (76). Because of this, we would hypothesize that tumor cells will be exposed to more Dll4 in vessels (as vessels sprout out and interact with tumor cells), which would corroborate our findings here that Notch downstream targets in OS cells are more sensitive to Dll4 ligand. Another interesting observation is that Hes1 and Hes4 are expressed at different time points (Figure 15) despite exposure to the same ligands for the same amount of time. This suggests that Notch downstream targets are regulated by something beyond the simple cleavage and activation of a Notch receptor by a Notch ligand. This adds yet another layer of complexity to Notch signaling, and allows Notch to become even more attuned to its micro-environment. This also begins to elucidate how Notch downstream targets may be differentially expressed in response to ligand to promote differing functions.

**CHAPTER 4. Notch downstream targets induce varying biological responses.**

**Rationale**

In Chapters 2 and 3, we demonstrated that dnMAM and ligand stimulation with Jag1 or Dll4 can promote different responses in Notch downstream target expression (Figures 11 & 15). We therefore hypothesized that activation of Notch at the receptor level will have a different biologic outcome than the activation of a downstream target of Notch. In this chapter, we seek to understand the effects of Notch downstream targets on proliferation, invasion, and OS patient outcome. We focused on (1) *Hes1*, the standard surrogate marker for Notch activation, and (2) *Hes4*, which has been shown to be a prognostic factor for response to GSI (48), and therefore may be indicative of OS cell response to Notch pathway modulation, because both targets increased upon Notch ligand stimulation (Chapter 3, Figures 14 & 15). This suggests that Hes1 and Hes4 are specific and responsive to Notch receptor signaling.

## Results

**Hes1 decreases proliferation by activating apoptosis while Hes4 does not change proliferation**

In order to understand how Hes1 and Hes4 affect the pathogenesis of OS, we transduced HOS and CCHD human OS cells with GFP containing retroviral MigR1 constructs with and without Hes1 or Hes4 (control: "CCHD/HOS-GFP"; Hes1 overexpressing: "CCHD/HOS-Hes1"; Hes4 overexpressing: CCHD/HOS-Hes4") (Figure 16A&B). The transduction of Hes1 resulted in a 4.7 fold (CCHD; $p<0.01$) and 6 fold (HOS; $p<0.01$) increase in Hes1 mRNA relative to GFP control (Figure 16C). Over-expression of Hes4 resulted in a 72 fold (CCHD; $p<0.01$) and 90 fold (HOS; $p<0.05$) increase in Hes4 mRNA relative to GFP control (Figure 16D). Using the Hes1 or Hes4 over-expression construct, we measured the effect of Hes1 or Hes4 on proliferation when compared to control CCHD/HOS-GFP cells in a competitive proliferation assay.

Interestingly, we observed a decrease in proliferation in CCHD-Hes1 and HOS-Hes1 cells, relative to control, (Figure 17A) but overexpression of Hes4 had no effect on proliferation (Figure 17B). To determine whether the effect of Hes1 on proliferation was due to reduced proliferation or increased cell death, we measured cell cycle and quantified caspase activity (Figure 18). Overexpression of Hes1 enriched the sub G1 population by 50% in HOS cells, indicative of cell death (Figure 18A). To determine if this increase in sub G1 was due to apoptosis, we measured the caspase activity with in cells after 48- and 72-hours post transduction with Hes1 (Figure 18B). Hes1 overexpression induced a 6- and 4-fold increase in caspase activity relative to control HOS-GFP cells, and this increase in caspase

activity was blocked using a pan-caspase inhibitor (Z-VAD). This suggests that increasing

Hes1 expression induces OS cell death via apoptosis.
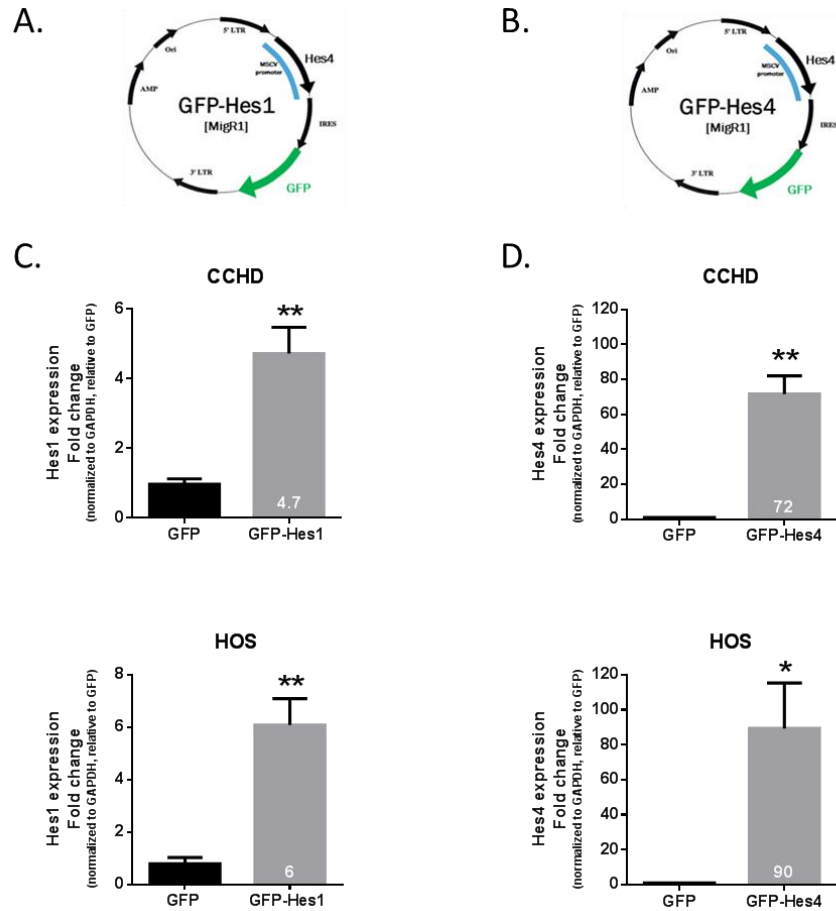


**Figure 16. Hes1 and Hes4 overexpression in CCHD and HOS cells.**
Schematic representation of Hes1 (A) and Hes4 (B) overexpression vector maps depicting the orientation of GFP and Hes1 or Hes4 within the retroviral MigR1 backbone. Expression is controlled by constitutively active 5' LTR promoter. The presence of an IRES causes production of Hes1 or Hes4 and GFP as 2 separate proteins, not a fusion protein.  (C) cDNA was prepared from RNA harvested from HOS and CCHD cells after transduction with GFP or GFP-Hes1. Real-time quantitative polymerase chain reaction (RTqPCR) was done to measure levels of Hes1 normalized to GAPDH, relative to GFP control cells. (D) cDNA was prepared from RNA harvested from HOS and CCHD cells after transduction with GFP or GFP-Hes4. Real-time quantitative polymerase chain reaction (RTqPCR) was done to measure levels of Hes4 normalized to GAPDH, relative to GFP control cells. *p≤0.05, **p ≤0.01, bars show mean +/- S.E.M, n=3.

**A. Hes1 decreases proliferation:**
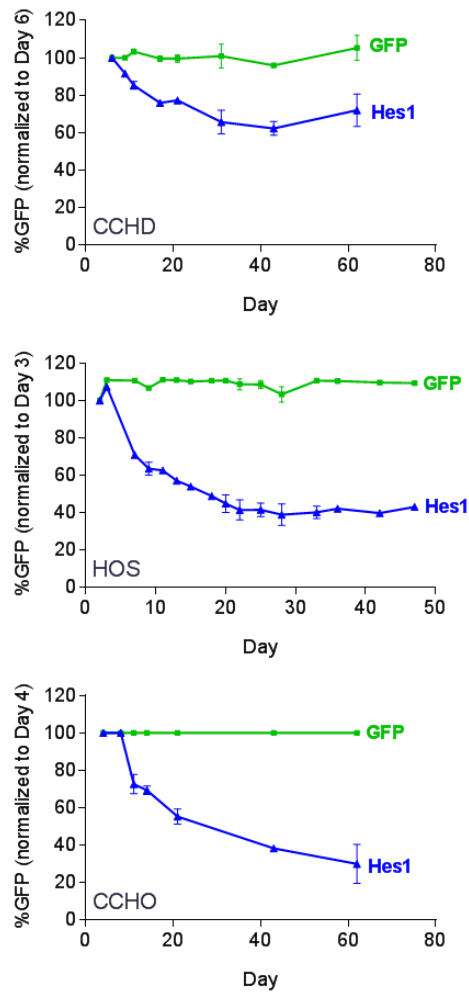
**B. Hes4 does not affect proliferation:**
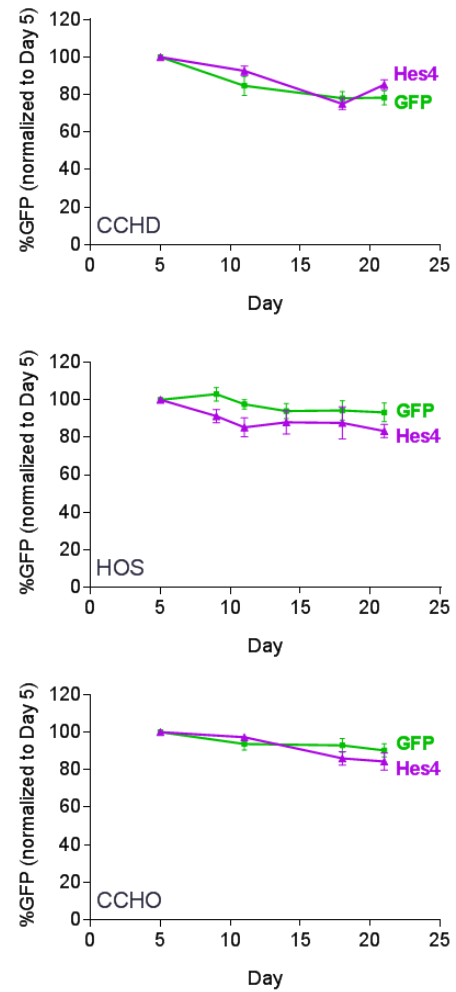
**Figure 17. Opposing roles of Hes1 and Hes4 in proliferation of OS: Hes1 decreases proliferation while Hes4 has no effect.**
Graph of the percentage of GFP+ OS cells (CCHD, HOS and CCHO) over time after stable retroviral transduction of vector alone (GFP) or containing dnMAM (normalized to day 6, 3, and 4, respectively, after transduction). (A) Hes1 decreases the rate of proliferation of HOS, CCHD and CCHO cells relative to control cells in a competitive proliferation assay. (B) Hes4 does not affect the rate of proliferation of HOS, CCHD and CCHO cells relative to control GFP cells in a competitive proliferation assay. N=3 per condition +/- S.E.M.

A.
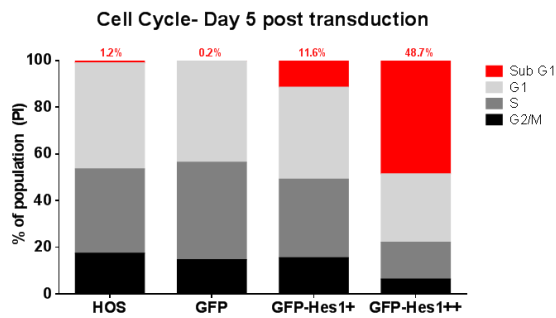


B.
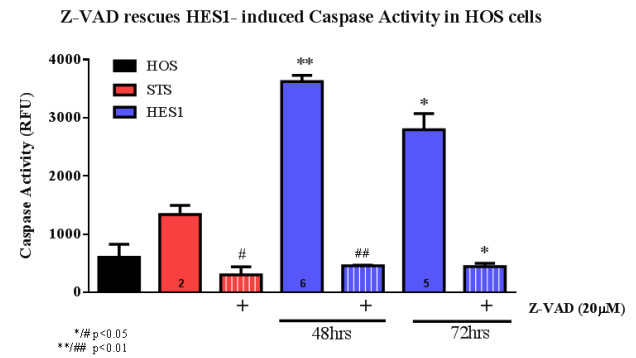


**Figure 18. Hes1 decreases proliferation by activating apoptosis.**
(A) Cell cycle analysis using PI staining on cells overexpressing Hes1 demonstrates the large proportion of cells (48.7%) in Sub G1, indicative of cell death. (B) Hes1 activates caspases 3 and 7 after 48 and 72 hrs post transduction. This activation can be blocked using a pan caspase inhibitor, Z-VAD (20uM).

**Hes1 decreases invasion while Hes4 increases invasion.**

To determine whether Hes1 or Hes4 overexpression affects OS cell migration or invasion, we quantified the number of cells that were able to migrate through Matrigel and traverse an 8-μm pore membrane. In HOS and CCHD cells, Hes1 transduction decreased invasion (Figure 19A), while Hes4 increased invasion (Figure 19B) relative to GFP control cells. This highlights the widely variable outcomes and phenotypes that different Notch downstream targets can promote.

35

A.



Hes1 decreases invasion:

CCHD

HOS
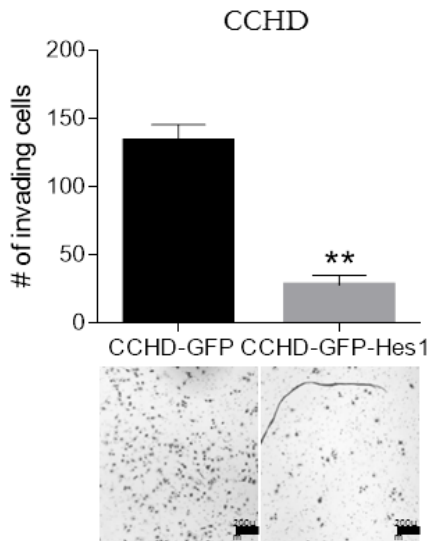
B.



Hes4 increases invasion:

CCHD

HOS
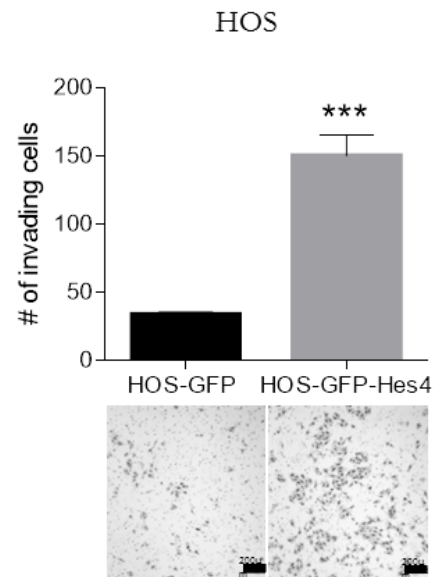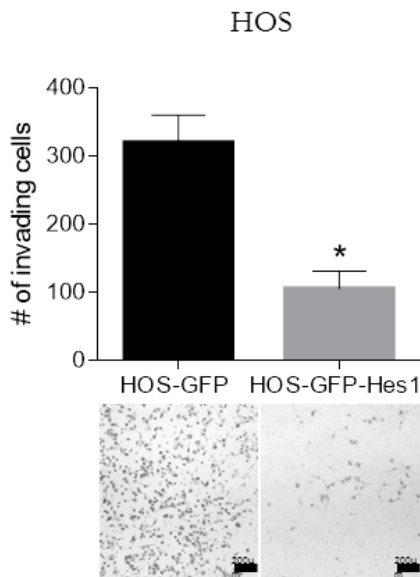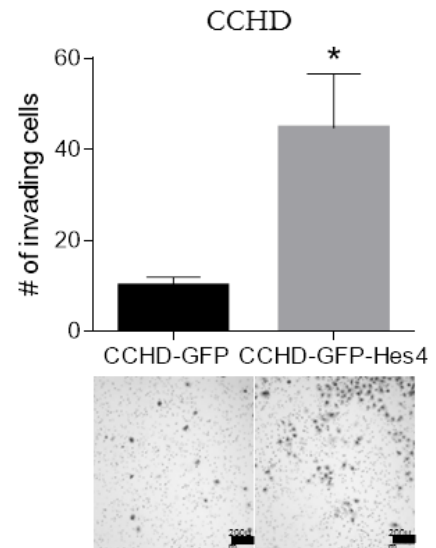
**Figure 19. Opposing roles of Hes1 and Hes4 in invasion: Hes1 decreases invasion while Hes4 increases invasion.**
CCHD and HOS cells were transduced with GFP, GFP-Hes1 (A) or GFP-Hes4 (B) and were sorted for GFP positivity. Invasiveness was measured using a 24-well BD BioCoat Matrigel invasion chamber with an 8-μm pore size (BD Biosciences, San Jose, CA). *p≤0.05, **p ≤0.01, ***p≤0.001, bars show mean +/- S.E.M, n=3.

**High Hes1 decreases the probability of metastases and increases overall survival while High Hes4 increases the probability of metastases and decreases overall survival.**

To determine the roles of Hes1 and Hes4 in the progression of OS in humans, we used the R2 Genomics Analysis and Visualization platform to create gene-based Kaplan-Meier survival curves using a mixed OS database set. Patients with high levels of Hes1 expression in their primary tumors had a significantly higher probability of survival than did those expressing low levels of Hes1 (overall survival: $p < 0.001$; Figure 20). In contrast, patients with high levels of Hes4 expression had a significantly lower probability of survival than did those expressing low levels of Hes4 (overall survival: $p < 0.01$; Figure 20). This patient data correlates with our *in vitro* data where overexpression of Hes1 decreased proliferation, increased apoptosis and decreased the invasive capacity of OS cells. By contrast, overexpression of Hes4 did not alter cell proliferation and increased tumor cell invasion.
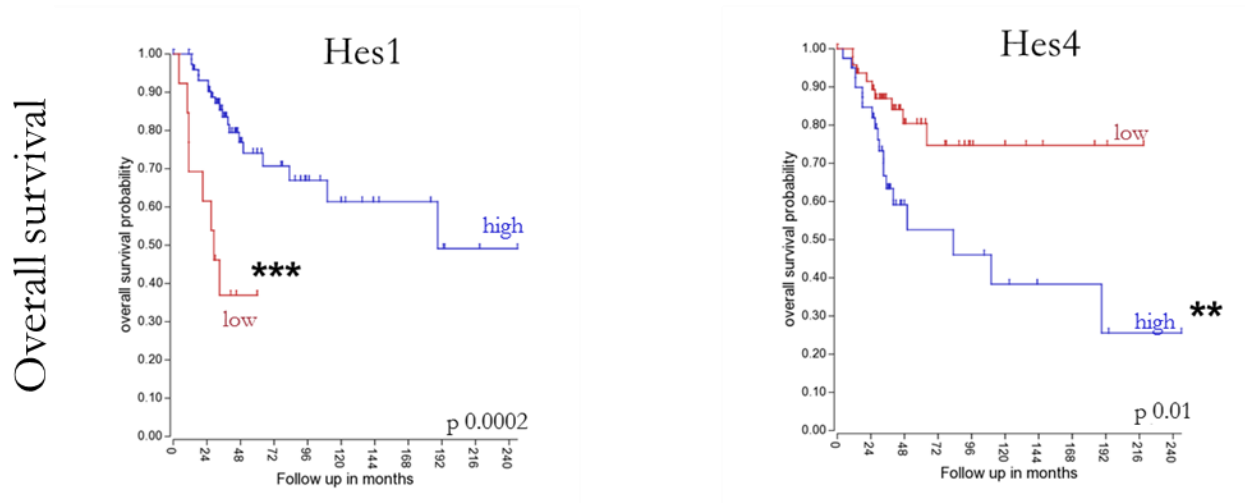
**Figure 20. Opposing roles of Hes1 and Hes4 in patient overall survival: High Hes1 correlates with beneficial outcome while High Hes4 expression correlates with worse patient outcome.**
The R2 Genomics Analysis and Visualization platform (Academic Medical Center, Amsterdam, The Netherlands; R2: Genomics Analysis and Visualization Platform; http://r2.amc.nl) was used to generate Kaplan-Meier overall survival curves using the 'Mixed Osteosarcoma - Kuijjer - 127 - vst - ilmnhwg6v2' dataset (77). Genome-wide gene expression analysis was performed on 84 pre-treatment high-grade osteosarcoma diagnostic biopsies, of which 29 overlapped with the 32 samples used for copy number analysis. Two different sets of control samples were used for comparison: osteoblasts (n=3) and mesenchymal stem cells (n=12, GEO accession number GSE28974). Primary tumors from OS patient samples were analyzed on the basis of High vs Low Hes1 or Hes4. The R2 generated "scan" cut-off modus was used to determine the threshold point that most significantly separates high relative gene expression vs. low relative gene expression. **p ≤0.01, ***p≤0.001.

**Hes1 and Hes4: potential for interaction**

Hes and Hey family members are known to hetero- and homodimerize to form repressive transcriptional complexes (37, 38, 78). Additionally, Hes1 can repress its own expression in a negative feedback loop to help promote oscillatory expression needed for a number of biological processes, for example the "segmentation clock" observed in vertebrate somitogenesis (79). The mechanisms by which Hes4 regulates target expression via hetero-

or homodimerization have not been defined. To determine whether Hes4 regulates Hes1, we
looked at Hes1 mRNA expression levels in HOS, CCHD, and SaOS2 cells that overexpress
Hes4.When Hes4 is overexpressed, Hes1 is significantly decreased (Figure 21). This suggests
that Hes4 may be directly or indirectly regulating Hes1 expression.
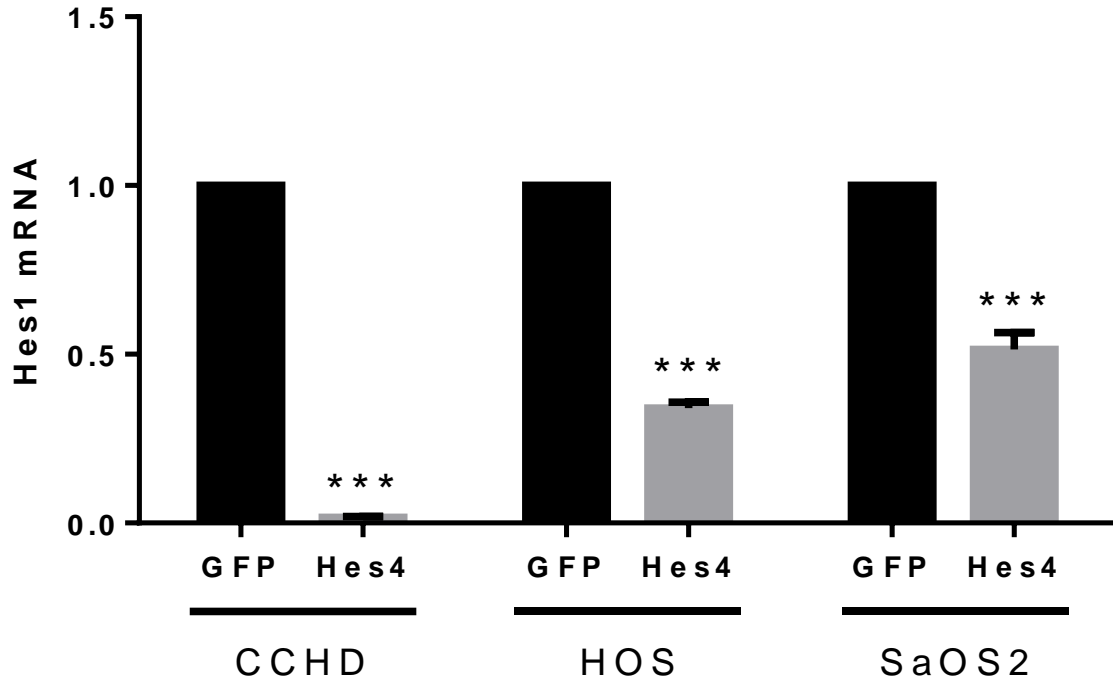


**Figure 21. Hes4 inhibits Hes1 expression**
cDNA was prepared from RNA harvested from HOS, CCHD and SaOS2 cells after
transduction with GFP or GFP-Hes4. Real-time quantitative polymerase chain reaction
(RTqPCR) was done to measure levels of Hes1 normalized to GAPDH, relative to GFP
control cells. ***$p \leq 0.001$, bars show mean +/- S.E.M, n=3.

## Summary and Discussion

Notch signaling can contribute to both oncogenic and tumor suppressive phenotypes within the same tumor type (54-59). Although studies have suggested that Notch plays an oncogenic role in OS (46, 60-62), these studies are limited in that they focus on inhibiting Notch at the receptor level, without considering how increasing Notch (or altering the expression of Notch downstream targets) affects OS tumor growth. In this chapter, we demonstrated that two Notch downstream targets (Hes1 and Hes4) can promote opposing functional outcomes in OS cells. Hes1 acts similar to a tumor suppressor in that it decreases OS cell proliferation by inducing apoptosis, and decreases invasion. High Hes1 expression in the patient primary tumor samples correlated with a superior overall survival (5-year overall survival: Hes1 high 75% versus Hes1 low = 35%; ***p<0.001) (Figures 17A, 18, 19A and 20). By contrast, Hes4 overexpression increased the invasive capacity of OS cells, and high Hes4 expression in patient primary tumors correlated with a significantly worse overall survival (5-year overall survival: Hes4 high 50% versus Hes4 low 80%; **p<0.01) (Figures 17B, 19B and 20). These data clearly indicate that activation of Notch at the receptor level is not the same as the activation of a specific downstream target of Notch. Our data is the first to show that Notch activation can have a dual role in OS. Our data is also the first to suggest that this dual role is secondary to the action of specific downstream targets. These data also underscore the importance of understanding how activation or inhibition of specific Notch downstream targets can affect the physiological properties of tumor cells, and that universal activation or inhibition at the receptor level may not be effectual.

There are multiple ways that Hes1 and Hes4 may be promoting differing outcomes in OS cells. One possibility is that Hes1 and Hes4 are being regulated upstream by differing

signaling pathways. Though both Hes1 and Hes4 expression increases in response to Notch-ligand-receptor mediated activation (Chapter 3, Figure 14 & 15), CSL-mediated inhibition using dnMAM results in variable Notch downstream target expression (40% decrease in Hes1 ($*p<0.05$) and no change in Hes4; Chapter 2, Figure 11). This suggests that Hes1 and Hes4 are both sensitive to, yet not limited to, Notch dependent signaling. Hes and Hey family members may be transcriptionally activated by other signaling pathways. For example, there are numerous reports that describe Notch-independent transcription of Hes1 by: sonic hedgehog (Shh) (67), activating transcription factor 2 (ATF2) (68), Nanog (69), c-Jun N-terminal kinase (JNK) (70, 71). Unfortunately, little is known about what non-Notch mechanisms may contribute to Hes4 expression. Because other pathways may play an important role in regulating the expression of Notch downstream targets, further studies are needed to understand the mechanisms that drive these targets individually.

Another possibility is that Hes1 and Hes4 differ in the targets they transcriptionally regulate. Although Hes1 and Hes4 both bind to the same promoter sequences (N- and E-boxes), Hes1 and Hes4 may be binding to different co-activator/co-repressor complexes to promote or inhibit specific targets. Hes1, for example, is known to complex with: c-myb to repress the transcriptional activation of the CD4 promoter (80), GATA1 to repress GATA1 activity (81), and RunX2 to enhance RunX2 activity by interfering with TLE1 and HDAC recruitment (37, 82-85).

Alternatively, Hes4 may transcriptionally inhibit Hes1. Because Hes and Hey family members are known to hetero- and homodimerize to form repressive transcriptional complexes and regulate each other's transcription (37, 38, 78), we explored the potential relationship between Hes1 and Hes4 and found that when Hes4 is overexpressed in OS, the

RNA expression of Hes1 decreases (Figure 21). This, along with our Dll4 ligand stimulation data (when Hes4 is high, Hes1 is low; Chapter 3, Figure 15), suggests that Hes4 may be repressing the expression of Hes1. To further study the potential transcriptional inhibition of Hes1 by Hes4, a luciferase reporter attached to the Hes1 promoter could be used to determine whether the addition of Hes4 affects Hes1 transcription. We could also use chromatin immunoprecipitation (ChIP) to investigate the interaction between Hes4 and the Hes1 promoter.

Similar to the possibility explained above, Hes4 may transcriptionally inhibit Hes1 by forming an inhibitory heterodimer with Hes1. Because Hes1 is known to repress its own expression via a negative feedback loops (79), and because both Hes1 and Hes4 bind to N- and E-boxes within the promoter region of their target, it is possible that Hes4 is similarly inhibiting the expression of Hes1 via inhibitory heterodimerization. To study whether Hes1 and Hes4 are physically interacting with one another via heterodimerization, we could use co-immunoprecipitation (Co-IP) to investigate the physiologic protein complexes that either Hes1 or Hes4 are involved with. Co-IP could provide insight into the function of the interaction within other biological mechanisms, for example: how Hes1 and Hes4 may interact to promote or prevent differentiation.

Future experiments that explore the relationship between Hes1 and Hes4 and analyze how these targets differ in their signaling are needed.

**CHAPTER 5. Hes4 promotes the growth of primary and metastatic OS.**

**Rationale**

In Chapter 4, we demonstrated that Hes4 promotes invasiveness without increasing proliferation *in vitro* (Chapter 4, Figures 18B & 19B). We also demonstrated that high Hes4 correlates with significantly worse OS patient overall survival (Chapter 4, Figure 20). These data together suggest that overexpression of Hes4 may play an important role in the progression of OS. In this Chapter, we evaluate the effect of Hes4 overexpression on *in vivo* tumor growth, tumor lysis, and the development of metastases using an orthotopic OS tumor model.

## Results

**Overexpression of Hes4 results in increased tumor growth *in vivo*.**

To determine the role of Hes4 in the progression of primary and metastatic OS, we used an *in vivo* CCHD xenograft mouse model (Figure 22). CCHD control cells take an average of 6-8 weeks to develop both primary and metastatic tumors. In contrast to the expected 6-8 weeks, this experiment was terminated after only four weeks post intratibial injection of CCHD-Hes4 cells into mice, due to excessive tumor burden in CCHD-Hes4 tumor bearing mice. Mice injected with CCHD-GFP control cells were also sacrificed at this time for comparison. We used X-ray images to determine the size of the primary tumors at euthanasia and quantified our results using arbitrary units (au). Mice injected with CCHD-Hes4 had significantly larger primary tumors than did the control CCHD-GFP mice (CCHD-GFP control: $38.93 \pm 0.62$ au; CCHD-Hes4 $64.60 \pm 3.86$ au; N=15; p≤0.001) (Figure 23).
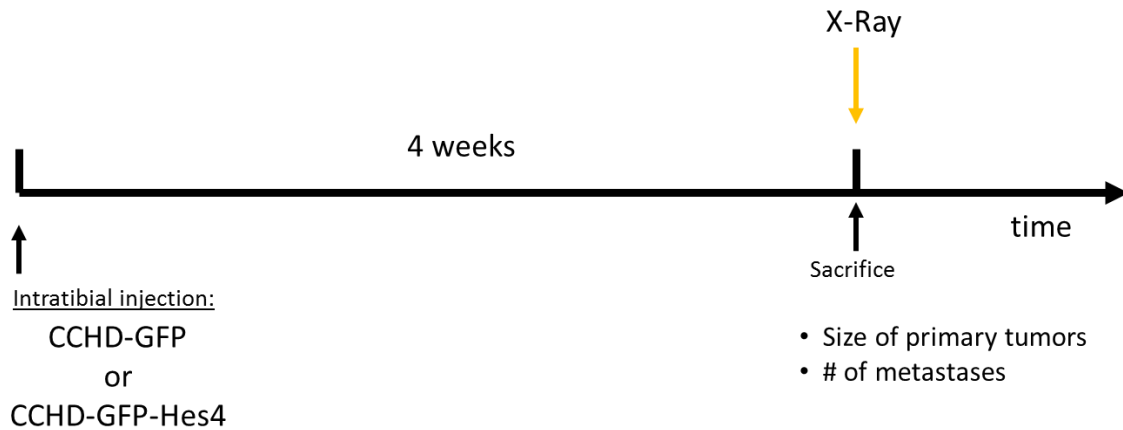


**Figure 22. Schematic diagram of mouse in vivo GFP versus Hes4 experimental design.** CCHD-GFP or CCHD-Hes4 cells ($1 \times 10^6$ suspended in 15 μl of sterile PBS) were injected into the right tibias of 6-week-old NOD/SCID/IL2Rγ-deficient mice. Mice were killed 4 weeks after inoculation due to excessive tumor burden in the CCHD-Hes4 group. Primary tumors and lungs were collected for analysis.
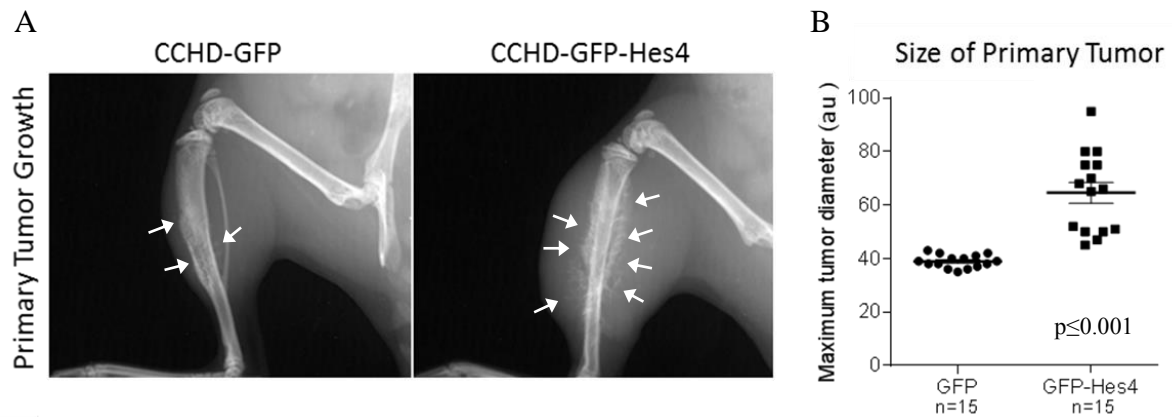
**Figure 23. Hes4 promotes large tumors *in vivo*.**
CCHD-GFP or CCHD-GFP-Hes4 expressing cells were injected orthotopically in NOD/SCID/IL2Rγ-deficient mice. Four weeks after the initial injection, mice were sacrificed, X-ray images were taken (A), and the size of the primary tumors was quantified (B) (au- arbitrary units) ***$p \leq 0.001$, each dot represents one mouse, lines show mean +/- S.E.M, n=15.

## Mice injected with Hes4 overexpressing OS cells develop more metastatic lesions than control mice.

We also evaluated the number of metastases that develop in mice injected with either CCHD-GFP or CCHD-Hes4 expressing cells. Mice injected with CCHD-Hes4 cells had significantly more metastases than did the control CCHD-GFP mice (average $0.60 \pm 0.19$ vs $44.73 \pm 10.58$; $p \leq 0.001$; n=15; Figure 24).
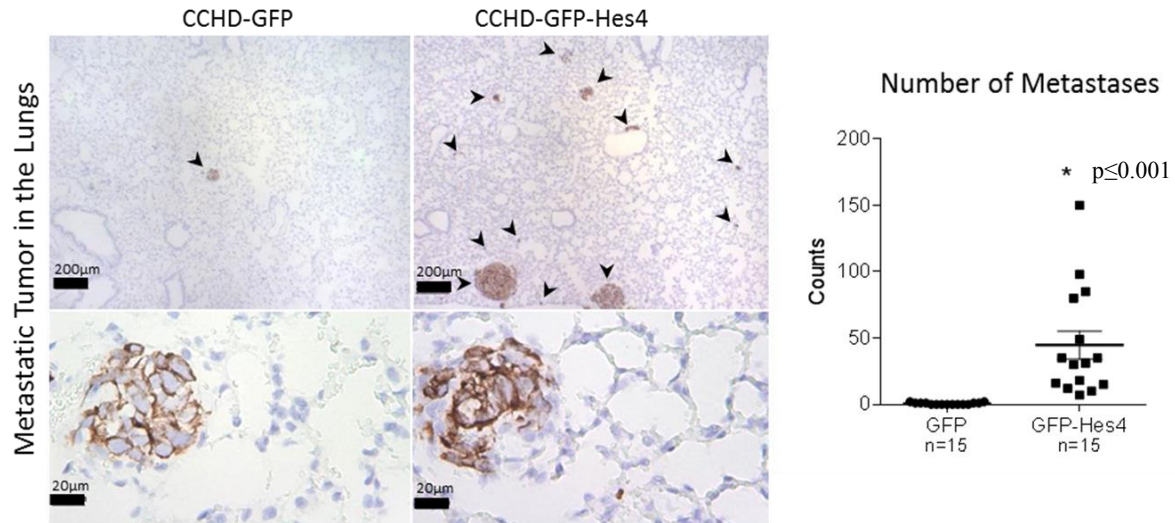
**Figure 24. Overexpression of Hes4 increases metastatic potential.**
Either CCHD-GFP or CCHD-GFP-Hes4 expressing cells were injected orthotopically in NOD/SCID/IL2Rγ-deficient mice. Four weeks after the initial injection, mice were sacrificed, and lung metastases were quantified. ***p≤0.001, each dot represents one mouse, lines show mean +/- S.E.M, n=15.

## Mice injected with Hes4 overexpressing OS cells develop lytic primary tumors independent of RANK/RANKL signaling.

We have demonstrated that the overexpression of Hes4 does not alter cell proliferation (Figure 17B), and increases the invasive capacity of OS cells *in vitro* (Figure 19B). When Hes4 overexpressing cells are injected *in vivo,* both tumor growth and the formation of metastases were accelerated (Figures 23 & 24). Since we showed no change in the proliferation-rate following Hes4 transduction, we hypothesized that the increase in tumor growth and metastatic potential *in vivo* was due to an increased invasive capacity and lytic phenotype.

In order for OS tumors to invade and form metastases, tumor cells must first degrade bone. To quantify the degradation of bone *in vivo,* we used radiographic imaging to measure the extent of bone lysis that occurred in response to CCHD-GFP or CCHD-Hes4 cells. The

extent of bone lysis was quantified using an established osteosarcoma radiographic grading scheme (86). In this scale, a grade of 0 represents no lysis, a grade of 1 represents minimal bone destruction in the medullary canal, a grade of 2 indicates moderate bone lysis within the medullary cortex with minimal destruction to the cortex, a grade of 3 is severe bone lysis with cortical disruption, and a grade of 4 indicates massive destruction with soft tissue extension of the tumor. In mice injected with CCHD-Hes4 cells, we observed a significant increase in bone lysis when compared to CCHD-GFP control injected mice (CCHD-GFP lytic grade $0.9 \pm 0.2$; CCHD-Hes4 lytic grade: $3.0 \pm 0.3$ N=15; p≤0.001; Figure 24).

A known contributor to lytic behavior is interleukin (IL)-1α, a potent cytokine secreted by osteosarcoma cells (19). IL1α promotes the expression of receptor activator of nuclear factor-κB ligand (RANKL) within mature osteoblasts. When RANKL interacts with its receptor, RANK, which is expressed in immature osteoclasts, RANKL allows for the maturation of osteoclast precursors to induce osteoclastic formation (Figure 26) (19, 87). It has been shown that osterix can transcriptionally suppress the expression of IL1α, and can thus inhibit osteolysis by preventing the IL1α/RANKL/RANK mediated maturation of osteoclasts (Figure 26). We investigated whether Hes4 promoted a lytic phenotype by a mechanism involving this IL1α/RANKL/RANK interaction. In cells overexpressing Hes4, however, we did not see any changes in the RNA expression levels of IL1α, RANK and RANKL (Figure 27).
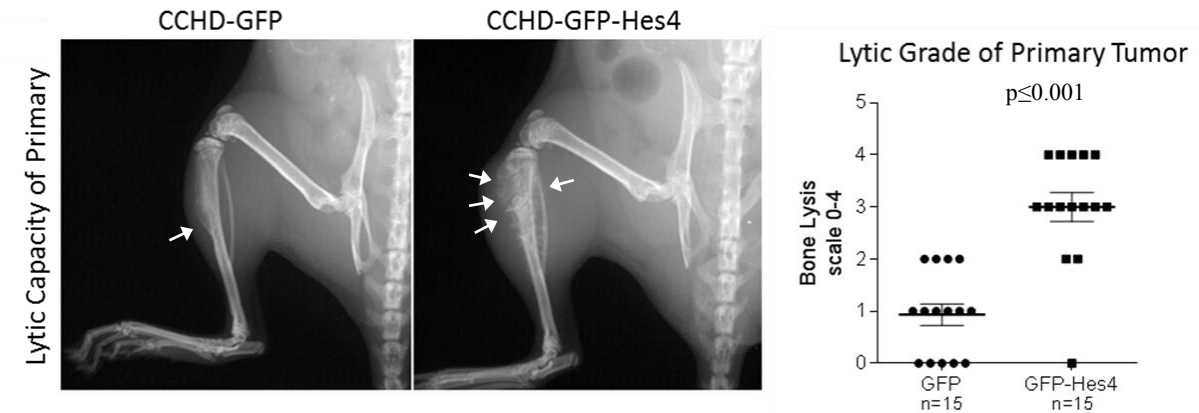
**Figure 25. Hes4 overexpression increases the lytic capacity of tumors *in vivo*.**
CCHD-GFP or CCHD-GFP-Hes4 expressing cells were injected orthotopically in NOD/SCID/IL2Rγ-deficient mice. Four weeks after the initial injection, mice were sacrificed, X-ray images were taken, and the lytic grade of the tumors was quantified using the following system: 0 = no lysis, 1 = minimal bone destruction in the medullary canal, 2 = moderate bone lysis within the medullary cortex with minimal destruction to the cortex, 3 = sever bone lysis with cortical disruption, and 4 = massive destruction with soft tissue extension of the tumor (based on a grading scheme developed by Kristy Weber (86). ***$p \leq 0.001$, each dot represents one mouse, lines show mean +/- S.E.M, n=15.
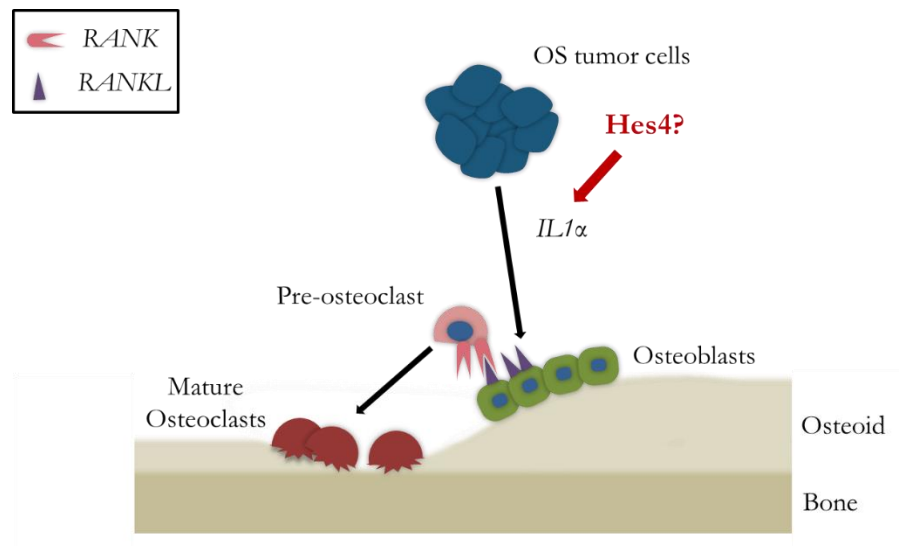


**Figure 26. Schematic depicting the role of IL1α, RANK, and RANKL in the promotion of lysis.**
IL1α is secreted by OS cancer cells, which stimulates the expression of RANKL on the surface of osteoblasts. RANKL on osteoblasts interacts with RANK on the surface of osteoclast precursors to promote the maturation of osteoclasts.
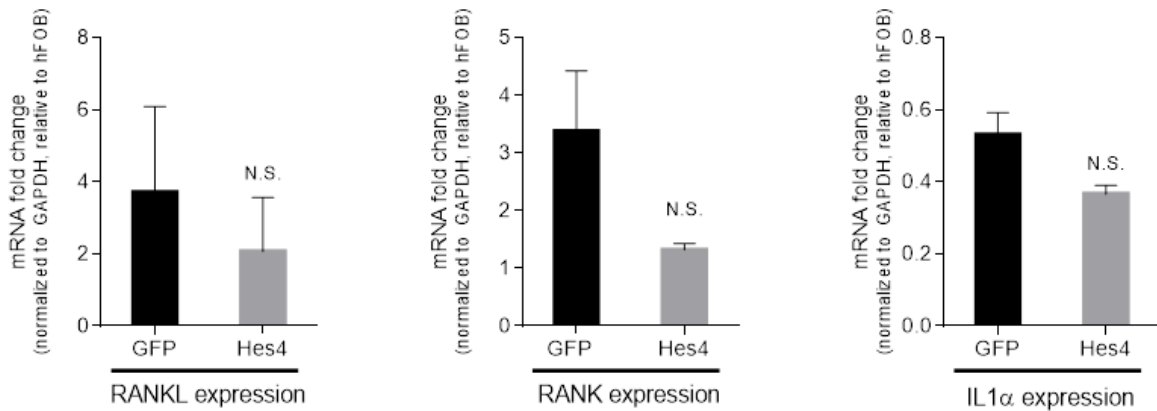
**Figure 27. Hes4 does not change the expression of RANKL/RANK/IL1α in HOS cells.** cDNA was prepared from RNA harvested from HOS cells after transduction with GFP or GFP-Hes4. Real-time quantitative polymerase chain reaction (RTqPCR) was done to measure levels of RANKL, RANK and IL1-α normalized to GAPDH, relative to hFOB control cells. Bars show mean +/- S.E.M, n=3; N.S.= not statistically significant.

**Human patients that express high levels of Hes4 have a higher probability of developing metastases.**

To determine whether Hes4 expression correlates with metastatic rates in human OS patients, we used the R2 Genomics Analysis and Visualization platform to create gene-based Kaplan-Meier survival curves using a mixed OS database set. Patients with high levels of Hes4 expression in their primary tumors had a significantly higher probability of developing metastases ($p < 0.05$) (Figure 28). This correlates with our *in vivo* data and further confirms the relevance of high Hes4 expression in the identification of patients at risk for relapse and poor response.
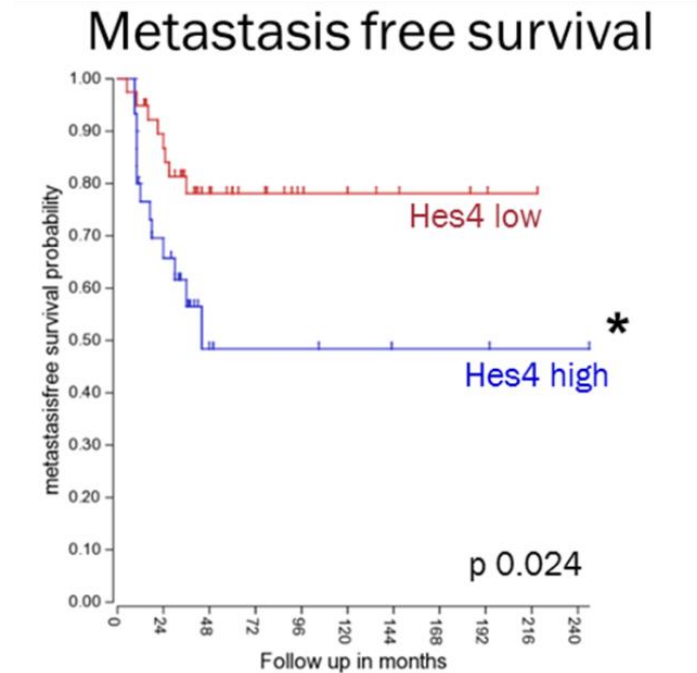
**Figure 28. High Hes4 expression correlates with an increased probability of developing metastases in OS patients.**

The R2 Genomics Analysis and Visualization platform (Academic Medical Center, Amsterdam, The Netherlands; R2: Genomics Analysis and Visualization Platform; http://r2.amc.nl) was used to generate Kaplan-Meier overall survival curves using the 'Mixed Osteosarcoma - Kuijjer - 127 - vst - ilmnhwg6v2' dataset (77). Genome-wide gene expression analysis was performed on 84 pre-treatment high-grade osteosarcoma diagnostic biopsies. Two different sets of control samples were used for comparison: osteoblasts (n=3) and mesenchymal stem cells (n=12, GEO accession number GSE28974). Primary tumors from OS patient samples were analyzed on the basis of High vs Low Hes4. The R2 generated "scan" cut-off modus was used to determine the threshold point that most significantly separates high relative gene expression vs. low relative gene expression. p<0.05.

## Summary and Discussion

To date, the role of Hes4 in OS has not been studied. For the first time, we demonstrate that overexpression of Hes4 significantly affects tumor growth using a human OS orthotopic mouse model. Mice injected with Hes4 overexpressing cells developed significantly larger primary tumors and more metastases than did control mice (Figures 23 & 24). OS tumor cells must first degrade bone in order to invade and form metastases. Because we have shown an increase in the invasive capacity of Hes4 overexpressing cells *in vitro,* we also quantified the lytic grade of Hes4 tumors. We found a significant increase in the lytic capacity of Hes4 overexpression tumors when compared with control tumors (Figure 24). A mechanism known to promote lytic behavior is the IL1α/RANKL/RANK mediated maturation of osteoclasts (19, 88). In cells overexpressing Hes4, however, we did not see any changes in the RNA expression levels of IL1α, RANK and RANKL (Figure 25). Further investigation is needed to understand the mechanisms responsible for the increased lytic phenotype observed in Hes4 overexpressing OS tumors.

Our findings that high expression of Hes4 correlates with a more aggressive phenotype in mice are consistent with decreased metastasis-free survival and overall patient survival. Patients with high levels of Hes4 in the primary tumor had a higher probability of developing metastases and lower overall survival (Figure 28).Our *in vitro, in vivo* and patient data suggest that the overexpression of Hes4 may play a critical role in the progression of OS and in the development of OS metastases. We tried to inhibit Hes4 expression using shRNA and CRISPR/Cas9 to see if blocking Hes4 prevents OS development. We confirmed knockdown in both cases. However, cells would quickly re-express Hes4 despite initial inhibition. This suggests that Hes4 may be necessary for OS survival. Therefore at this time

we cannot conclude that Hes4 is necessary for OS progression. If Hes4 is indeed necessary for OS, therapeutic development to target Hes4 may result in better inhibition of OS than inhibition of the Notch receptor signaling.

In conclusion, our data suggests that Hes4 plays a critical role both in the progression of OS and in the development of metastases. Our data also suggest that Hes4 may be the mediator of Notch promotion of OS tumor growth.

**CHAPTER 6. Hes4 overexpression prevents terminal differentiation and the progression from committed osteoprogenitor to early osteoblast.**

**Rationale**

In Chapter 5, we demonstrated that Hes4 significantly increased the size and lytic capacity of OS primary tumors and increased the number of metastatic lesions *in vivo* (Chapter 5, Figure 23-25), which correlated with a higher probability of developing metastases and worse patient outcome (Figure 28). In this Chapter, we examine the mechanisms that may drive this aggressive tumor phenotype. The formation of primary and metastatic osteosarcoma relies on a number of distinct biological processes. In order for a tumor to develop, there must be a tumor initiating event that allows for uncontrolled cellular regulation. One such mechanism relies on the disruption of osteogenic differentiation, which could not only lead to the initiation of OS, but may also promote the progression of OS into metastatic spread. Defects of osteogenic differentiation can occur at any stage within the differentiation process; defects at early stages within the differentiation process are believed to lead to the development of more undifferentiated and aggressive OS, while defects at later stages may lead to the development of more differentiated and less aggressive OS (89). It has also been shown that undifferentiated tumor cells (stem-like cancer cells) may be more likely to metastasize and develop drug resistance due to their greater abilities to self-renew, active DNA repair, higher expression of drug transporters and resistance to apoptosis (90). In Chapter 5, we demonstrated that mice injected with OS cells that overexpress Hes4 have larger more lytic primary tumors and more metastases than control mice; this may be the result of dysregulation osteogenic differentiation.

As described in Chapter 1 ("Normal Bone Development and Homeostasis"), bone formation relies on a multistep differentiation pathway in which various transcription factors control the progression from an immature stem-like state (MSC) through osteogenic lineage

commitment to terminal differentiation into osteoblasts/osteocytes (8-17). This process is defined and regulated by the presence or absence of a number of transcription factors and can be divided into 4 main stages (Chapter 1, Figure 2; Reprinted below as Figure 29). The first stage, "pluripotency," is comprised of pluripotent MSCs which are characterized by the expression of Nanog, Sox2 and Oct4. The second stage is comprised of committed osteoprogenitors and is induced by the expression of RunX2 and osterix. These transcription factors promote the commitment of pluripotent mesenchymal stem cells into the osteogenic pathway, and are key transcriptional switches that allow for proper osteogenic differentiation. Committed osteoprogenitors differentiate into early and mature osteoblasts, which give rise to bone forming osteocytes during the third and final stage which is characterized by the expression of alkaline phosphatase, osteopontin, and osteocalcin. This final stage of differentiation results in the deposition of osteoid, a matrix that allows for bone formation.

The role of Hes4 in bone differentiation remains poorly defined. Cakouros *et al*. have previously shown that Hes4 promotes the differentiation of bone marrow stromal cells into osteoblasts by interacting with Twist1 to release RunX2 and promote the expression of osterix, thus inducing the progression of the differentiation pathway toward mature osteoblasts (27). Although Hes4 was shown to promote differentiation in normal bone marrow stromal cells, we demonstrated in Chapter 5 that the overexpression of Hes4 in OS tumor cells leads to a more malignant phenotype in mice, and high expression of Hes4 correlates with worse outcome in human OS patients (Figures 23-25, 28). Because of this, we hypothesize that overexpression of Hes4 may inhibit differentiation in tumor cells which in turn promotes a more aggressive phenotype. In this Chapter, calcium staining and the

quantification of key differentiation transcription factors was used to determine the effect of

Hes4 overexpression in the differentiation of OS.

For reader convenience, Chapter 1, Figure 2 is re-printed here:
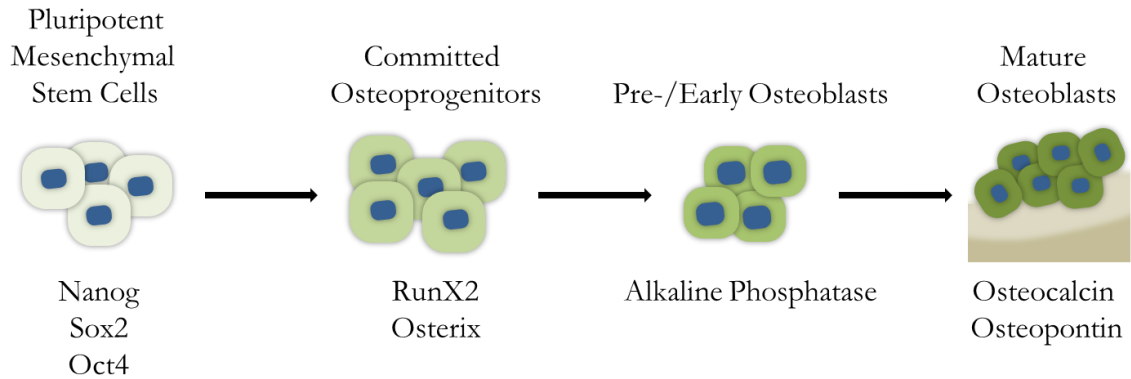


**Figure 29. A schematic of normal osteogenic bone differentiation and associated transcription factors.**
This process is defined and regulated by the presence or absence of a number of transcriptions factors and can be divided into 4 main stages: pluripotency, osteogenic commitment, pre/early osteoblast, and maturation.

## Results

**Hes4 decreases calcium deposition.**

The development of OS is caused by genetic and epigenetic disruptions of osteogenic terminal differentiation. Human OS tumors are extremely heterogeneous, and can contain populations of cells that represent all stages of the osteogenic differentiation pathway, ranging from highly differentiated to undifferentiated phenotypes (11). The quantification of calcium deposition is a commonly used method to determine the extent of osteogenic differentiation. More calcium indicates more differentiation into mature osteoblasts. We measured calcium deposition using alizarin red staining to determine the effect of Hes4 overexpression on osteoid production in OS cells treated with osteogenic differentiation-inducing media. HOS and CCHD human OS cells were transduced with GFP containing retroviral MigR1 constructs with and without Hes4 (Chapter 4, Figure 16). HOS-GFP cells developed calcium nodules more slowly than CCHD-GFP cells (21 days vs. 9 days; data not shown). This demonstrates the heterogeneity of OS cells. In addition to dark red points of thick calcium buildup, a thin layer of a calcium sheet can be seen, shown in Figure 30A as a smooth bright red surface. This suggests that differentiation media is able to successfully induce the differentiation of control GFP OS tumor cells into mature, calcium producing osteoclasts. Interestingly, despite the presence of differentiation media, HOS-Hes4 OS cells have significantly fewer calcium nodules, and almost no calcium sheets when compared to the GFP control cells (GFP: 133.7±11.7 nodules; GFP-Hes4: 27.7±7.2 nodules; **p=0.0015; Figure 30B). This suggests that Hes4 overexpression prevents calcium deposition and differentiation. Calcium deposition is dependent on the presence of differentiated, mature osteoblasts and osteocytes. The overexpression of Hes4 almost completely abrogated calcium

deposition. This indicates that the differentiation of immature tumor cells is inhibited when

Hes4 is overexpressed. We next evaluated the stage at which Hes4 overexpression inhibited

differentiation using RTq-PCR to quantify the expression of key mediators of differentiation.
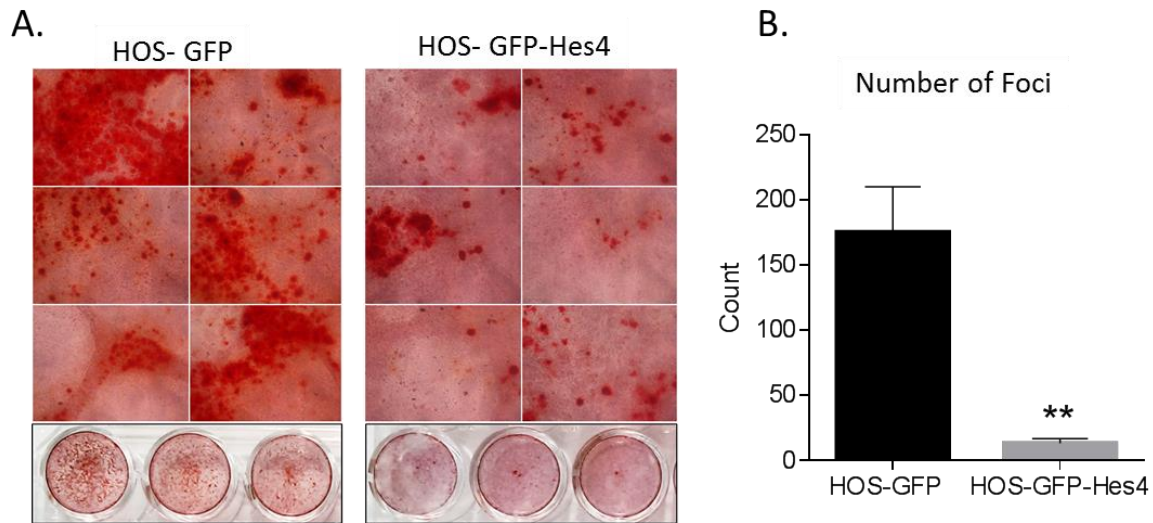


**Figure 30. Hes4 over-expression decreases calcium deposition in human OS cells.**
Alizarin Red (Calcium deposition) staining was performed on HOS-GFP or HOS-GFP-Hes4
cells after 21 days in differentiation media. (A) Representative images are shown. (B). Mean
number of foci per well +/- S.E.M., n=3. **p ≤0.01

**Hes4 increases markers of pluripotency and osteogenic commitment (Nanog, Sox2,**

**Oct4, RunX2 and Osterix) and decreases markers of pre-osteoblasts and maturation**

**(Alkaline Phosphatase and Osteocalcin).**

The multistep progression of MSCs to terminally differentiated osteocytes is well

established and defined by the presence or absence of various transcription factors (Figure

33). To determine the stage of differentiation at which Hes4 overexpressing cells are

arrested, we quantified the change in transcriptional expression of proteins that are indicative

of MSCs (Nanog, Sox2, and Oct4), committed osteoprogenitors/preosteoblasts (RunX2 and osterix), early osteoblasts (alkaline phosphatase), and mature osteoblasts and osteocytes (osteocalcin and osteopontin) in control or Hes4 over-expressing cells. In HOS cells, Hes4 overexpression resulted in increased Nanog, Sox2, Oct4, RunX2, and osterix RNA levels (Figures 31 & 32) and decreased alkaline phosphatase and osteocalcin (Figure 33). In CCHD cells, Oct4 is increased by Hes4 overexpression, but Nanog and Sox2 are decreased. The fold change increase in RunX2 and Osterix are much higher in CCHD cells than those seen in HOS cells that overexpress Hes4 (8- and 120- fold in CCHD, 1.8 and 1.5-fold in HOS, respectively). As evidenced by our studies described above, time to differentiation takes longer in HOS cells than CCHD cells. These differences in gene expression, along with the calcium deposition data in Figure 30, suggest that HOS cells are less differentiated than CCHD cells and are stalled at the *progenitor state* while CCHD cells are blocked at the stage of *osteogenic commitment*. Overall, our differentiation gene expression data indicate that there is a block in the maturation of osteoblasts (neither cell line progressed beyond the pre-osteoblastic stage) when Hes4 is over-expressed.

# Markers of Pluripotency
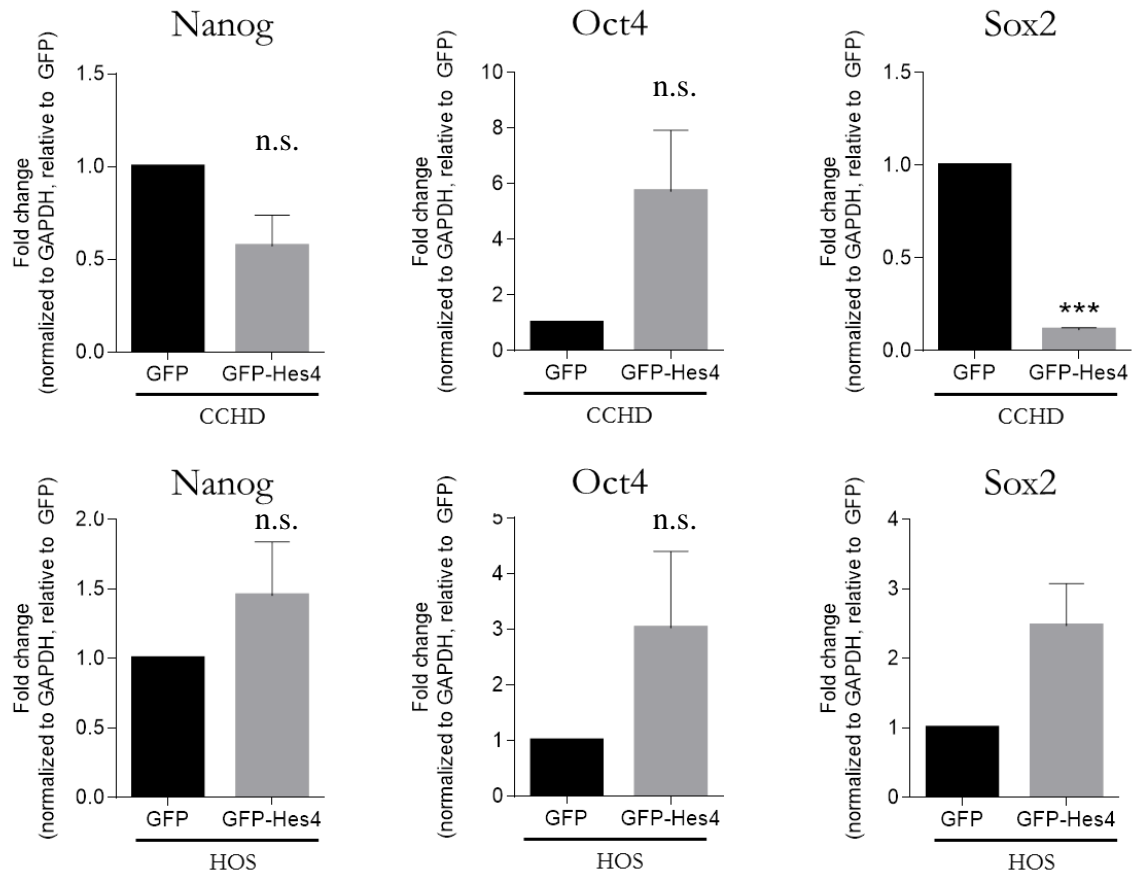


**Figure 31. Effect of Hes4 overexpression on the expression of transcription factors involved in pluripotency.**

cDNA was prepared from RNA harvested from CCHD and HOS cells 3-5 days after transduction with GFP or GFP-Hes4. Real-time quantitative polymerase chain reaction (RTqPCR) was done to measure levels of Nanog, Oct4, and Sox2, normalized to GAPDH, relative to GFP control cells

***n.s. is not significant, $p \leq 0.001$, bars show mean +/- S.E.M, N=3.

# Markers of Osteogenic Commitment
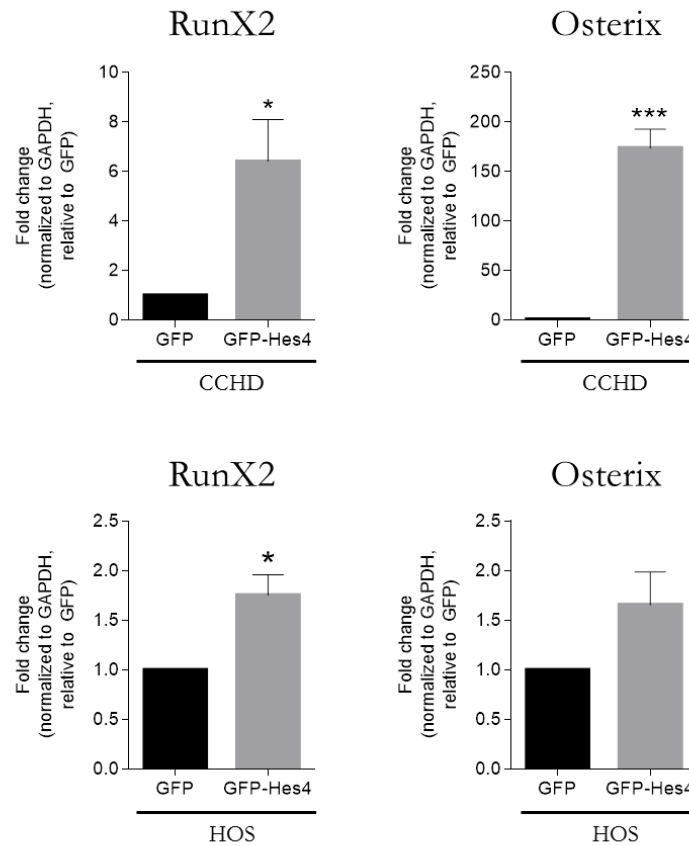


**Figure 32. Hes4 overexpression results in the increase of the RunX2 and Osterix transcription factors involved in osteogenic commitment.**
cDNA was prepared from RNA harvested from CCHD and HOS cells 3-5 days after transduction with GFP or GFP-Hes4. Real-time quantitative polymerase chain reaction (RTqPCR) was done to measure levels of RunX2 and osterix, normalized to GAPDH, relative to GFP control cells.
*p≤0.05, ***p≤0.001, bars show mean +/- S.E.M, N=3.

# Pre-Osteoblasts    Markers of Maturation
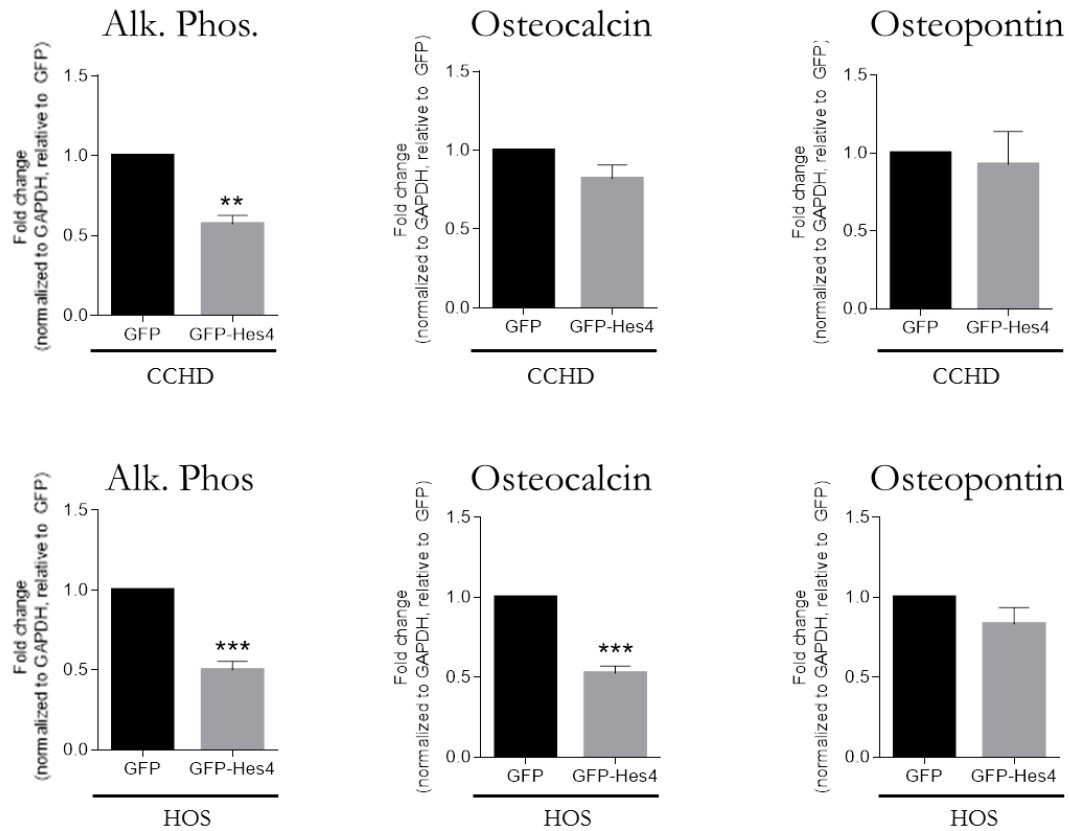


**Figure 33. Hes4 overexpression results in the decreased expression of pre-osteoblasts and maturation**

cDNA was prepared from RNA harvested from CCHD and HOS cells 3-5 days after transduction with GFP or GFP-Hes4. Real-time quantitative polymerase chain reaction (RTqPCR) was done to measure levels of Alkaline Phosphatase, Osteocalcin and Osteopontin, normalized to GAPDH, relative to GFP control cells. $**p \leq 0.01$, $***p \leq 0.001$, bars show mean +/- S.E.M, n=3.

**Overexpression of Hes4 inhibits the expression of alkaline phosphatase in response to differentiation media.**

Because OS tumor cells are inherently immature, one might expect to see an already high baseline level of MSC markers (Nanog, Sox2, and Oct4) and markers of committed osteoprogenitors/preosteoblasts (RunX2 and osterix). With naturally low expression of drivers of early osteoblasts (alkaline phosphatase) and mature osteoblasts and osteocytes (osteocalcin and osteopontin). To confirm that overexpression of Hes4 can block differentiation, we treated HOS and CCHD GFP and Hes4 overexpressing cells with differentiation media. RNA was isolated at time points half way to differentiation (day 4 for CCHD and day 9 for HOS), and the expression of alkaline phosphatase was quantified using RT-qPCR. Even in the presence of media that triggers differentiation, the overexpression of Hes4 inhibited the increase in alkaline phosphatase, a key factor that is synonymous with terminal osteogenic differentiation (Figure 34).
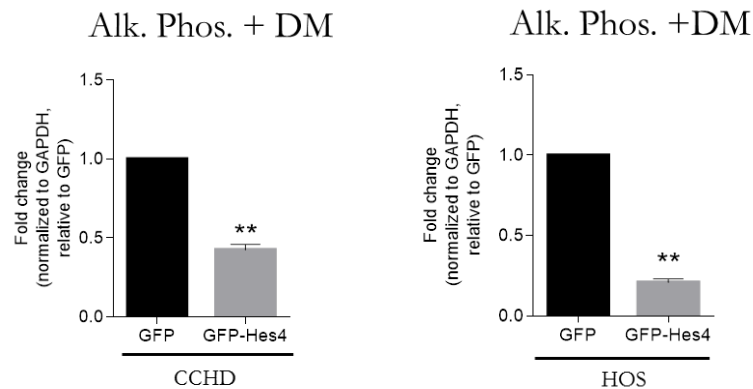


**Figure 34. Hes4 overexpression results in decreased of alkaline phosphatase expression in the presence of differentiation media.**
cDNA was prepared from RNA harvested from CCHD and HOS cells 10-15 days after transduction with GFP or GFP-Hes4, incubated with differentiation media for 4 (CCHD) or 9 days (HOS). Real-time quantitative polymerase chain reaction (RTqPCR) was done to measure levels of Alkaline Phosphatase, normalized to GAPDH, relative to GFP control cells **p $\leq$ 0.01, bars show mean +/- S.E.M, N=3.

**High RunX2 and Osterix, similar to high Hes4, correlate with poor patient outcome**

High Hes4 expression correlates with a higher probability of developing metastases and a lower overall survival (Chapter 4, Figure 20 & Chapter 5, Figure 28). If increased Hes4 blocks differentiation resulting in sustained increase in RunX2 and osterix, and if differentiation is indeed linked to worse patient outcome, then high expression of RunX2 and osterix, should also correlate with worse patient outcome. To determine whether RunX2 and osterix correlate with prognosis, we used the R2 Genomics Analysis and Visualization platform to generate gene-based Kaplan-Meier survival curves based on gene expression within pretreatment, high grade, OS biopsies using a mixed OS database set. Patients with high levels of RunX2 or osterix expression in their primary tumors had a significantly higher probability of developing metastases (p<0.05) and a significantly worse overall survival, similar to high Hes4 expression (Figure 35). This corroborates our findings *in vitro* and suggests that high He4 in the primary tumor results in high RunX2 and osterix, a less differentiated tumor phenotype and a poor patient prognosis. This also suggests that differentiation status may indeed play an important role in the aggressiveness of OS (91). Furthermore, RunX2 expression has been shown to correlate with poor response to chemotherapy in OS (92), which suggests that RunX2 has both clinical and prognostic significance in OS.
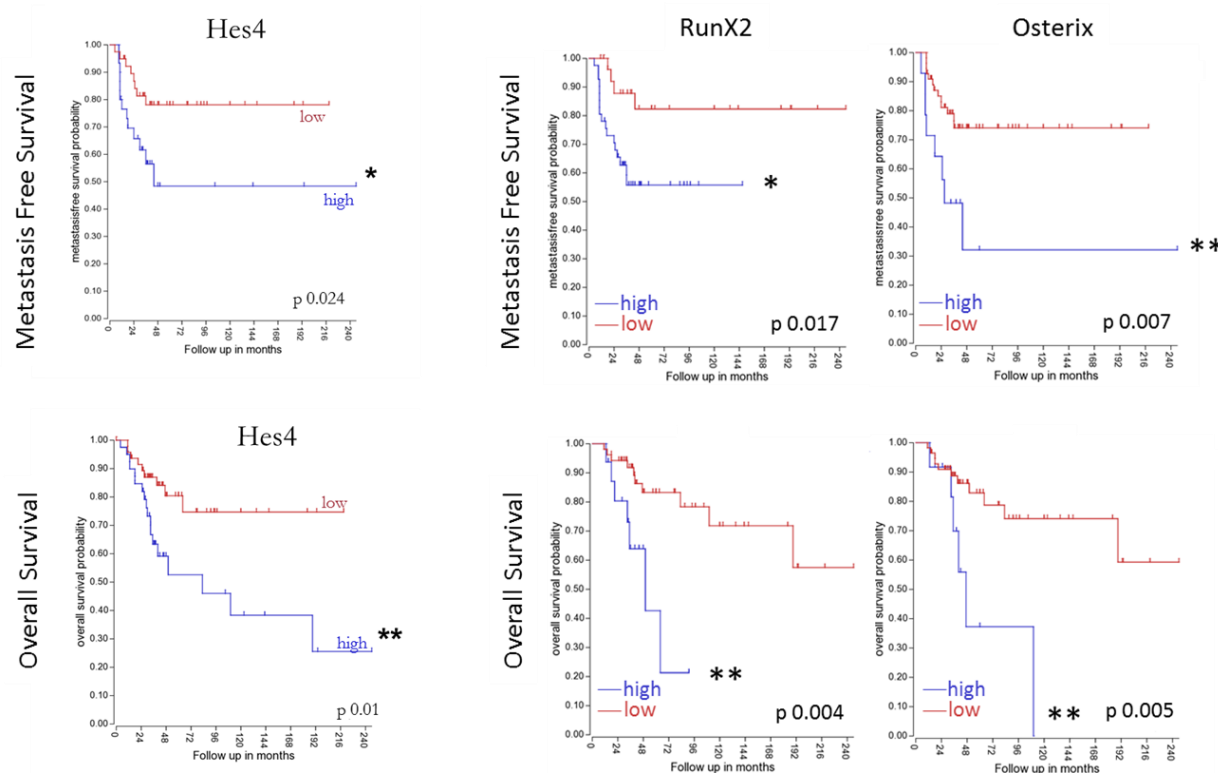
**Figure 35. High expression of Hes4, RunX2 or Osterix correlates with worse patient outcome.**

The R2 Genomics Analysis and Visualization platform (Academic Medical Center, Amsterdam, The Netherlands; R2: Genomics Analysis and Visualization Platform; http://r2.amc.nl) was used to generate Kaplan-Meier overall survival curves using the 'Mixed Osteosarcoma - Kuijjer - 127 - vst - ilmnhwg6v2' dataset (77). Genome-wide gene expression analysis was performed on 84 pre-treatment high-grade osteosarcoma diagnostic biopsies, of which 29 overlapped with the 32 samples used for copy number analysis. Two different sets of control samples were used for comparison: osteoblasts (n=3) and mesenchymal stem cells (n=12, GEO accession number GSE28974). Primary tumors from OS patient samples were analyzed on the basis of High vs Low Hes4, RunX2, or Osterix. The R2 generated "scan" cut-off modus was used to determine the threshold point that most significantly separates high relative gene expression vs. low relative gene expression. Patients with high levels of Hes4, RunX2 or Osterix expression have a higher probability of developing metastases and a significantly lower probability of overall survival than did those expressing low levels of Hes4, RunX2, or Osterix (Metastasis Free Survival: Hes4 p<0.05, RunX2 p<0.05, Osterix p<0.01; Overall Survival: Hes4 p<0.01, RunX2 p<0.01, Osterix p<0.01).

**Hes4 may be a prognostic factor and/or predictive biomarker of tumor response in the patients with OS.**

The current standard of care in treating newly diagnosed osteosarcoma patients involves 10-12 weeks of preoperative chemotherapy (high-dose methotrexate, doxorubicin, and cisplatin; MAP), followed by surgery and then several more months of postoperative chemotherapy (4). To date, the single most important prognostic factor in determining OS patient outcome is the histological response to preoperative chemotherapy within the surgically resected tumor, which cannot be determined until 10-12 weeks after the initial diagnosis (5-7). A good histological response is defined as >90% necrosis in a resected tumor specimen. In patients with good histological response, the 5-year survival is 70-80% while the 5-year survival for poor responders (those with <90% tumor necrosis) is 30-60% (5-7). Biological biomarkers such as p53, VEGF, and HIF1-α expression in the primary tumor at the time of diagnosis have been studied as potential prognostic and/or predictive factors for OS. To date, however, a biomarker with high enough specificity or sensitivity to be clinically relevant has not been identified (93-97).

Because high Hes4 contributes significantly to the pathogenesis and progression of OS, and because tumor response to neoadjuvant chemotherapy correlates with patient outcome, we hypothesized that low Hes4 expression may act as a predictor of good response to chemotherapy. Indeed, the overall survival of patients that were good responders (>90% necrosis) in the recently published international European and American Osteosarcoma Study (EURAMOS; results presented at the annual meeting of the Connective Tissue Oncology Society Annual Meeting, Berlin, Germany, 2014), and the overall survival of patients that express low levels of Hes4 in the tumor at the time of diagnosis are superimposable (Figure

36). This suggests that Hes4 expression in the primary tumor before neoadjuvant

chemotherapy is a potential prognostic biomarker to identify good responders, and also poor

responders and those at high risk for relapse.
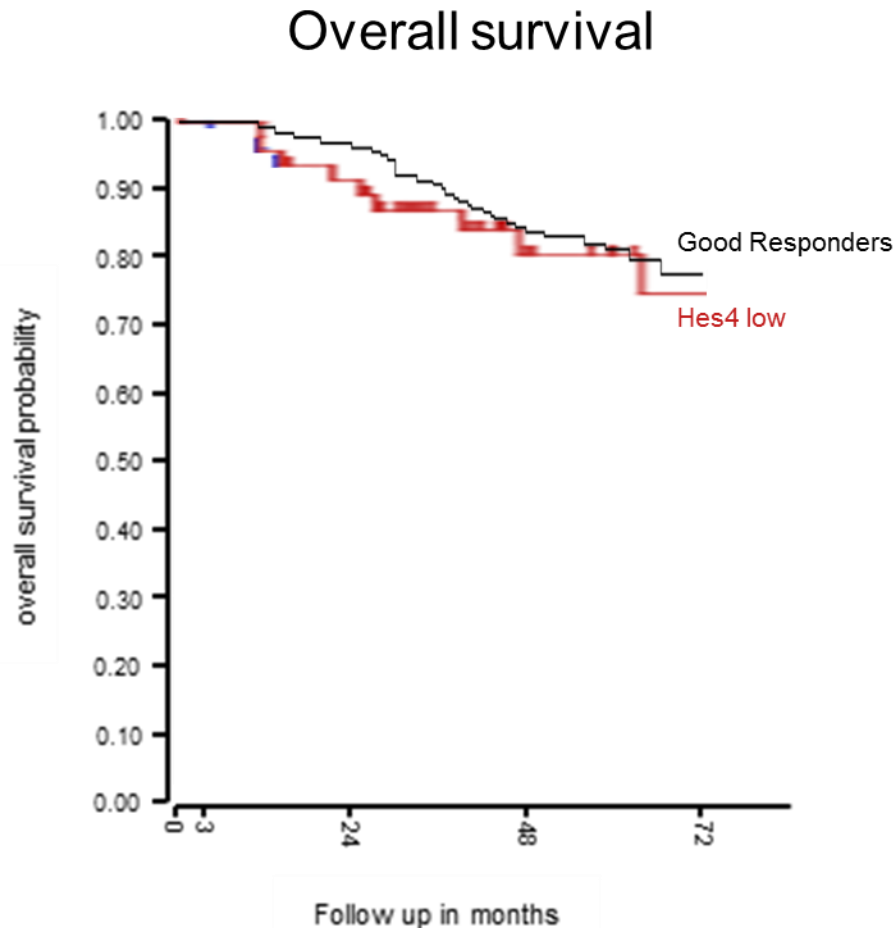


**Figure 36. Low Hes4 expression and patients with good response (>90% necrosis of surgical resection after 10-12 weeks chemotherapy) have similar overall survival.** Kaplan Meir overlay. In red: overall survival in patients that express low levels of Hes4 expression [The R2 Genomics Analysis and Visualization platform (Academic Medical Center, Amsterdam, The Netherlands; R2: Genomics Analysis and Visualization Platform; http://r2.amc.nl) was used to generate Kaplan-Meier overall survival curves using the 'Mixed Osteosarcoma - Kuijjer - 127 - vst - ilmnhwg6v2' dataset (77). Genome-wide gene expression analysis was performed on 84 pre-treatment high-grade osteosarcoma diagnostic biopsies, of which 29 overlapped with the 32 samples used for copy number analysis. Two different sets of control samples were used for comparison: osteoblasts (n=3) and mesenchymal stem cells (n=12, GEO accession number GSE28974). In black: overall survival in patients that have >90% necrosis at tumor resection (7).

## Summary and Discussion

In this Chapter, we demonstrated that overexpression of Hes4 blocks differentiation by promoting an immature phenotype and/or by inhibiting osteogenic maturation. These results support our hypothesis that a block in differentiation increases the malignant potential resulting in larger more lytic primary tumors and more metastases, as was demonstrated in mice injected with cells that overexpress Hes4 in Chapter 5 (Figures 23-25).

In contrast to our findings, Cakouros *et al* recently demonstrated that overexpression of Hes4 in normal bone marrow stromal cells promoted the expression of RunX2, osteopontin, and osteocalcin. This increase in expression resulted in the mineralization and terminal differentiation of bone marrow stromal cells (27). In contrast, we found that overexpression of Hes4 in OS cells prohibited terminal differentiation. This discrepancy in Hes4 mediated differentiation may be due to differences in normal and tumorigenic cells. We examined the expression of a wide range of key mediators of cellular differentiation at multiple steps of the differentiation process to determine the stage of differentiation in which OS cells and normal bone marrow stromal cells responded differently to Hes4 overexpression. These results are summarized in Table 1. In OS cells, Hes4 blocks differentiation as osteoprogenitors/preosteoblasts differentiate into early osteoblasts. This information enabled us to elucidate key differences in Notch-mediated differentiation under normal and tumorigenic circumstances, and suggests that there is something specific in tumor cells that allows Hes4 to block differentiation. Future studies are needed to identify potential factors that are differentially expressed in BMSCs versus OS cells. One such factor may be p53 as the majority of OS tumors have and abnormality in this pathway.

**Table 1. Comparison in expression of differentiation markers in normal bone marrow stromal cells (27) versus in OS after over-expression of Hes4.**

| Protein | Expression in Normal BMSC after + Hes4 | Expression in OS after + Hes4 |
|---|---|---|
| Nanog/Sox2/Oct4 | not determined | increased |
| RunX2 | increased | increased |
| Osterix | not determined | increased |
| Alkaline Phosphatase | not determined | decreased |
| Osteocalcin | increased | decreased |
| Osteopontin | increased | no change |

Based on our results, we hypothesized that Hes4 is binding directly to the promoters of RunX2, osterix, or alkaline phosphatase to regulate their transcription. However, there are no N- (CACNAG) or E- (CANNTG) box binding sites (data not shown), suggesting that Hes4 does not transcriptionally regulate these targets directly. Hes4 may instead regulate these factors indirectly. Interactions between other Notch effectors have been shown to regulate the expression of RunX2. For example, in an osteoblast precursor cell line, MC3T3-E1, Hes1 was shown to stabilize RunX2 on DNA to promote the transcription of type I collagen and osteopontin, leading to osteoblastic differentiation (24). Because this Hes1/RunX2 complex is inhibited by the Notch effector Hey2 (24, 98), it is possible that Hes4 is acting similar to Hey2 in inhibiting the ability for Hes1 to bind to and stabilize RunX2, thus preventing terminal differentiation. Hes4 could be inhibiting Hes1 either by forming a repressive heterodimer (37, 38, 78), or Hes4 could be inhibiting the expression of Hes1, as supported by our observation in Chapter 4, Figure 21. Future studies are needed to

discover the mechanism by which Hes4 interacts with RunX2/osterix/alkaline phosphatase to inhibit terminal differentiation.

Metastatic tumors are generally more aggressive and resistant to chemotherapy (3). With this in mind, it is important to identify ways to classify and distinguish between aggressive, mostly undifferentiated tumors with poor outcome and moderate, mostly differentiated tumors with higher likelihoods of survival. Our data suggests that due to its significant relationship to differentiation state and patient outcome, Hes4 may be a promising prognostic factor and/or predictive biomarker in newly diagnosed untreated patients. Future prospective studies to determine whether Hes4 status can be utilized as a biomarker to predict patient response to standard pre-operative chemotherapy and identify poor-risk patients at the time of diagnosis are warranted.

**CHAPTER 7. Discussion**

## I. Targeting Notch at the receptor level does not inhibit OS growth

Normal bone development is tightly regulated by a multistep differentiation pathway in which various transcription factors control the progression from an immature stem-like state through osteogenic lineage commitment to terminal differentiation (13, 17, 99-107). Because disruption of osteogenic differentiation is thought to lead to the development and progression of osteosarcoma (50, 102), we sought to expand our understanding of the OS tumor cell differentiation by studying the molecular mechanisms that control normal bone development. One such mechanism relies on the Notch signaling pathway, which has been shown to mediate cell differentiation and is critical for normal bone development.

Notch signaling can contribute to both oncogenic or tumor suppressive phenotypes depending on the cancer (51-53), and in some cases, can play both roles within the same tumor type (54-59). Because of the potential oncogenic role Notch has been shown to play in osteosarcoma (46, 60-62), we inhibited Notch signaling and examined the effect on OS tumor progression. While GSIs are tested clinically due to the ease of delivery as a pharmacologic agent, more specific targeting of Notch pathway activity is achieved with dnMAM which can be introduced by retroviral transduction into various experimental systems (46, 60, 66). In Chapter 2, we demonstrated that inhibiting Notch using dnMAM does not affect proliferation, cell viability, the formation of colonies, or the ability to invade in OS cells. Although dnMAM expression was reported to decrease tumor burden in an OS subcutaneous model in nude mice (46), we did not observe tumor growth inhibition using an orthotopic OS model in NSG mice. Orthotopic tumor models are more clinically relevant and better predictive models of tumor growth and metastasis than subcutaneous models due to the fact that tumor cells are implanted directly into the organ of origin. This allows injected

tumor cells to interact with the microenvironment that better mimics clinical OS. This data altogether allows us to conclude that broad inhibition of Notch signaling at the receptor level is not an effective method of inhibiting OS tumor growth in an orthotopic murine model.

In Chapter 2, we also showed that inhibiting Notch receptor signaling using dnMAM can have varying effects on Notch downstream targets. Although Hes and Hey family members are considered Notch downstream targets, they may also be transcriptionally activated by other signaling pathways. For example, there have been several reports that describe Notch-independent transcription of Hes1 by: sonic hedgehog (Shh) (67), activating transcription factor 2 (ATF2) (68), Nanog (69), and c-Jun N-terminal kinase (JNK) (70, 71). This suggests that other pathways may play an important role in regulating the expression of Notch downstream targets, and further studies are needed to understand the mechanisms that drive these targets individually. Perhaps targeting a Notch downstream target instead of the receptor will be more effective in treating OS.

Due to our observation that targeting Notch using dnMAM did not inhibit OS growth, and our observation of variant Notch downstream target responses to dnMAM in Chapter 2, we sought to better understand Notch signaling both up- and downstream of the Notch receptor. We found that notch downstream targets are variably expressed in OS cell lines when unstimulated, and when stimulated with the Notch ligands Jag1 and Dll4 the expression of Hes1, Hes4 and Hey1 increases. We focused on Hes1, the standard surrogate marker for Notch activation, and Hes4, which has been shown to be a prognostic factor for response to GSI (108). In assessing the kinetics of Hes1 and Hes4 expression in response to ligand stimulation over time, we discovered that Dll4 promoted temporally different changes in Hes1 and Hes4 expression, suggesting that Notch downstream targets are not all activated in

the same way. This data demonstrates that it is possible to promote differential expression of Notch downstream targets despite similar contexts. Further investigation is needed to more thoroughly understand how the downstream targets of Notch interact with one another and contribute to downstream signaling.

## II. Hes1 and Hes4 have different effects in OS

Because we demonstrated that dnMAM and ligand stimulation with Dll4 can promote greatly different responses in Notch downstream target expression, we hypothesized that activation of Notch at the receptor level will have a different biologic outcome than the activation of a downstream target of Notch. Indeed, Hes1 and Hes4 had opposing roles in proliferation, invasion and, importantly, patient outcome. Hes1 acted similar to a tumor suppressor in that it (1) decreased OS cell proliferation by inducing apoptosis, (2) decreased invasion, and (3) correlated with improved patient overall. In contrast, Hes4 acts similar to an oncogene in that it (1) increases invasion (2) promotes an increase in tumor size, lytic grade and metastatic burden *in vivo*, and (3) correlates with significantly worse patient overall survival. Because Hes and Hey family members are known to hetero- and homodimerize to form repressive transcriptional complexes (37, 38, 78), we explored the potential relationship between Hes1 and Hes4 and found that when Hes4 is overexpressed in OS, the RNA expression of Hes1 decreases. This, along with our Dll4 ligand stimulation data that shows when Hes4 is high, Hes1 is low, suggests that Hes4 may be repressing the expression of Hes1. Because Hes1 is known to repress its own expression via a negative feedback loop (79), and because both Hes1 and Hes4 bind to DNA N- and E-boxes within the promoter region of their target, it is possible that Hes4 is similarly inhibiting the expression of Hes1. Future experiments are needed to explore and understand the relationship between Hes1 and

Hes4. To further study the potential transcriptional inhibition of Hes1 by Hes4, a luciferase reporter attached to the Hes1 promoter, with or without Hes4 overexpression, could be used. We could also use chromatin immunoprecipitation (ChIP) to investigate the interaction between Hes4 and the Hes1 promoter. We hypothesize that Hes4 is directly binding to the Hes1 promoter via its N-box to inhibit Hes1 transcription, thereby inhibiting Hes1-mediated OS cell apoptosis. To study whether Hes1 and Hes4 are physically interacting with one another via heterodimerization, we could use co-immunoprecipitation (Co-IP) to investigate the physiologic protein complexes that either Hes1 or Hes4 are involved with. Co-IP could provide insight into the interaction within biological mechanisms, for example: how Hes1 and Hes4 may interact to promote or prevent differentiation.

### III. Hes4 promotes OS growth *in vivo*

To date, the effect of Hes4 on the development of primary and metastatic OS has not been studied. For the first time, we demonstrate the effect of Hes4 overexpression on the progression and phenotype of the primary tumor and on the metastatic potential of human OS cells in an orthotopic mouse model. Mice injected with Hes4-transduced OS cells developed significantly larger primary tumors than did those injected with the control cells. Because OS tumors must first degrade bone in order to invade and form metastases, we also quantified the lytic grade of the Hes4 transduced tumors. We found a significant increase in the lytic capacity of Hes4 overexpressing tumors versus control tumors. A known contributor to lytic behavior is interleukin (IL)-1$\alpha$, a potent cytokine secreted by osteosarcoma cells (19). IL1$\alpha$ promotes the expression of receptor activator of nuclear factor-$\kappa$B ligand (RANKL) within mature osteoblasts. When RANKL interacts with its receptor, RANK, which is expressed in immature osteoclasts, RANKL allows for the maturation of osteoclast precursors to induce

osteoclastic formation (19, 87). Interestingly, osterix can transcriptionally suppress the expression of IL1α, and can thus inhibit osteolysis by preventing the IL1α/RANKL/RANK mediated maturation of osteoclasts. We evaluated whether Hes4 promotes a lytic phenotype via this IL1α/RANKL/RANK mechanism. In cells overexpressing Hes4, however, we did not see any changes in the RNA expression levels of IL1α, RANK and RANKL. Further investigation is needed to understand the mechanisms that drive the lytic phenotype observed in Hes4 overexpressing OS *in vivo* tumors.

Our findings that overexpression of Hes4 correlates with a more malignant and metastatic phenotype in mice are consistent with the patient data, which shows that patients that express high levels of Hes4 in their primary tumors have a lower overall survival and a higher probability of developing metastases. Together, this suggests that overexpression of Hes4 plays a critical role both in the progression of OS and in the development of OS metastases. Future studies that knockdown Hes4 to see if blocking Hes4 prevents OS development are needed to conclude that Hes4 is critical for OS development and progression. If Hes4 is indeed necessary, identifying agents that target Hes4 may result in better inhibition of OS than inhibition of the Notch receptor signaling.

## IV. Hes4 regulates OS cell differentiation

The formation of primary and metastatic osteosarcoma relies on a number of distinct biological processes. In order for a tumor to develop, there must be a tumor initiating event that allows for uncontrolled cellular regulation. One such mechanism relies on the disruption of osteogenic differentiation, which could not only lead to the initiation of OS, but may also promote OS metastases. Defects of osteogenic differentiation can occur at any stage within the differentiation process; defects at early stages within the differentiation process are

believed to lead to the development of more undifferentiated and aggressive OS, while defects at later stages may lead to the development of more differentiated and less aggressive OS (89). It has also been shown that undifferentiated tumor cells (stem-like cancer cells) may be more likely to metastasize and develop drug resistance due to their greater abilities to self-renew, active DNA repair, higher expression of drug transporters and resistance to apoptosis (90).

The work presented in Chapter 6 provides insight into the mechanism by which Hes4 promotes tumor growth and metastasis in OS. Hes4 overexpression results in a block of OS differentiation, as demonstrated by increased stem cell and osteogenic commitment markers (Nanog, Sox2, Oct4, RunX2, and osterix) and decreased markers of osteogenic maturation (alkaline phosphatase and osteocalcin). This suggests that Hes4 overexpression in OS cells blocks terminal differentiation at the transition from osteoprogenitors/preosteoblasts to osteoblasts. Because Hes4 is important in differentiation, and if differentiation is indeed linked to worse patient outcome, genes that are upregulated in the presence of Hes4 (i.e. RunX2 and osterix) should also be high in tumors with high Hes4 and their levels should therefore correlate with patient outcome. Indeed, patients with high levels of RunX2 or osterix expression in their primary tumors have significantly higher probabilities of developing metastases ($p<0.05$) and correlate with significantly worse overall survival, similar to Hes4 expression. Further studies are needed to quantify the percentage of patients that are simultaneously high for Hes4, RunX2 and osterix. This data corroborates our findings *in vitro* and suggests that Hes4 works with RunX2 and osterix. Our data is also in line with the findings of other investigators: the differentiation status plays an important role in the aggressiveness of OS (91). Furthermore, RunX2 expression has been shown to

correlate with poor response to chemotherapy in OS (92), which suggests that RunX2 may have clinical and prognostic potential in OS.

Based on our results, we hypothesized that Hes4 is binding directly to the promoters of RunX2, osterix or alkaline phosphatase to regulate their transcription. However, there were no N- (CACNAG) or E- (CANNTG) box binding sites, which suggests Hes4 does not directly transcriptionally regulate these targets. Hes4 may regulate these factors indirectly. Interactions between other Notch effectors have been shown to regulate expression of RunX2. For example, Hes1 is known to stabilize RunX2 to promote transcription resulting in osteoblast differentiation (24). This is inhibited by the Notch effector Hey2, and regulated by Inhibitor of DNA binding 4 (Id4) (24, 98). We did not detect changes in Id4 as a result of Hes4 over-expression, but the possibility of interaction between Hes4 and Hes1 or other Notch downstream targets in order to regulate RunX2 expression remains. As mentioned previously, it is known that Hes and Hey family members are able to heterodimerize to repress transcription (37, 38, 78). Hes4 may therefore heterodimerize with Hes1 in a way that prevents RunX2 stabilization, thus preventing OS differentiation. Alternatively, Hes4 may heterodimerize with Hey1, and not Hes1, to prevent differentiation. In MSCs, it was shown that bone morphogenetic protein (BMP) 9, one of the most potent inducers of osteogenic differentiation, directly regulates the transcription of Hey1 which acts synergistically with RunX2 to promote differentiation (109, 110).

Alternatively, Hes4 may be interacting with a non-Notch target to prevent differentiation. In normal bone marrow stromal/stem cells, Twist-1 binds to RunX2 to prevent osteogenic differentiation (27). When Hes4 is over-expressed in these cells, Hes4 binds to Twist-1 to reverse this repression, and allows for differentiation. It is possible that in

OS Hes4 is not able to bind to Twist-1 which allows for a block in normal differentiation, thus resulting in a tumorigenic and immature state.

Hes4 may also regulate differentiation via modulation of osterix. In previous studies, mice injected with cells that over-express osterix developed fewer tumors and metastases which promoted survival (19, 22). This may be a result of differentiation: higher osterix results in more differentiation which results in fewer tumors and metastases and better survival. We however observed increased osterix in cells that overexpress Hes4, and when Hes4 over-expressing cells are injected into mice, there is an increase in tumor size and metastases. Interestingly, the disparity between our findings and those reported by Cao *et al.* may be due to the fact that mice do not express Hes4. The model used by Cao *et al.* was K7M2 cells, a mouse OS cell line. Therefore, in the absence of Hes4, high osterix results in smaller primary tumors, fewer metastases, and increased survival, but in the presence of Hes4, high osterix results in larger primary tumors, more metastases, and decreased survival. This suggests that Hes4 acts downstream of osterix. Though it has been shown that Hes4 binds to Twist-1 to allow RunX2 to promote the transcription of osterix (27), to date it is unknown how Hes4 may be interacting with osterix, the transcription of osterix targets, or downstream effector factors like alkaline phosphatase. Future studies are needed to explore the role of Hes4 downstream of RunX2.

## V. Hes4 as a prognostic/predictive biomarker

Despite major advancements over the last 40 years in the treatment of OS using multidisciplinary applications of chemotherapy, radiotherapy and surgical resection, the overall cure rate has not improved (4, 5). This is most likely due to our limited understanding of the molecular mechanisms that drive OS tumorigenesis, and a lack of good diagnostic,

prognostic and predictive clinical markers for this disease. Although osteosarcomas are inherently very heterogeneous, OS is oftentimes treated similarly (111-117). The current standard of care in treating Pediatric osteosarcomas relies on the use of 10-12 weeks of preoperative chemotherapy (high-dose methotrexate, doxorubicin, and cisplatin; MAP), followed by surgery and then several more months of postoperative chemotherapy (4). To date, the single most important prognostic factor in determining OS patient outcome is the histological response to preoperative chemotherapy within the surgically resected tumor, which cannot be determined until 10-12 weeks after the initial diagnosis (5, 6). A good histological response is defined as >90% necrosis in a resected tumor specimen. In patients with good histological response, the 5-year survival is 80-90% while the 5-year survival for poor responders (those with <90% tumor necrosis) is 30-65% (5, 6). Though biological markers like p53, VEGF, and HIF1-α have been studied as potential prognostic and/or predictive factors for OS, researchers have not been successful in finding a biomarker with high enough specificity or sensitivity to be clinically relevant (93-97).

Because we found that Hes4 contributes significantly to the pathogenesis and progression of OS and correlates with worse overall survival, we explored the potential use of Hes4 as an indicator of good or poor response to pre-operative chemotherapy. In comparing the overall survival of patients with low Hes4 to those that are considered good responders (with >90% necrosis), the survival curve of patients with low Hes4 expression aligns with the survival curve of good responders indicating that the level of expression of Hes4 in the primary tumor has potential as a prognostic marker. If the expression of Hes4 in the primary tumor can be used to identify between good and poor responders, and because Hes4 expression can be quantified at diagnosis, identifying poor-risk patients at the time of

diagnosis may allow for modification of pre-operative therapy rather than waiting until the post-operative assessment. This may assist in the stratification of patients earlier and be useful for future clinical trials in osteosarcoma.

Our data suggests that due to its significant relationship to differentiation state and patient outcome, Hes4 may be a promising prognostic factor and/or predictive biomarker that can be used at the time of diagnosis and thus aid in the management of high risk OS patients. Future prospective studies to determine whether Hes4 status can be utilized as a biomarker to predict patient response to standard pre-operative chemotherapy and identify poor-risk patients at the time of diagnosis are warranted.

In order to validate Hes4 as a true prognostic marker, we can request response data (% necrosis after surgical resection) from the gene expression database used to generate our patient outcome data to compare response versus Hes4 expression. This will allow us to determine how many Hes4 low patients were indeed also good responders. We can also probe frozen tumor samples taken from an internal cohort of patients with known response data and correlate this to Hes4 expression. To further validate Hes4 as potential markers, the sensitivity, specificity, positive predictive value, negative predictive value and the likelihood ratio should be determined using the equations outlined in Table 2 (118).

**Table 2. Clinical Tests used to validate biomarkers. Equations reprinted from (118)**

| Test | Equation | Definition |
|---|---|---|
| *Sensitivity* | $= \dfrac{True\ Positives}{True\ Positives + False\ Negatives}$ | Percentage chance that the test will correctly identify a person who truly has the disease. |
| *Selectivity* | $= \dfrac{True\ Negatives}{True\ Negatives + False\ Positives}$ | Percentage chance that the test will correctly identify a person who is disease free. |
| *Positive Predictive value* | $= \dfrac{True\ Positives}{True\ Positives + False\ Positives}$ | The likelihood that a patient has the disease, given that the test result is positive. |
| *Negative Predictive value* | $= \dfrac{True\ Negatives}{True\ Negatives + False\ Negatives}$ | The likelihood that a patient does not have the disease given that the test result is negative. |
| *Likelihood ratio* | $= \dfrac{Sensitivity}{1 - Specificity}$ | The likelihood that a patient who tests positive has the disease compared with one who tests negative. |

If Hes4 is validated as a predictive/prognostic biomarker, this could have significant impact on the clinical treatment of OS. Using Hes4 expression at diagnosis has the potential to identify patients who will experience a good histological response (>90% tumor necrosis) to chemotherapy. This allows patients and clinicians to identify and stratify patients based on Hes4 expression into good or poor response groups 3-4 months sooner than the current standard. Using this information, clinicians and researchers can design clinical studies to determine the potential of increasing chemotherapy in patients identified as poor responders, or decreasing chemotherapy in patients identified as good responders. Though EURAMOS

showed definitively that the addition of ifosfamide and etoposide to post-operative chemotherapy (MAP) for OS patients with poor necrosis increased toxicity without improving survival (results presented at the annual meeting of the Connective Tissue Oncology Society Annual Meeting, Berlin, Germany, 2014), it is unknown if adding ifosfamide and etoposide will benefit poor responders if given pre-operatively. It is possible that the first 10-12 weeks is the most critical time that highly aggressive treatment of OS will result in the most tumor necrosis, and therefore, benefit the patients most. Conversely, in patients that are likely to be good responders, it may be possible to reduce chemotherapy to minimize debilitating side effects. Indeed, childhood sarcoma survivors treated with anthracyclines have a 5.3 fold increased likelihood of developing breast cancer 10-34 years after their primary diagnosis (119). Reducing the levels of chemotherapy while maintaining the highest possible overall survival could drastically impact the quality of life for pediatric OS patients.

## Major Conclusions and Significance.

We demonstrated that manipulating Notch activity at the receptor level can promote different responses in Notch downstream target expression, and the activation of Notch at the receptor level has a different biologic outcome than the activation of a specific downstream target of Notch. Indeed, Hes1 and Hes4 had opposing roles in proliferation, invasion and patient outcome.

For the first time, we describe the role of Hes4 in bone differentiation within a malignant context. We found that Hes4 promotes the development and progression of primary and metastatic OS by blocking terminal differentiation and promoting an immature preosteoblastic phenotype. When injected orthotopically into a mouse tibia, Hes4 overexpressing cells promote the growth of large OS tumors. In patients, high expression of Hes4 correlated with worse overall survival. Consistent with this, we showed that the overexpression of Hes4 increased invasiveness *in vitro* and the lytic capacity *in vivo*, and promotes significantly more metastatic disease *in vivo* in mice. High Hes4 expression also correlated with a higher incidence of metastases in patients.

Defects in OS cell differentiation have been postulated to produce more aggressive OS tumors (3). In this study, we confirmed this link between OS tumor differentiation and patient outcome. We showed that high Hes4/RunX2/osterix correlated with worse patient overall survival, and a higher incidence of developing metastases. This suggests that there is indeed a link between the differentiation status of OS and patient outcome, and that link may be Hes4 mediated. We also demonstrated the potential for Hes4 as a predictive biomarker in the prognosis of OS, which has the potential for major clinical impact as it may also allow for the stratification of risk groups several months earlier than current techniques allow.

**Table 3. Major Observations, Significance and Future Directions**

| *Major Observation* | Novelty | Significance | Future Directions |
|---|---|---|---|
| **Inhibiting Notch using dnMAM does not affect** *in vitro* **OS tumor cell growth, or** *in vivo* **orthotopic tumor growth**<br>*Chapter 2* | Orthotopic inhibition of Notch in OS has never been performed. | Broad inhibition of Notch receptor signaling may not have therapeutic relevance. | Assess the potential of targeting specific Notch downstream genes. |
| **dnMAM and Dll4 promote differing responses in Notch downstream target (Hes1 and Hes4) expression**<br>*Chapter 2, Figure 11; Chapter 3, Figure 19;* | The complexities of Notch downstream target activation are not fully understood. | Notch receptor activation or inhibition is not synonymous with broad activation or inhibition of Notch downstream targets. This greatly shapes the design of Notch targeting therapeutics. | Explore the biological context cues that drive differing activation and regulation of Notch downstream targets. |
| **Hes1 acts as a tumor suppressor while Hes4 acts like an oncogene in OS**<br>*Chapter 4* | The dual role of Notch downstream targets in cancer has not been characterized | Understanding how specific Notch downstream targets affect OS or other cancers can shape the way | Explore the relationship between Hes1 and Hes4 and analyze how these targets differ in their signaling. |
| **Hes4 overexpression results in larger more lytic tumors and more metastases when compared to control OS cells in an orthotopic OS mouse model**<br>*Chapter 5* | The *in vivo* effect of Hes4 overexpression has never been assessed within a tumorigenic context. | Hes4 overexpression may significantly contribute to the pathogenesis of OS. | Inhibit Hes4 expression using shRNA or CRISPR and assess primary tumor and metastatic growth. |

| | | | |
|---|---|---|---|
| **High Hes4 correlates with a significantly higher probability of developing metastases, and a significantly lower probability of overall survival when compared to the overall survival of patients whose tumor expresses low levels of Hes4** *Chapter 4, Figure 20* *Chapter 5, Figure 28* | This is the first time that Hes4 expression has been linked to OS patient outcome. | Because Hes4 is significantly correlated with worse patient outcome, it is possible that Hes4 contributes biologically to the pathogenesis and progression of OS. | Analyze patient samples for their expression in Hes4. Compare the expression of Hes4 in patients with known outcomes. |
| **Hes4 blocks differentiation via RunX2/Osterix/Alkaline Phosphatase signaling** *Chapter 6* | The mechanisms that inhibit differentiation in OS are not fully understood. | Hes4 may contribute to a sustained immature state in OS. | Explore the role of Hes4 downstream of RunX2 and osterix. |
| **High RunX2 and high osterix, like high Hes4, correlate with a significantly higher probability of developing metastases, and a significantly lower probability of overall survival that low Hes4** *Chapter 6, Figure 35* | This is the first time Hes4, RunX2 and osterix have been proposed to work together in OS patients. | Our proposed *in vitro/in vivo* mechanism regarding Hes4/RunX2/Osterix signaling may also be relevant in patients. | Assess the expression of Hes4/RunX2/Osterix in patient samples and determine how geographical and temporal networks within these pathways correlate with patient outcome. |
| **Low Hes4 results in similar patient overall survival as good response (>90% to necrosis at surgical resection 10-12 weeks post diagnosis)** *Chapter 6, Figure 36* | The identification of clinically relevant biomarkers in OS has been unsuccessful. Hes4 may be a potential marker for response in patients. | Scientists can design clinical studies to determine the potential of increasing chemotherapy in patients identified as poor responders, or decreasing chemotherapy in patients identified as good responders. | Determine whether Hes4 status can be utilized as a biomarker to predict patient response to standard pre-operative chemotherapy and identify poor-risk patients at the time of diagnosis |

**CHAPTER 8. Materials and Methods**

## Cell culture

The human OS cell lines HOS, SaOS2, LM7, CCHO and CCHD, and 293T normal kidney fibroblasts, were maintained in high-glucose Dulbecco's modified Eagle's medium (DMEM; Invitrogen, Carlsbad, CA) supplemented with 10% fetal bovine serum (HyClone, Logan, UT) and 1% penicillin-streptomycin (Gemini Bio-Products, Woodland, CA). All cells were incubated in a humidified atmosphere at 37°C with 5% $CO_2$. HOS, SaOS2, and 293T cells were purchased from the American Type Culture Collection (Manassas, VA). CCHD and CCHO are primary OS cell lines derived from patients at the Children's Cancer Hospital at The University of Texas MD Anderson Cancer Center. CCHD was obtained via a core needle biopsy of a proximal femur lesion in an 18-year-old man who also presented with pulmonary metastases. CCHO was derived from a core needle biopsy of hip lesion in a 22 year old male who presented with T5 spinal metastases. Cells were maintained between 20-80% confluency, and EDTA-free Trypsin (GIBCO) was used to passage cells.

## GSI treatment (Appendix)

OS cells were treated with increasing amounts of GSI (Compound E; Abcam) for 72 hours. CCHD, HOS and CCHO cells were treated with 10, 100, and 1000nM GSI while.

## Retroviral transduction of dnMAM, Hes1, Hes4

All MigR1 plasmids were gifts from Dr. Zweidler-McKay (MD Anderson). MigR1-green fluorescent protein (GFP) or MigR1-GFP-dnMAM, MigR1-GFP-Hes1, or MigR1-GFP-Hes4 was used to make a replication-incompetent retrovirus that was then used to infect HOS, SaOS2, and CCHD cells. To generate the virus, 293T cells were seeded initially at a density of 140,000 cells/well in a six-well dish. After 24 hours, the following were incubated for 5 minutes: tube A, 2 μg of MigR1-GFP vectors, 2 μg of VSVG, 2 μg of PCGP (gifts from

Dr. Zweidler-McKay), and 250 µl of Opti-MEM (Invitrogen); tube B, 12 µl of Lipofectamine (Invitrogen); and 250 µl of Opti-MEM. The contents of tubes A and B were then combined and incubated at room temperature for 30 minutes. Afterward, 500 µl of the resulting complex was added to one well of a six-well plate containing 293T cells. After 8 hours, the complex was removed from the well, fresh medium was added, and the plate was incubated in a humidified atmosphere at 32°C with 5% CO2. The supernatant was collected at 24 hours and centrifuged at 2,500 rpm for 2 minutes. Next, 2.5 ml of viral supernatant and 8 µg/ml Polybrene (Sigma, St. Louis, MO) were added to plates containing HOS, SaOS2, and CCHD cells. These plates were centrifuged at 2,500 rpm for 1 hour and then incubated at 32°C for 24 hours. Next, the viral medium was removed from the treated wells, and fresh medium was added. By 48 hours after the initial virus exposure, infected cells had begun to express GFP. Stably transduced GFP-positive OS cells were selected by fluorescence-activated cell sorting using BD FACSAria Fusion sorter (Becton Dickinson).

**Proliferation**

Cell count assay: Cells were seeded in triplicate into 6-well plates at the density of $2x10^4$ (HOS), $5x10^4$ (CCHD), $10x10^4$ (LM7, CCHO) cells/well. After treatment with either GSI or dnMAM as described above, the number of viable cells was counted after 2, 4, 6 and 8 days of culture by using an automated Vi-Cell Analyzer (Beckman Coulter). Cells were prepared as follows: medium was removed from the culture plates and the cells were rinsed with PBS to remove the dead cells and debris. Cells were treated with 0.25 ml of Trypsin at room temperature for 5 minutes. DMEM (0.25ml) was added and the total (0.5 ml) solution containing cell nuclei was transferred into an autosampler cup for further processing by the automated Vi-Cell Analyzer.

Competitive proliferation assay: HOS, SaOS2, and CCHD cells were transduced with MigR1 or Hes4 as described above, and cells were seeded in six-well plates in triplicate. Cells were collected every other day and analyzed using a FACSCalibur flow cytometer (Becton Dickinson, Franklin Lakes, NJ). The ratio of GFP-positive to GFP-negative cells was observed over time to determine the effect of MigR1 and Hes4 on the rate of OS cell growth.

Cell count assay: HOS, SaOS2, and CCHD cells were transduced with either MigR1 or Hes4 and sorted for GFP positivity to generate a polyclonal population of transduced cells. These cells were seeded in triplicate into six-well plates at concentrations of 2,000 cells per well for HOS, and 5,000 cells per well for CCHD. Cells were collected at 3, 5, 7, 9, and 11 days after seeding and counted using an automated Vi-Cell Cell Viability Analyzer (Beckman Coulter, Fullerton, CA).

Colony formation assay: $1 \times 10^3$ HOS cells were seeded in 6-well plates in triplicate. Cells were treated with 0.1, 0.5, 1, 10, 50, 100, and 1000nM GSI for 7 days (media was changed every 24hours and fresh GSI was added). After 7 days, cells were washed with PBS and incubated with crystal violet. Excess crystal violet was washed and the3 number of stained colonies were counted.

## Cell-cycle analysis

HOS, SaOS2, and CCHD cells transduced with either MigR1 or Hes4 were sorted for GFP to generate a polyclonal population of transduced cells. Dead and live cells were collected and incubated overnight at 4ºC with 0.005% propidium iodide and 0.1% Triton X-100 diluted in phosphate-buffered saline (PBS). Cells were analyzed using a FACSCalibur

flow cytometer (Becton Dickinson), and the percentages of cells in the various phases of the cell cycle were quantified as described previously (reference).

## Caspase Activity Assay

HOS cells were transduced with Hes1 (as mentioned above). Cells were sorted for GFP positivity and seeded into 96 well plates. 48- and 72- hours after transduction, the caspase activity of caspases 3 and 7 was measured using the Caspase-Glo3/7 Assay (Promega, Madison, WI). The 96-well plate was removed from the incubator and allowed to cool to room temperature; 100ul of Caspase-Glo 3/7 reagent was added to each well, plates were agitated to promote thorough mixing, and were incubated at room temperature for 3 hours. The luminescence was measured using the plate-reading luminometer, SpectraMax plus 384 (Molecular Devices, Sunnyvale, CA). Staurasporin was used as a positive control. The pan-caspase inhibitor, Z-VAD (20uM, R&D Systems, Minneapolis, MN) was used to block the activation of caspases and acted as a negative control.

## Cellular Invasion

HOS, SaOS2, and CCHD cells transduced with MigR1, dnMAM, Hes1 or Hes4 were sorted for GFP, and their invasiveness was measured using a 24-well BD BioCoat Matrigel invasion chamber with an 8-µm pore size (BD Biosciences, San Jose, CA). Briefly, 2.5 x 104 cells suspended in 500 µl of serum-free Dulbecco's modified Eagle's medium were seeded in triplicate into the upper chamber of an assay plate. A medium with 10% fetal bovine serum was added to the bottom chamber and acted as the chemoattractant for the cells. After 48 hours of incubation at 37°C, the migrated cells were fixed, stained with Hema-3 (Thermo Fisher Scientific, Waltham, MA), and counted under a microscope at 20x magnification.

## Differentiation

**Alizarin Red Staining:** HOS, SaOS2, and CCHD cells transduced with either MigR1 or Hes4 and sorted for GFP expression were seeded into 24-well plates and cultured to confluency. Once cells were 100% confluent, the cell medium was supplemented with a differentiation supplement (10 mM β-glycerophosphate and 50 µg/ml ascorbic acid). The medium and differentiation supplement was refreshed every 3 days for 21 days. On day 21, cells were gently washed with PBS and fixed with 10% paraformaldehyde for 15 minutes at room temperature. Excess paraformaldehyde was removed with a PBS wash two times for 5 minutes each. Cells were stained for calcium deposition using 40 mM Alizarin Red (pH 4.2) for 30 minutes. Excess Alizarin Red was removed via a PBS wash two times for 5 minutes each. Water was added to the wells containing cells, and cells were imaged using an inverted microscope (Eclipse Ti, Nikon Instruments).

**Quantification of the expression of differentiation markers:** To determine the stage at which Hes4 blocked osteoblastic differentiation, polymerase chain reaction (PCR) was used to quantify the change in the transcriptional expression of markers of MSCs (Nanog, Sox2, and Oct4), committed osteoprogenitors/preosteoblasts (RunX2 and osterix), early osteoblasts (alkaline phosphatase), and mature osteoblasts and osteocytes (osteocalcin and osteopontin). Briefly, total RNA was extracted from OS cells using an RNeasy Mini Kit (QIAGEN, Valencia, CA). cDNA was constructed using an Omniscript Reverse Transcriptase Kit (QIAGEN) with oligo(dT)s (Invitrogen) according to the manufacturer's protocol. Real-time PCR analysis was performed using an iCycler iQ quantitative PCR system (Bio-Rad, Hercules, CA) with SYBR Green PCR Master Mix (Bio-Rad) following the manufacturer's protocol. The primers used were: Runx2 (5'-

GACACCACCAGGCCAATC-3' and 5'-AGAACAAGGGGGCCGTTA-3'), Osterix (5'-

TGGAAAGCCAGTCTCATGGTGA-3' and 5'-TTGGGTATCTCCTTGCATGCCT-3'),

Alkaline Phosphatase (5'-TGATGAATGCTTGCGAAGGGT-3' and 5'-

TCTCCGCATTGCATTTTCTGCT-3'), Osteocalcin (5′-

CTCTGTCTCTCTGACCTCACAG-3′ and 5′-GGAGCTGCTGTGACATCCATAC-3′), and

Osteopontin (5′-TGACCCATCTCAGAAGCAG-3′ and 5′-GCTGACTTGACTCATGGCT-

3′). The Taqman probes used were: Hes1 (Hs00172878_m1), Hes4 (Hs00368353_g1), Nanog

(Hs04399610_g1), Sox2 (Hs01053049_s1), Oct4 (Hs00999632_g1) and GAPDH

(Hs02758991_g1).

## In vivo mouse xenograft

All animal experiments were approved by the MD Anderson Institutional Animal

Care and Use Committee.

**Intratibial injection:** CCHD cells ($1 \times 10^6$ suspended in 15 µl of sterile PBS) were

injected into the right tibias of 6-week-old NOD/SCID/IL2Rγ-deficient mice (The Jackson

Laboratory, Bar Harbor, ME). Mice were killed 4-8 weeks after inoculation, their lungs were

inflated with 10% formaldehyde via transtracheal injection, and their primary tumors and

lungs were fixed in formalin and embedded in paraffin. Five-micron sections of the primary

tumors and metastatic lesions in the lungs were mounted on glass slides for analysis, and

staining of them with hematoxylin and eosin as well as human vimentin was performed by

our core laboratory personnel.

**Microscopy and immunohistochemical quantification of metastases:**

Representative images of lung tumor burden were obtained using a cooled charge-coupled

device Hamamatsu C5810 camera (Hamamatsu Photonics, Bridgewater, NJ) and the Optimas

imaging software program (Media Cybernetics, Bethesda, MD). Lung sections obtained from mice intratibially injected with CCHD MigR1 or CCHD Hes4 were stained with human vimentin for easy identification. Lung sections were scanned at 10X, and all positively stained lesions were counted.

**Quantification of Lysis:** In order to determine the extent of lysis in the bone as a result of OS tumor burden, we used a radiographic grading scheme previously developed by Kristy Weber (86). Briefly, radiographs of the tibia were taken on the day the experiment was terminated (week 4) using the Xtreme X-ray machine (insert company name). A grading system using numerical values from 0 to 4 was used to quantify the extent of bone destruction, where a grade of 0 represents no lysis, a grade of 1 represents minimal bone destruction in the medullary canal, 2 is moderate bone lysis within the medullary cortex with minimal destruction to the cortex, 3 is sever bone lysis with cortical disruption, and 4 is massive destruction with soft tissue extension of the tumor.

## Patient survival and probability of metastasis

The R2 Genomics Analysis and Visualization platform (Academic Medical Center, Amsterdam, The Netherlands; R2: Genomics Analysis and Visualization Platform; http://r2.amc.nl) was used to generate Kaplan-Meier overall survival curves using the 'Mixed Osteosarcoma - Kuijjer - 127 - vst - ilmnhwg6v2' dataset (77). Genome-wide gene expression analysis was performed on 84 pre-treatment high-grade osteosarcoma diagnostic biopsies, of which 29 overlapped with the 32 samples used for copy number analysis. Two different sets of control samples were used for comparison: osteoblasts (n=3) and mesenchymal stem cells (n=12, GEO accession number GSE28974). Primary tumors from

OS patient samples were analyzed on the basis of High vs Low Hes1, Hes4, RunX2, or Osterix. Determination of high versus low cut-off was based on gene expression.

## Statistics

Significance was assessed using the Student t-test (GraphPad Software Inc) with an alpha error threshold of 0.05. All experiments were conducted at least three times unless stated otherwise. Log-rank test was used for assessment of survival curves. A p-value of $<0.05$, $<0.01$, and $<0.001$ was indicated using *, **, or *** respectively.

**APPENDIX**

**Rationale**

       The cleavage and activation of a Notch receptor relies on a two-step proteolytic cleavage, first by a metalloprotease (ADAM-10/TACE or ADAM-17), then by gamma secretase (33, 120). Gamma secretase is comprised of a catalytic subunit (either presenilin 1 or presenilin 2), a seven pass transmembrane protein, and accessory subunits (nicastrin (NCT), anterior pharynx-defective 1 (APH1), and presenilin enhancer 2 (PEN-2)) (121). Once cleaved by gamma secretase, the intracellular domain of Notch (ICN) translocates to the nucleus where it interacts with the co-activator mastermind-like 1-3 (MAM) and CSL (C promoter binding factor-1 [CBF-1], suppressor of hairless, Lag-1) to form a transcriptional complex which promotes the expression of a number of target genes (28-30). These Notch effectors are transcription factors that regulate the expression of diverse targets, allowing Notch receptors to act as master regulators of gene cohorts to control cellular outcome (33).

       Because of the potential oncogenic role Notch has played in osteosarcoma (46, 60-62), we inhibited Notch signaling and examined the effect on OS tumor progression. There are numerous genetic and pharmacologic approaches to blocking Notch pathway activity (63-65). In this chapter, we will focus on the inhibition of gamma secretase mediated cleavage of Notch receptors using gamma secretase inhibitors (GSIs).

       There are over 100 GSIs that have been synthesized to date (122). Of these, 5 are currently in clinical trials (63). A phase I/II clinical trial using a GSI in combination with Erivedge® (vismodegib), an inhibitor of the hedgehog pathway, for the treatment of metastatic sarcomas completed recruiting patients in June 2015, and has yet to report any conclusions (ClinicalTrials.gov Identifier: NCT01154452). The GSI's that will be discussed in this dissertation are DAPT and Compound E (123). Both DAPT and Compound E are

small molecule inhibitors with similar structures and functional properties, with poorly understood mechanisms of action. It is thought that these compounds inhibit gamma secretase cleavage by binding to the C-terminal section of transmembrane segment 7 in presenilin 1, which could be in proximity to the substrate-docking cavity and the active site aspartates (122-125). Gamma secretase contributes to a number of important biological processes and thus has multiple targets including ERBB4, APP, Cd44, N- and E-cadherin (63). Because of the wide range of GSI targets, GSIs can cause a wide range of side effects, most notably within the gastrointestinal tract (63, 122).

## Results

**GSI increases the invasiveness of OS cells**

In order to determine whether there are changes in migration or invasion in OS cells in response to GSI, we quantified the number of cells that were able to migrate through Matrigel and traverse an 8-μm pore membrane. HOS cells were treated with 0.1, 0.5, 1, 10, 50nM GSI while CCHO and LM7 were treated with 3, 10, or 30nM GSI for 72 hours. The invasiveness of all 3 cell lines increased with GSI treatment (Figure 37).
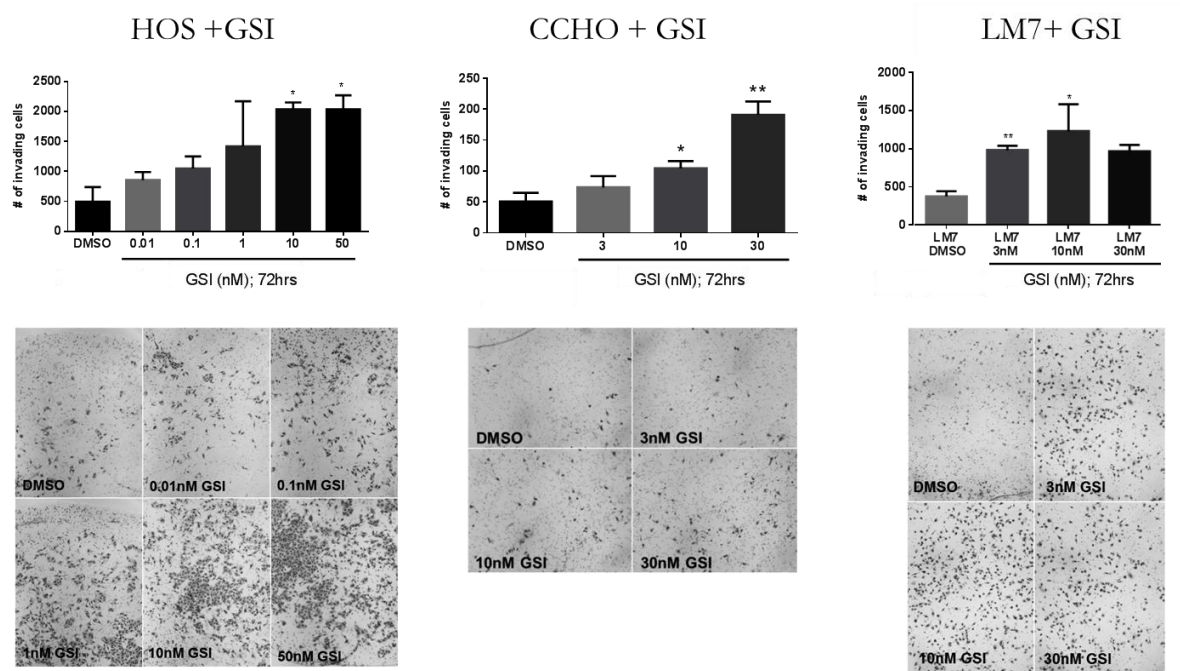


**Figure 37. GSI increases the invasiveness of HOS, CCHO and LM7 OS cells.**
HOS cells were treated with 0.1, 0.5, 1, 10, or 50nM GSI while CCHO and LM7 3, 10, or 30nM GSI for 72 hours. Invasiveness was measured using a 24-well BD BioCoat Matrigel invasion chamber with an 8-μm pore size. *p≤0.05, **p ≤0.01, bars show mean +/- S.E.M, n=3.

**GSI does not affect proliferation, viability or ability to form colonies in OS tumor cells**

Variable *in vitro* proliferative responses of OS cells to GSI treatment have been reported (46). Therefore, we examined the effect of Compound E on proliferation in LM7, CCHO and HOS cells. Cell count and cell viability in LM7 and CCHO cells were not affected by 3, 10 and 30nM GSI in LM7 or CCHO (Figures 38A&B). Similarly, the ability of HOS cells to form colonies did not change after treatment with 0.1, 0.5, 1, 10, 50, 100, and 1000nM GSI (Figure 39). This suggests that even with high amounts of GSI, OS cells do not experience cytotoxic effects.
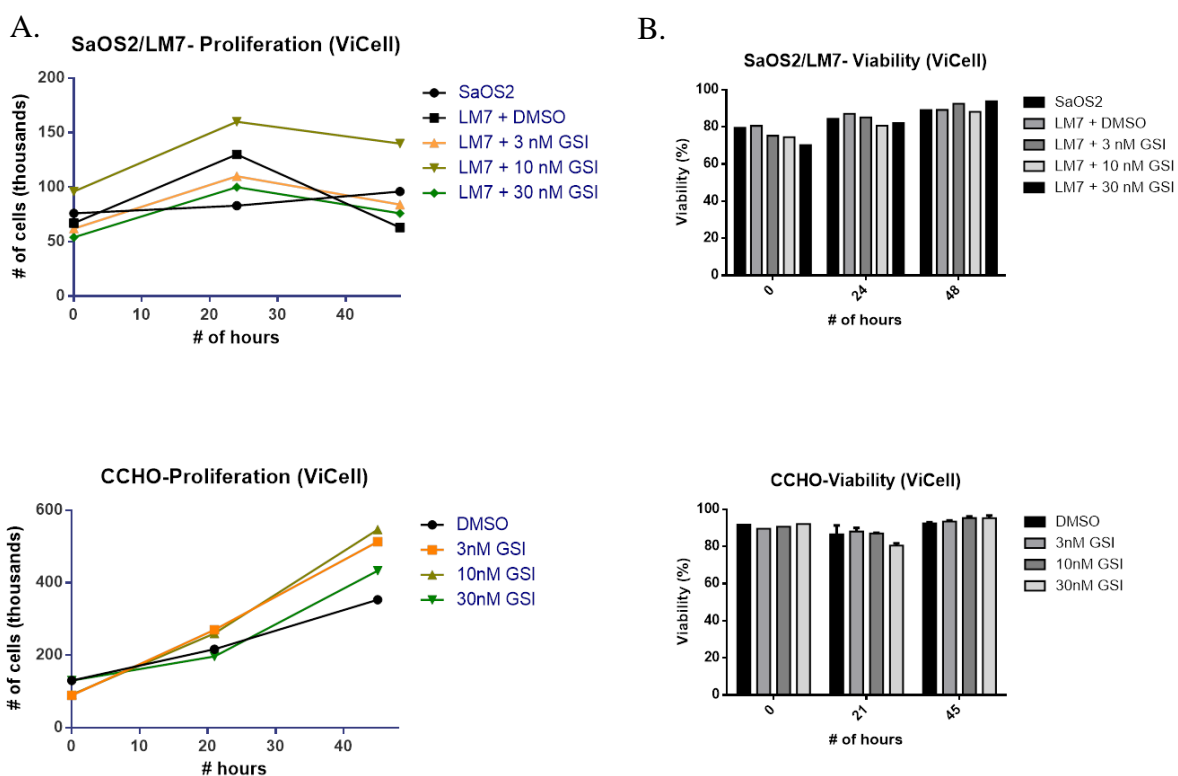


**Figure 38. GSI does not affect cell count, cell viability, or proliferation of OS cells.**
(A) Cell counts of SaOS2, LM7 and CCHO cells treated with 3, 10, or 30nM GSI (Compound E) over a 48 hour period. (B) Cell viability of SaOS2, LM7 and CCHO cells treated with 3, 10, or 30nM GSI (Compound E) over a 48 hour period.
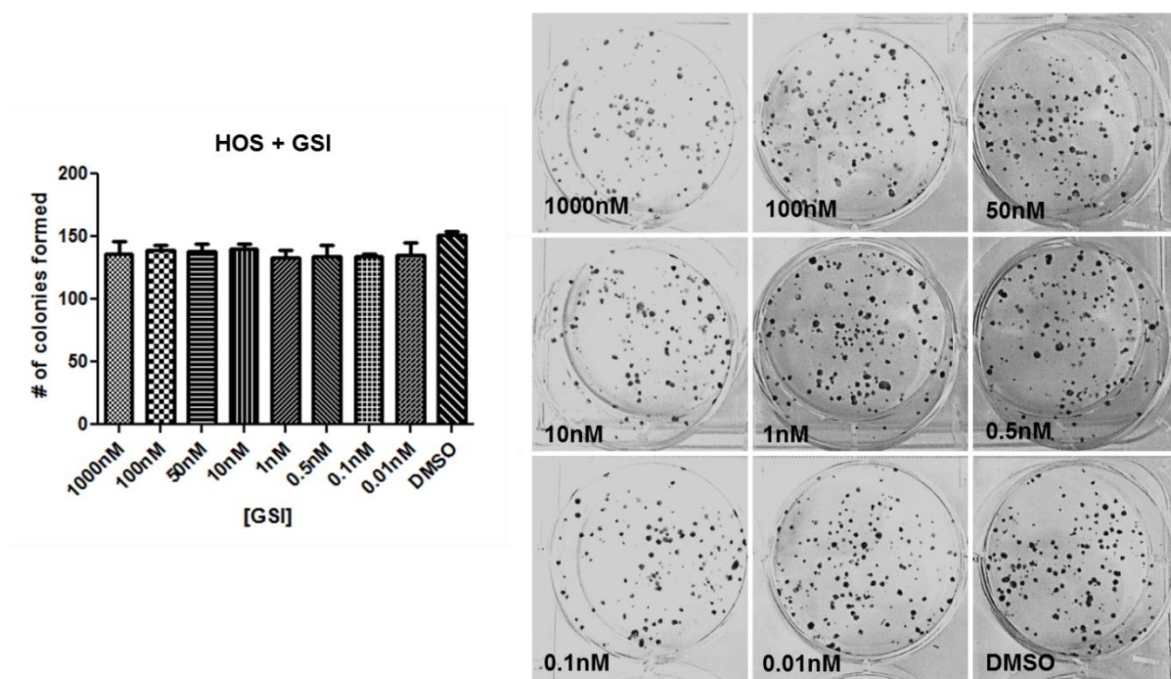
**Figure 39. GSI does not affect colony formation.**
HOS cells were treated with 0.1, 0.5, 1, 10, 50, 100, and 1000nM GSI (Compound E), 500 cells were seeded on day 0 and stained for crystal violet on day 7. The graph shows the average number of colonies formed from 3 wells per condition.

**GSI decreases the expression of the Notch downstream targets, Hes1 and Hes4**

We used RTq-PCR to confirm inhibition of Notch receptor signaling by monitoring the expression of the Notch downstream targets, Hes1 and Hes4, in response to increasing amounts of GSI (Compound E). CCHD, HOS and CCHO cells were treated with 10, 100 and 1000nM GSI 72 hours. GSI treatment in CCHD, HOS and CCHO cells resulted in up to a 50% decrease in Hes1 and Hes4 expression (Figure 40A & B). This suggests that the Notch targets Hes1 and Hes4 are sensitive to GSI mediated Notch inhibition.
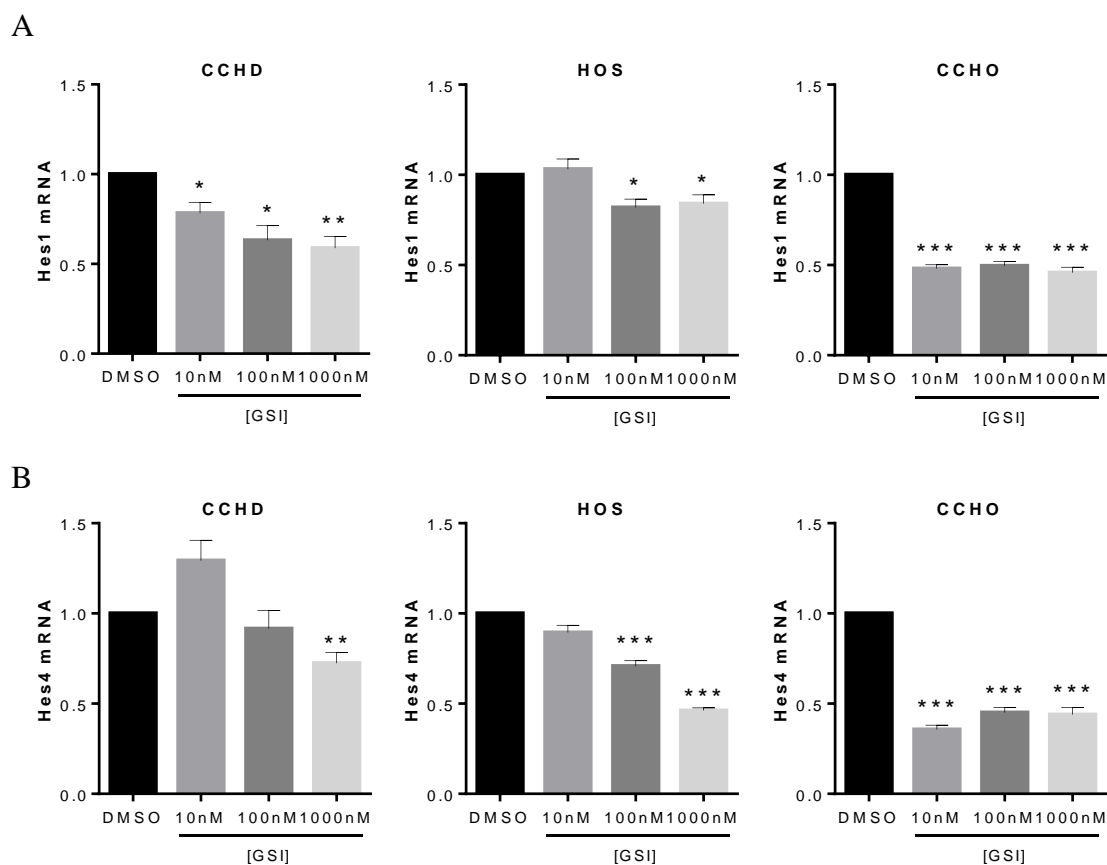
**Figure 40. GSI inhibits the expression of Notch downstream targets, Hes1 and Hes4 in OS cell lines.**

RTq-PCR was used to quantify the expression of (A) Hes1 and (B) Hes4 in CCHD, HOS and CCHO cells treated with increasing amounts of GSI (Compound E) for 72 hours. *p≤0.05, **p ≤0.01, ***p≤0.001, relative to DMSO controls; bars show mean +/- S.E.M, n=3.

## Summary and Discussion

In this Chapter, we showed that GSI increased invasion in multiple OS cell lines (Figure 37). In Chapter 2, the more specific inhibition of Notch receptor signaling using dnMAM had no effect (Figure 7). This discrepancy could be attributed to the fact that GSI has multiple targets that could affect invasion, including CD44 and E- and N-cadherin (63), while dnMAM more specifically targets CSL-dependent Notch transcription. This suggests that GSI is affecting invasion not through Notch, but rather one of its other target mechanisms. The fact that GSI increased invasion *in vitro* may suggest that GSI may increase the ability for OS cells to metastasize *in vivo,* as was demonstrated in neuroblastoma and breast cancer models (126). This highlights the need to understand the molecular mechanisms within each individual tumor type before treating patients with GSIs.

We found that the GSI Compound E did not decrease OS cell proliferation. This is in contrast to a prior report in which another GSI (DAPT) was reported to decrease proliferation (46). Although DAPT and Compound E are both small molecule GSIs that affect the same region within the catalytic subunit of gamma secretase, these results suggest that DAPT and Compound E have differing potencies in OS, and need to be further studied to understand subtleties in target specificities (123, 127).  Additionally, our findings may differ from those reported with DAPT because we used a different model of OS: our study used CCHD, HOS and CCHO cells, while the report by Engin *et al.* used SJSA and SaOS2 cells. Finally, it is possible that *in vitro* response using GSI (Compound E or DAPT) does not correlate with *in vivo* effects. Therefore, future studies should be done looking a t the ability for DAPT or Compound E to reduce tumor burden in an orthotopic model. Understanding the mechanisms that differentiate GSIs and allow for target selectivity may allow for future use of GSIs in the

clinic; however, due to severe GSI associated toxicities, this class of drugs is not yet clinically useful.

## Bibliography

1.      Hayden, J. B., and B. H. Hoang. 2006. Osteosarcoma: basic science and clinical implications. *The Orthopedic clinics of North America* 37: 1-7.
2.      Marina, N., M. Gebhardt, L. Teot, and R. Gorlick. 2004. Biology and therapeutic advances for pediatric osteosarcoma. *Oncologist* 9: 422-441.
3.      Tang, N., W.-X. Song, J. Luo, R. Haydon, and T.-C. He. 2008. Osteosarcoma development and stem cell differentiation. *Clinical orthopaedics and related research* 466: 2114-2130.
4.      Jaffe, N. 2009. Osteosarcoma: review of the past, impact on the future. The American experience. *Cancer Treat Res* 152: 239-262.
5.      Mirabello, L., R. J. Troisi, and S. A. Savage. 2009. Osteosarcoma incidence and survival rates from 1973 to 2004: data from the Surveillance, Epidemiology, and End Results Program. *Cancer* 115: 1531-1543.
6.      Bielack, S., H. Jurgens, G. Jundt, M. Kevric, T. Kuhne, P. Reichardt, A. Zoubek, M. Werner, W. Winkelmann, and R. Kotz. 2009. Osteosarcoma: the COSS experience. *Cancer Treat Res* 152: 289-308.
7.      Bielack, S. S., S. Smeland, J. S. Whelan, N. Marina, G. Jovic, J. M. Hook, M. D. Krailo, M. Gebhardt, Z. Papai, J. Meyer, H. Nadel, R. L. Randall, C. Deffenbaugh, R. Nagarajan, B. Brennan, G. D. Letson, L. A. Teot, A. Goorin, D. Baumhoer, L. Kager, M. Werner, C. C. Lau, K. Sundby Hall, H. Gelderblom, P. Meyers, R. Gorlick, R. Windhager, K. Helmke, M. Eriksson, P. M. Hoogerbrugge, P. Schomberg, P. U. Tunn, T. Kuhne, H. Jurgens, H. van den Berg, T. Bohling, S. Picton, M. Renard, P. Reichardt, J. Gerss, T. Butterfass-Bahloul, C. Morris, P. C. Hogendoorn, B. Seddon, G. Calaminus, M. Michelagnoli, C. Dhooge, M. R. Sydes, M. Bernstein, and E.-. investigators. 2015. Methotrexate, Doxorubicin, and Cisplatin (MAP) Plus Maintenance Pegylated Interferon Alfa-2b Versus MAP Alone in Patients With Resectable High-Grade Osteosarcoma and Good Histologic Response to Preoperative MAP: First Results of the EURAMOS-1 Good Response Randomized Controlled Trial. *J Clin Oncol* 33: 2279-2287.
8.      Deng, Z. L., K. A. Sharff, N. Tang, W. X. Song, J. Luo, X. Luo, J. Chen, E. Bennett, R. Reid, D. Manning, A. Xue, A. G. Montag, H. H. Luu, R. C. Haydon, and T. C. He. 2008. Regulation of osteogenic differentiation during skeletal development. *Front Biosci* 13: 2001-2021.
9.      Ducy, P., M. Starbuck, M. Priemel, J. Shen, G. Pinero, V. Geoffroy, M. Amling, and G. Karsenty. 1999. A Cbfa1-dependent genetic pathway controls bone formation beyond embryonic development. *Genes Dev* 13: 1025-1036.
10.     Ducy, P., R. Zhang, V. Geoffroy, A. L. Ridall, and G. Karsenty. 1997. Osf2/Cbfa1: a transcriptional activator of osteoblast differentiation. *Cell* 89: 747-754.
11.     Haydon, R. C., H. H. Luu, and T. C. He. 2007. Osteosarcoma and osteoblastic differentiation: a new perspective on oncogenesis. *Clin Orthop Relat Res* 454: 237-246.
12.     Hong, J. H., E. S. Hwang, M. T. McManus, A. Amsterdam, Y. Tian, R. Kalmukova, E. Mueller, T. Benjamin, B. M. Spiegelman, P. A. Sharp, N. Hopkins, and M. B. Yaffe. 2005. TAZ, a transcriptional modulator of mesenchymal stem cell differentiation. *Science* 309: 1074-1078.

13. Karsenty, G. 2000. Role of Cbfa1 in osteoblast differentiation and function. *Semin Cell Dev Biol* 11: 343-346.
14. Lian, J. B., G. S. Stein, A. Javed, A. J. van Wijnen, J. L. Stein, M. Montecino, M. Q. Hassan, T. Gaur, C. J. Lengner, and D. W. Young. 2006. Networks and hubs for the transcriptional control of osteoblastogenesis. *Rev Endocr Metab Disord* 7: 1-16.
15. Nakashima, K., X. Zhou, G. Kunkel, Z. Zhang, J. M. Deng, R. R. Behringer, and B. de Crombrugghe. 2002. The novel zinc finger-containing transcription factor osterix is required for osteoblast differentiation and bone formation. *Cell* 108: 17-29.
16. Otto, F., A. P. Thornell, T. Crompton, A. Denzel, K. C. Gilmour, I. R. Rosewell, G. W. Stamp, R. S. Beddington, S. Mundlos, B. R. Olsen, P. B. Selby, and M. J. Owen. 1997. Cbfa1, a candidate gene for cleidocranial dysplasia syndrome, is essential for osteoblast differentiation and bone development. *Cell* 89: 765-771.
17. Yamaguchi, A., T. Komori, and T. Suda. 2000. Regulation of osteoblast differentiation mediated by bone morphogenetic proteins, hedgehogs, and Cbfa1. *Endocrine reviews* 21: 393-411.
18. Hsu, H., D. L. Lacey, C. R. Dunstan, I. Solovyev, A. Colombero, E. Timms, H. L. Tan, G. Elliott, M. J. Kelley, I. Sarosi, L. Wang, X. Z. Xia, R. Elliott, L. Chiu, T. Black, S. Scully, C. Capparelli, S. Morony, G. Shimamoto, M. B. Bass, and W. J. Boyle. 1999. Tumor necrosis factor receptor family member RANK mediates osteoclast differentiation and activation induced by osteoprotegerin ligand. *Proc Natl Acad Sci U S A* 96: 3540-3545.
19. Cao, Y., S. F. Jia, G. Chakravarty, B. de Crombrugghe, and E. S. Kleinerman. 2008. The osterix transcription factor down-regulates interleukin-1 alpha expression in mouse osteosarcoma cells. *Molecular cancer research : MCR* 6: 119-126.
20. Myers, D. E., F. M. Collier, C. Minkin, H. Wang, W. R. Holloway, M. Malakellis, and G. C. Nicholson. 1999. Expression of functional RANK on mature rat and human osteoclasts. *FEBS letters* 463: 295-300.
21. Gorlick, R., and P. A. Meyers. 2003. Osteosarcoma necrosis following chemotherapy: innate biology versus treatment-specific. *J Pediatr Hematol Oncol* 25: 840-841.
22. Cao, Y., Z. Zhou, B. de Crombrugghe, K. Nakashima, H. Guan, X. Duan, S. F. Jia, and E. S. Kleinerman. 2005. Osterix, a transcription factor for osteoblast differentiation, mediates antitumor activity in murine osteosarcoma. *Cancer Res* 65: 1124-1128.
23. Watanabe, T., T. Oyama, M. Asada, D. Harada, Y. Ito, M. Inagawa, Y. Suzuki, S. Sugano, K. Katsube, G. Karsenty, T. Komori, M. Kitagawa, and H. Asahara. 2013. MAML1 enhances the transcriptional activity of Runx2 and plays a role in bone development. *PLoS genetics* 9: e1003132.
24. Suh, J. H., H. W. Lee, J. W. Lee, and J. B. Kim. 2008. Hes1 stimulates transcriptional activity of Runx2 by increasing protein stabilization during osteoblast differentiation. *Biochem Biophys Res Commun* 367: 97-102.
25. Hilton, M., X. Tu, X. Wu, S. Bai, H. Zhao, T. Kobayashi, H. Kronenberg, S. Teitelbaum, F. Ross, R. Kopan, and F. Long. 2008. Notch signaling maintains bone marrow mesenchymal progenitors by suppressing osteoblast differentiation. *Nature medicine* 14: 306-314.

26.	Engin, F., Z. Yao, T. Yang, G. Zhou, T. Bertin, M. Jiang, Y. Chen, L. Wang, H. Zheng, R. Sutton, B. Boyce, and B. Lee. 2008. Dimorphic effects of Notch signaling in bone homeostasis. *Nature medicine* 14: 299-305.

27.	Cakouros, D., S. Isenmann, S. E. Hemming, D. Menicanin, E. Camp, A. C. Zannettino, and S. Gronthos. 2015. Novel basic Helix Loop Helix Transcription Factor Hes4 Antagonizes the Function of Twist-1 to Regulate Lineage Commitment of Bone Marrow Stromal/ Stem Cells. *Stem cells and development*.

28.	Mumm, J. S., and R. Kopan. 2000. Notch signaling: from the outside in. *Developmental biology* 228: 151-165.

29.	Bray, S. J. 2006. Notch signalling: a simple pathway becomes complex. *Nat Rev Mol Cell Biol* 7: 678-689.

30.	Kopan, R., and M. X. Ilagan. 2009. The canonical Notch signaling pathway: unfolding the activation mechanism. *Cell* 137: 216-233.

31.	Andersson, E. R., R. Sandberg, and U. Lendahl. 2011. Notch signaling: simplicity in design, versatility in function. *Development* 138: 3593-3612.

32.	Guruharsha, K. G., M. W. Kankel, and S. Artavanis-Tsakonas. 2012. The Notch signalling system: recent insights into the complexity of a conserved pathway. *Nature reviews. Genetics* 13: 654-666.

33.	Schroeter, E. H., J. A. Kisslinger, and R. Kopan. 1998. Notch-1 signalling requires ligand-induced proteolytic release of intracellular domain. *Nature* 393: 382-386.

34.	Bessho, Y., R. Sakata, S. Komatsu, K. Shiota, S. Yamada, and R. Kageyama. 2001. Dynamic expression and essential functions of Hes7 in somite segmentation. *Genes Dev* 15: 2642-2647.

35.	Kageyama, R., and T. Ohtsuka. 1999. The Notch-Hes pathway in mammalian neural development. *Cell Res* 9: 179-188.

36.	Ishibashi, M., S. L. Ang, K. Shiota, S. Nakanishi, R. Kageyama, and F. Guillemot. 1995. Targeted disruption of mammalian hairy and Enhancer of split homolog-1 (HES-1) leads to up-regulation of neural helix-loop-helix factors, premature neurogenesis, and severe neural tube defects. *Genes Dev* 9: 3136-3148.

37.	Fischer, A., and M. Gessler. 2007. Delta-Notch--and then? Protein interactions and proposed modes of repression by Hes and Hey bHLH factors. *Nucleic Acids Res* 35: 4583-4596.

38.	Davis, R. L., and D. L. Turner. 2001. Vertebrate hairy and Enhancer of split related proteins: transcriptional repressors regulating cellular differentiation and embryonic patterning. *Oncogene* 20: 8342-8357.

39.	Liu, P., Y. Ping, M. Ma, D. Zhang, C. Liu, S. Zaidi, S. Gao, Y. Ji, F. Lou, F. Yu, P. Lu, A. Stachnik, M. Bai, C. Wei, L. Zhang, K. Wang, R. Chen, M. I. New, D. W. Rowe, T. Yuen, L. Sun, and M. Zaidi. 2016. Anabolic actions of Notch on mature bone. *Proc Natl Acad Sci U S A*.

40.	Tezuka, K., M. Yasuda, N. Watanabe, N. Morimura, K. Kuroda, S. Miyatani, and N. Hozumi. 2002. Stimulation of osteoblastic cell differentiation by Notch. *J Bone Miner Res* 17: 231-239.

41.	Yamada, T., H. Yamazaki, T. Yamane, M. Yoshino, H. Okuyama, M. Tsuneto, T. Kurino, S. Hayashi, and S. Sakano. 2003. Regulation of osteoclast development by Notch signaling directed to osteoclast precursors and through stromal cells. *Blood* 101: 2227-2234.

42. Dallas, D. J., P. G. Genever, A. J. Patton, M. I. Millichip, N. McKie, and T. M. Skerry. 1999. Localization of ADAM10 and Notch receptors in bone. *Bone* 25: 9-15.

43. Swiatek, P. J., C. E. Lindsell, F. F. del Amo, G. Weinmaster, and T. Gridley. 1994. Notch1 is essential for postimplantation development in mice. *Genes Dev* 8: 707-719.

44. Conlon, R. A., A. G. Reaume, and J. Rossant. 1995. Notch1 is required for the coordinate segmentation of somites. *Development* 121: 1533-1545.

45. Shen, J., R. T. Bronson, D. F. Chen, W. Xia, D. J. Selkoe, and S. Tonegawa. 1997. Skeletal and CNS defects in Presenilin-1-deficient mice. *Cell* 89: 629-639.

46. Engin, F., T. Bertin, O. Ma, M. M. Jiang, L. Wang, R. E. Sutton, L. A. Donehower, and B. Lee. 2009. Notch signaling contributes to the pathogenesis of human osteosarcomas. *Hum Mol Genet* 18: 1464-1470.

47. Zhang, C. C., A. Pavlicek, Q. Zhang, M. E. Lira, C. L. Painter, Z. Yan, X. Zheng, N. V. Lee, M. Ozeck, M. Qiu, Q. Zong, P. B. Lappin, A. Wong, P. A. Rejto, T. Smeal, and J. G. Christensen. 2012. Biomarker and pharmacologic evaluation of the γ-secretase inhibitor PF-03084014 in breast cancer models. *Clinical cancer research : an official journal of the American Association for Cancer Research* 18: 5008-5019.

48. Stoeck, A., S. Lejnine, A. Truong, L. Pan, H. Wang, C. Zang, J. Yuan, C. Ware, J. MacLean, P. W. Garrett-Engele, M. Kluk, J. Laskey, B. B. Haines, C. Moskaluk, L. Zawel, S. Fawell, G. Gilliland, T. Zhang, B. E. Kremer, B. Knoechel, B. E. Bernstein, W. S. Pear, X. S. Liu, J. C. Aster, and S. Sathyanarayanan. 2014. Discovery of biomarkers predictive of GSI response in triple-negative breast cancer and adenoid cystic carcinoma. *Cancer discovery* 4: 1154-1167.

49. Messersmith, W. A., G. I. Shapiro, J. M. Cleary, A. Jimeno, A. Dasari, B. Huang, M. N. Shaik, R. Cesari, X. Zheng, J. M. Reynolds, P. A. English, K. R. McLachlan, K. A. Kern, and P. M. LoRusso. 2014. A Phase I, Dose-Finding Study in Patients with Advanced Solid Malignancies of the Oral γ-Secretase Inhibitor PF-03084014. *Clinical cancer research : an official journal of the American Association for Cancer Research* 21: 60-67.

50. Thomas, D., and M. Kansara. 2006. Epigenetic modifications in osteogenic differentiation and transformation. *Journal of cellular biochemistry* 98: 757-769.

51. Weng, A. P., A. A. Ferrando, W. Lee, J. P. t. Morris, L. B. Silverman, C. Sanchez-Irizarry, S. C. Blacklow, A. T. Look, and J. C. Aster. 2004. Activating mutations of NOTCH1 in human T cell acute lymphoblastic leukemia. *Science* 306: 269-271.

52. Morimura, T., R. Goitsuka, Y. Zhang, I. Saito, M. Reth, and D. Kitamura. 2000. Cell cycle arrest and apoptosis induced by Notch1 in B cells. *J Biol Chem* 275: 36523-36531.

53. Jundt, F., K. S. Probsting, I. Anagnostopoulos, G. Muehlinghaus, M. Chatterjee, S. Mathas, R. C. Bargou, R. Manz, H. Stein, and B. Dorken. 2004. Jagged1-induced Notch signaling drives proliferation of multiple myeloma cells. *Blood* 103: 3511-3515.

54. Leong, K. G., and A. Karsan. 2006. Recent insights into the role of Notch signaling in tumorigenesis. *Blood* 107: 2223-2233.

55. Radtke, F., and K. Raj. 2003. The role of Notch in tumorigenesis: oncogene or tumour suppressor? *Nat Rev Cancer* 3: 756-767.

56. Roy, M., W. S. Pear, and J. C. Aster. 2007. The multifaceted role of Notch in cancer. *Curr Opin Genet Dev* 17: 52-59.

57.     Maillard, I., and W. S. Pear. 2003. Notch and cancer: best to avoid the ups and downs. *Cancer cell* 3: 203-205.

58.     Wilson, A., and F. Radtke. 2006. Multiple functions of Notch signaling in self-renewing organs and cancer. *FEBS letters* 580: 2860-2868.

59.     Avila, J. L., and J. L. Kissil. 2013. Notch signaling in pancreatic cancer: oncogene or tumor suppressor? *Trends Mol Med* 19: 320-327.

60.     Zhang, P., Y. Yang, R. Nolo, P. A. Zweidler-McKay, and D. P. Hughes. 2010. Regulation of NOTCH signaling by reciprocal inhibition of HES1 and Deltex 1 and its role in osteosarcoma invasiveness. *Oncogene* 29: 2916-2926.

61.     Mu, X., C. Isaac, N. Greco, J. Huard, and K. Weiss. 2013. Notch Signaling is Associated with ALDH Activity and an Aggressive Metastatic Phenotype in Murine Osteosarcoma Cells. *Frontiers in oncology* 3: 143.

62.     Engin, F., and B. Lee. 2010. NOTCHing the bone: insights into multi-functionality. *Bone* 46: 274-280.

63.     Andersson, E. R., and U. Lendahl. 2014. Therapeutic modulation of Notch signalling--are we there yet? *Nature reviews. Drug discovery* 13: 357-378.

64.     Miele, L., H. Miao, and B. J. Nickoloff. 2006. NOTCH signaling as a novel cancer therapeutic target. *Current cancer drug targets* 6: 313-323.

65.     Espinoza, I., and L. Miele. 2013. Notch inhibitors for cancer treatment. *Pharmacology & therapeutics* 139: 95-110.

66.     Gonzalez-Garcia, S., M. Garcia-Peydro, E. Martin-Gayo, E. Ballestar, M. Esteller, R. Bornstein, J. L. de la Pompa, A. A. Ferrando, and M. L. Toribio. 2009. CSL-MAML-dependent Notch1 signaling controls T lineage-specific IL-7R{alpha} gene expression in early human thymopoiesis and leukemia. *J Exp Med* 206: 779-791.

67.     Wall, D. S., A. J. Mears, B. McNeill, C. Mazerolle, S. Thurig, Y. Wang, R. Kageyama, and V. A. Wallace. 2009. Progenitor cell proliferation in the retina is dependent on Notch-independent Sonic hedgehog/Hes1 activity. *J Cell Biol* 184: 101-112.

68.     Sanalkumar, R., C. L. Indulekha, T. S. Divya, M. S. Divya, R. J. Anto, B. Vinod, S. Vidyanand, B. Jagatha, S. Venugopal, and J. James. 2010. ATF2 maintains a subset of neural progenitors through CBF1/Notch independent Hes-1 expression and synergistically activates the expression of Hes-1 in Notch-dependent neural progenitors. *Journal of neurochemistry* 113: 807-818.

69.     Katoh, M., and M. Katoh. 2007. Integrative genomic analyses on HES/HEY family: Notch-independent HES1, HES3 transcription in undifferentiated ES cells, and Notch-dependent HES1, HES5, HEY1, HEY2, HEYL transcription in fetal tissues, adult tissues, or cancer. *Int J Oncol* 31: 461-466.

70.     Curry, C. L., L. L. Reed, B. J. Nickoloff, L. Miele, and K. E. Foreman. 2006. Notch-independent regulation of Hes-1 expression by c-Jun N-terminal kinase signaling in human endothelial cells. *Lab Invest* 86: 842-852.

71.     Lin, C. H., and E. H. Lee. 2012. JNK1 inhibits GluR1 expression and GluR1-mediated calcium influx through phosphorylation and stabilization of Hes-1. *J Neurosci* 32: 1826-1846.

72.     Stewart, K. S., Z. Zhou, P. Zweidler-McKay, and E. S. Kleinerman. 2011. Delta-like ligand 4-Notch signaling regulates bone marrow-derived pericyte/vascular smooth muscle cell formation. *Blood* 117: 719-726.

73. Lobov, I., R. Renard, N. Papadopoulos, N. Gale, G. Thurston, G. Yancopoulos, and S. Wiegand. 2007. Delta-like ligand 4 (Dll4) is induced by VEGF as a negative regulator of angiogenic sprouting. *Proceedings of the National Academy of Sciences of the United States of America* 104: 3219-3224.

74. Thomas, J.-L., K. Baker, J. Han, C. Calvo, H. Nurmi, A. Eichmann, and K. Alitalo. 2013. Interactions between VEGFR and Notch signaling pathways in endothelial and neural cells. *Cellular and molecular life sciences : CMLS* 70: 1779-1792.

75. Benedito, R., C. Roca, I. Sörensen, S. Adams, A. Gossler, M. Fruttiger, and R. Adams. 2009. The notch ligands Dll4 and Jagged1 have opposing effects on angiogenesis. *Cell* 137: 1124-1135.

76. McManus, M. M., K. R. Weiss, and D. P. Hughes. 2014. Understanding the role of Notch in osteosarcoma. *Adv Exp Med Biol* 804: 67-92.

77. Kuijjer, M. L., H. Rydbeck, S. H. Kresse, E. P. Buddingh, A. B. Lid, H. Roelofs, H. Burger, O. Myklebost, P. C. Hogendoorn, L. A. Meza-Zepeda, and A. M. Cleton-Jansen. 2012. Identification of osteosarcoma driver genes by integrative analysis of copy number and gene expression data. *Genes, chromosomes & cancer* 51: 696-706.

78. Kageyama, R., T. Ohtsuka, and T. Kobayashi. 2007. The Hes gene family: repressors and oscillators that orchestrate embryogenesis. *Development* 134: 1243-1251.

79. Momiji, H., and N. A. Monk. 2008. Dissecting the dynamics of the Hes1 genetic oscillator. *Journal of theoretical biology* 254: 784-798.

80. Allen, R. D., 3rd, H. K. Kim, S. D. Sarafova, and G. Siu. 2001. Negative regulation of CD4 gene expression by a HES-1-c-Myb complex. *Mol Cell Biol* 21: 3071-3082.

81. Ishiko, E., I. Matsumura, S. Ezoe, K. Gale, J. Ishiko, Y. Satoh, H. Tanaka, H. Shibayama, M. Mizuki, T. Era, T. Enver, and Y. Kanakura. 2005. Notch signals inhibit the development of erythroid/megakaryocytic cells by suppressing GATA-1 activity through the induction of HES1. *J Biol Chem* 280: 4929-4939.

82. McLarren, K. W., F. M. Theriault, and S. Stifani. 2001. Association with the nuclear matrix and interaction with Groucho and RUNX proteins regulate the transcription repression activity of the basic helix loop helix factor Hes1. *J Biol Chem* 276: 1578-1584.

83. Shen, Q., and S. Christakos. 2005. The vitamin D receptor, Runx2, and the Notch signaling pathway cooperate in the transcriptional regulation of osteopontin. *J Biol Chem* 280: 40589-40598.

84. McLarren, K. W., R. Lo, D. Grbavec, K. Thirunavukkarasu, G. Karsenty, and S. Stifani. 2000. The mammalian basic helix loop helix protein HES-1 binds to and modulates the transactivating function of the runt-related factor Cbfa1. *J Biol Chem* 275: 530-538.

85. Lee, J. S., D. M. Thomas, G. Gutierrez, S. A. Carty, S. Yanagawa, and P. W. Hinds. 2006. HES1 cooperates with pRb to activate RUNX2-dependent transcription. *J Bone Miner Res* 21: 921-933.

86. Weber, K. L., M. Doucet, J. E. Price, C. Baker, S. J. Kim, and I. J. Fidler. 2003. Blockade of epidermal growth factor receptor signaling leads to inhibition of renal cell carcinoma growth in the bone of nude mice. *Cancer Res* 63: 2940-2947.

87. van Breugel, F. M. 1971. The action of the Notch locus in Drosophila hydei. *Genetica* 42: 25-41.

88.     Jimi, E., M. Shin, H. Furuta, Y. Tada, and J. Kusukawa. 2013. The RANKL/RANK system as a therapeutic target for bone invasion by oral squamous cell carcinoma (Review). *Int J Oncol* 42: 803-809.
89.     Wagner, E., B.-C. He, L. Chen, G.-W. Zuo, W. Zhang, Q. Shi, Q. Luo, X. Luo, B. Liu, J. Luo, F. Rastegar, C. He, Y. Hu, B. Boody, H. Luu, T.-C. He, Z.-L. Deng, and R. Haydon. 2010. Therapeutic Implications of PPARgamma in Human Osteosarcoma. *PPAR research* 2010: 956427.
90.     Monteiro, J., and R. Fodde. 2010. Cancer stemness and metastasis: therapeutic consequences and perspectives. *Eur J Cancer* 46: 1198-1203.
91.     Tang, N., W. X. Song, J. Luo, R. C. Haydon, and T. C. He. 2008. Osteosarcoma development and stem cell differentiation. *Clin Orthop Relat Res* 466: 2114-2130.
92.     Sadikovic, B., P. Thorner, S. Chilton-Macneill, J. W. Martin, N. K. Cervigne, J. Squire, and M. Zielenska. 2010. Expression analysis of genes associated with human osteosarcoma tumors shows correlation of RUNX2 overexpression with poor response to chemotherapy. *BMC Cancer* 10: 202.
93.     Yu, X. W., T. Y. Wu, X. Yi, W. P. Ren, Z. B. Zhou, Y. Q. Sun, and C. Q. Zhang. 2014. Prognostic significance of VEGF expression in osteosarcoma: a meta-analysis. *Tumour biology : the journal of the International Society for Oncodevelopmental Biology and Medicine* 35: 155-160.
94.     Chen, D., Y. J. Zhang, K. W. Zhu, and W. C. Wang. 2013. A systematic review of vascular endothelial growth factor expression as a biomarker of prognosis in patients with osteosarcoma. *Tumour biology : the journal of the International Society for Oncodevelopmental Biology and Medicine* 34: 1895-1899.
95.     Chen, Y., C. M. Wang, Y. Q. Shi, and Y. Yang. 2012. [Expression of hypoxia-inducible factor 1alpha in osteosarcoma and its value in predicting chemosensitivity]. *Zhonghua zhong liu za zhi [Chinese journal of oncology]* 34: 899-904.
96.     Rastogi, S., R. Kumar, S. R. Sankineani, K. Marimuthu, L. Rijal, S. Prakash, D. Jalan, S. A. Khan, and M. C. Sharma. 2012. Role of vascular endothelial growth factor as a tumour marker in osteosarcoma: a prospective study. *Int Orthop* 36: 2315-2321.
97.     Pakos, E. E., P. A. Kyzas, and J. P. Ioannidis. 2004. Prognostic significance of TP53 tumor suppressor gene expression and mutations in human osteosarcoma: a meta-analysis. *Clin Cancer Res* 10: 6208-6214.
98.     Tokuzawa, Y., K. Yagi, Y. Yamashita, Y. Nakachi, I. Nikaido, H. Bono, Y. Ninomiya, Y. Kanesaki-Yatsuka, M. Akita, H. Motegi, S. Wakana, T. Noda, F. Sablitzky, S. Arai, R. Kurokawa, T. Fukuda, T. Katagiri, C. Schonbach, T. Suda, Y. Mizuno, and Y. Okazaki. 2010. Id4, a new candidate gene for senile osteoporosis, acts as a molecular switch promoting osteoblast differentiation. *PLoS genetics* 6: e1001019.
99.     Deng, Z.-L., K. Sharff, N. Tang, W.-X. Song, J. Luo, X. Luo, J. Chen, E. Bennett, R. Reid, D. Manning, A. Xue, A. Montag, H. Luu, R. Haydon, and T.-C. He. 2008. Regulation of osteogenic differentiation during skeletal development. *Frontiers in bioscience : a journal and virtual library* 13: 2001-2021.
100.    Ducy, P., M. Starbuck, M. Priemel, J. Shen, G. Pinero, V. Geoffroy, M. Amling, and G. Karsenty. 1999. A Cbfa1-dependent genetic pathway controls bone formation beyond embryonic development. *Genes & development* 13: 1025-1036.

101. Ducy, P., R. Zhang, V. Geoffroy, A. Ridall, and G. Karsenty. 1997. Osf2/Cbfa1: a transcriptional activator of osteoblast differentiation. *Cell* 89: 747-754.

102. Haydon, R., H. Luu, and T.-C. He. 2007. Osteosarcoma and osteoblastic differentiation: a new perspective on oncogenesis. *Clinical orthopaedics and related research* 454: 237-246.

103. Hong, J.-H., E. Hwang, M. McManus, A. Amsterdam, Y. Tian, R. Kalmukova, E. Mueller, T. Benjamin, B. Spiegelman, P. Sharp, N. Hopkins, and M. Yaffe. 2005. TAZ, a transcriptional modulator of mesenchymal stem cell differentiation. *Science (New York, N.Y.)* 309: 1074-1078.

104. Karsenty, G. 2000. How many factors are required to remodel bone? *Nat Med* 6: 970-971.

105. Lian, J., G. Stein, A. Javed, A. van Wijnen, J. Stein, M. Montecino, M. Hassan, T. Gaur, C. Lengner, and D. Young. 2006. Networks and hubs for the transcriptional control of osteoblastogenesis. *Reviews in endocrine & metabolic disorders* 7: 1-16.

106. Nakashima, K., X. Zhou, G. Kunkel, Z. Zhang, J. Deng, R. Behringer, and B. de Crombrugghe. 2002. The novel zinc finger-containing transcription factor osterix is required for osteoblast differentiation and bone formation. *Cell* 108: 17-29.

107. Otto, F., A. Thornell, T. Crompton, A. Denzel, K. Gilmour, I. Rosewell, G. Stamp, R. Beddington, S. Mundlos, B. Olsen, P. Selby, and M. Owen. 1997. Cbfa1, a candidate gene for cleidocranial dysplasia syndrome, is essential for osteoblast differentiation and bone development. *Cell* 89: 765-771.

108. Stoeck, A., S. Lejnine, A. Truong, L. Pan, H. Wang, C. Zang, J. Yuan, C. Ware, J. MacLean, P. W. Garrett-Engele, M. Kluk, J. Laskey, B. B. Haines, C. Moskaluk, L. Zawel, S. Fawell, G. Gilliland, T. Zhang, B. E. Kremer, B. Knoechel, B. E. Bernstein, W. S. Pear, X. S. Liu, J. C. Aster, and S. Sathyanarayanan. 2014. Discovery of biomarkers predictive of GSI response in triple-negative breast cancer and adenoid cystic carcinoma. *Cancer Discov* 4: 1154-1167.

109. Lamplot, J. D., J. Qin, G. Nan, J. Wang, X. Liu, L. Yin, J. Tomal, R. Li, W. Shui, H. Zhang, S. H. Kim, W. Zhang, J. Zhang, Y. Kong, S. Denduluri, M. R. Rogers, A. Pratt, R. C. Haydon, H. H. Luu, J. Angeles, L. L. Shi, and T. C. He. 2013. BMP9 signaling in stem cell differentiation and osteogenesis. *American journal of stem cells* 2: 1-21.

110. Sharff, K. A., W. X. Song, X. Luo, N. Tang, J. Luo, J. Chen, Y. Bi, B. C. He, J. Huang, X. Li, W. Jiang, G. H. Zhu, Y. Su, Y. He, J. Shen, Y. Wang, L. Chen, G. W. Zuo, B. Liu, X. Pan, R. R. Reid, H. H. Luu, R. C. Haydon, and T. C. He. 2009. Hey1 basic helix-loop-helix protein plays an important role in mediating BMP9-induced osteogenic differentiation of mesenchymal progenitor cells. *J Biol Chem* 284: 649-659.

111. Batanian, J. R., L. R. Cavalli, N. M. Aldosari, E. Ma, C. Sotelo-Avila, M. B. Ramos, J. D. Rone, C. M. Thorpe, and B. R. Haddad. 2002. Evaluation of paediatric osteosarcomas by classic cytogenetic and CGH analyses. *Molecular pathology : MP* 55: 389-393.

112. Lim, G., J. Karaskova, B. Beheshti, B. Vukovic, J. Bayani, S. Selvarajah, S. K. Watson, W. L. Lam, M. Zielenska, and J. A. Squire. 2005. An integrated mBAND and submegabase resolution tiling set (SMRT) CGH array analysis of focal

amplification, microdeletions, and ladder structures consistent with breakage-fusion-bridge cycle events in osteosarcoma. *Genes, chromosomes & cancer* 42: 392-403.

113. Lim, G., J. Karaskova, B. Vukovic, J. Bayani, B. Beheshti, M. Bernardini, J. A. Squire, and M. Zielenska. 2004. Combined spectral karyotyping, multicolor banding, and microarray comparative genomic hybridization analysis provides a detailed characterization of complex structural chromosomal rearrangements associated with gene amplification in the osteosarcoma cell line MG-63. *Cancer genetics and cytogenetics* 153: 158-164.

114. Sandberg, A. A., and J. A. Bridge. 2003. Updates on the cytogenetics and molecular genetics of bone and soft tissue tumors: osteosarcoma and related tumors. *Cancer genetics and cytogenetics* 145: 1-30.

115. Selvarajah, S., M. Yoshimoto, G. Maire, J. Paderova, J. Bayani, J. A. Squire, and M. Zielenska. 2007. Identification of cryptic microaberrations in osteosarcoma by high-definition oligonucleotide array comparative genomic hybridization. *Cancer genetics and cytogenetics* 179: 52-61.

116. Squire, J. A., J. Pei, P. Marrano, B. Beheshti, J. Bayani, G. Lim, L. Moldovan, and M. Zielenska. 2003. High-resolution mapping of amplifications and deletions in pediatric osteosarcoma by use of CGH analysis of cDNA microarrays. *Genes, chromosomes & cancer* 38: 215-225.

117. Zielenska, M., P. Marrano, P. Thorner, J. Pei, B. Beheshti, M. Ho, J. Bayani, Y. Liu, B. C. Sun, J. A. Squire, and X. S. Hao. 2004. High-resolution cDNA microarray CGH mapping of genomic imbalances in osteosarcoma using formalin-fixed paraffin-embedded tissue. *Cytogenetic and genome research* 107: 77-82.

118. Lalkhen, A. G., and McCluskey, A. . 2008. Clinical tests: sensitivity and specificity. *Contin Educ Anaesth Crit Care Pain* 8: 221-223.

119. Henderson, T. O., C. S. Moskowitz, J. F. Chou, A. R. Bradbury, J. P. Neglia, C. T. Dang, K. Onel, D. Novetsky Friedman, S. Bhatia, L. C. Strong, M. Stovall, L. B. Kenney, D. Barnea, E. Lorenzi, S. Hammond, W. M. Leisenring, L. L. Robison, G. T. Armstrong, L. R. Diller, and K. C. Oeffinger. 2016. Breast Cancer Risk in Childhood Cancer Survivors Without a History of Chest Radiotherapy: A Report From the Childhood Cancer Survivor Study. *J Clin Oncol* 34: 910-918.

120. Struhl, K. 1998. Histone acetylation and transcriptional regulatory mechanisms. *Genes Dev* 12: 599-606.

121. Lai, E. C. 2002. Notch cleavage: Nicastrin helps Presenilin make the final cut. *Current biology : CB* 12: R200-202.

122. Olsauskas-Kuprys, R., A. Zlobin, and C. Osipo. 2013. Gamma secretase inhibitors of Notch signaling. *OncoTargets and therapy* 6: 943-955.

123. Svedruzic, Z. M., K. Popovic, and V. Sendula-Jengic. 2013. Modulators of gamma-secretase activity can facilitate the toxic side-effects and pathogenesis of Alzheimer's disease. *PLoS One* 8: e50759.

124. Clarke, E. E., I. Churcher, S. Ellis, J. D. Wrigley, H. D. Lewis, T. Harrison, M. S. Shearman, and D. Beher. 2006. Intra- or intercomplex binding to the gamma-secretase enzyme. A model to differentiate inhibitor classes. *J Biol Chem* 281: 31279-31289.

125. Morohashi, Y., T. Kan, Y. Tominari, H. Fuwa, Y. Okamura, N. Watanabe, C. Sato, H. Natsugari, T. Fukuyama, T. Iwatsubo, and T. Tomita. 2006. C-terminal fragment

of presenilin is the molecular target of a dipeptidic gamma-secretase-specific inhibitor DAPT (N-[N-(3,5-difluorophenacetyl)-L-alanyl]-S-phenylglycine t-butyl ester). *J Biol Chem* 281: 14670-14676.

126.    Banerjee, D., A. Kadenhe-Chiweshe, and D. J. Yamashiro. 2015. Inhibition of Notch promotes liver metastasis. *Aging* 7: 603-604.

127.    Yang, T., D. Arslanova, Y. Gu, C. Augelli-Szafran, and W. Xia. 2008. Quantification of gamma-secretase modulation differentiates inhibitor compound selectivity between two substrates Notch and amyloid precursor protein. *Molecular brain* 1: 15.

**Vita**

Madonna Michelle McManus was born in El Paso, Texas on November 14th, 1986. She is the daughter of Rita Garcia-McManus and Larry George McManus. After completing high school at St. Pius X, Albuquerque, New Mexico in 2005, she entered Trinity University in San Antonio, Texas. She received a Bachelor of Science degree with a major in Biochemistry from Trinity University in May, 2009. From August 2009 to May 2010, Madonna worked at The University of Texas Health Science Center at Houston Medical School in the Center for Translation Injury Research (CTIR). In August 2010, she entered The University of Texas Health Science Center at Houston Graduate School of Biomedical Sciences and MD Anderson Cancer Center. In spring 2016, she received a Doctorate of Philosophy in Experimental Therapeutics.

Mailing address: 6026 Effingham Dr., Houston, Texas 77035